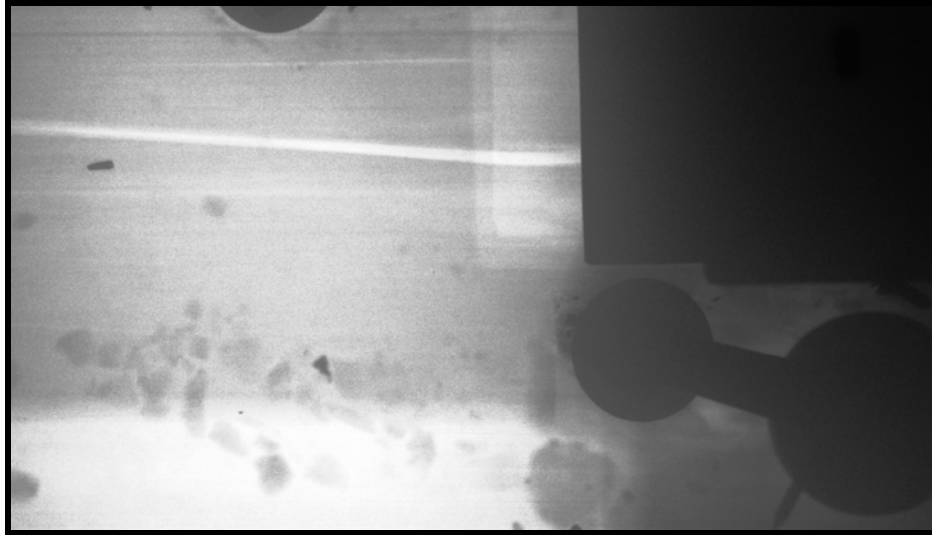


Report:

Advances in Digital Radioscopy for
Use in Historic Preservation
Grant Number MT-2210-03-NC-07



Submitted to:

National Center for Preservation Technology and Training
645 College Avenue
Natchitoches, LA 71457

Submitted by:

Historic Fort Collins Development Corporation
P. O. Box 271732
Fort Collins, CO 80527-1732

Anthony & Associates, Inc.
P. O. Box 271400
Fort Collins, CO 80527-1400

City Visions, Inc.
314 South Sherwood Street
Fort Collins, CO 80521

December 2005

Acknowledgements

The technical work on this project was conducted by Ron Anthony and Deb Anthony of Anthony & Associates, Inc. and Chris Koziol and Katherine Woods of City Visions, Inc. This report builds on research conducted by Ron Anthony of Anthony & Associates, Inc. , which is summarized in a report entitled “Investigating Wood in Historic Structures Using Real-Time X-ray Technology”, funded by the Kress Mid-Career Grant of the James Marston Fitch Charitable Foundation. The body of the Fitch report, with modification, is contained within the NCPTT report for continuity. The ability to leverage research funds from different sources is largely what made the extent of the research reported herein possible.

This project would not have been possible without the generous support of the National Center for Preservation Technology and Training. Additional financial support to research the historical context on x-rays and the preliminary laboratory research was provided by the James Marston Fitch Charitable Foundation and the Kress Foundation. The opportunity to collect field data on historic structures in the Czech Republic was provided by the National Science Foundation. Logos Imaging LLC, SAIC and Golden Engineering, Inc. provided technical support. Vicen Alvarez, Gretchen Lear and Peter Koziol provided laboratory and analytical assistance throughout the project. Logistical and material support was provided by many individuals and organizations. Special thanks go to the Dr. Milos Drdacky and the Czech Academy of Sciences, Mr. Peter Weiss of ELP GmbH and Dr. Bo Kasal of Penn State University for their assistance in the Czech Republic. Mr. Karl Koski, Mr. Jack Smoot of Bollinger Mill State Historic Park (Burfordville, Missouri) and Mr. Mark Miller of Trail Ridge Timber Frames (Masonville, Colorado) kindly provided materials for the laboratory research.

This publication was developed under a grant from the National Park Service and the National Center for Preservation Technology and Training. Its contents are solely the responsibility of the authors and do not necessarily represent the official position or policies of the National Park Service or the National Center for Preservation Technology and Training.

Cover photo: Radiograph of a horizontal fracture in a wooden truss chord showing a steel side plate and bolt at one of the joints, New York State Capitol.

Executive Summary

In the interest of saving as much historic fabric as possible and not altering or scarring historic materials as a result of investigative probes, architectural conservators look to nondestructive testing methods for the evaluation and identification of materials, conditions and alterations made to structures over time. As the answers to these and many other questions are typically concealed in a historic structure, nondestructive techniques of investigation are a necessity, but few are available. Digital radiography is one of those techniques.

The goal of this work was to advance the use of digital radiography for assessing wood in historic structures. The work focused on:

- Investigating historic fabric and construction details using stereo-radiography
- Evaluating the extent of wood deterioration using digital imaging techniques
- Investigating licensing and regulatory requirements for use of portable x-ray equipment
- Investigating safety measures needed to operate the equipment in historic structures

In distilling the findings related to post-processing of digital radiographs, three main points are relevant. First, digital imaging affords the field operator the opportunity to modify image capture techniques based on real-time or near real-time (i.e., field processing) image production. This is particularly important in building investigation where conditions are variable, and future access may be difficult.

Second, the availability of relatively inexpensive mass-market (e.g., Adobe® Photoshop®) and multi-market specialty software (e.g., Photoflair®, Photomodeler) raise the possibility that software applications can be found and tweaked so as to extend the power of digital radiography for building investigation without a prohibitively large outlay of research and development (R&D) resources.

Finally, while the intuitively legible graphic (i.e., pictorial) output of radiographic investigation can provide convincing information, the efficient investigator must weigh whether increasing data inputs is worth the investment, and under what circumstances interpretive experience, multi-method data corroboration, and tacit knowledge suffice.

As demonstrated in this project, the potential that real-time digital radiography investigation presents is exciting and could have great positive impact in the

field of historic preservation. Practical use can be found in some of the following areas:

- Historic structures reports.
- Documentation of original construction details.
 - Documentation of the chronology of construction of a historic structure,
 - Documentation of material dimensions,
 - Documentation of tool markings,
 - Documentation of fastener shapes and sizes.
- Identification of the alteration of such details due to modifications.
- Structural evaluation of conditions and construction details.

Table of Contents

Acknowledgements.....	i
Executive Summary.....	ii
Introduction	1
Discovery of X-rays	1
The Physics of X-Rays	4
Portable X-ray Equipment.....	6
XR200® X-ray Source.....	7
RTR-4™ Imager	7
EPIX Scanner and Imaging Plates	9
Comparisons Between the SAIC® and Logos Radioscopy Systems	10
Safety Procedures	11
Operator Training and Radiation Safety Officer.....	13
Safe Operation (Safe Distance, Signage, Source Key Protocol)	13
Monitoring for Radiation Exposure.....	14
State Notification and Licensing Requirements	16
Licensing.....	17
Additional Resources on Regulations Governing Radiation Safety.....	17
Training.....	18
Survey of States.....	18
Previous Use of X-rays in Historic Buildings	18
Investigation of Metal Fasteners in Timber – Built-Up Timber Trusses	22
Investigation of Metal Fasteners in Timber-Iron Rods Embedded in Beams.....	25
Investigation of Metal Fasteners in Timber – Failure of Double Shear Joints	26
Investigation of Deterioration – Simulated Termite Damage.....	27
Investigating and Imaging Construction Details Non-Intrusively	29
Geometry	29
Producing Contrast	33
Identifying the Location and Condition of Fasteners and Connections.....	37
Metal Connections.....	37
Wood Connections	39
Identifying Wood Deterioration.....	42
General Image Enhancement.....	50
Introduction.....	50
Imaging System Software: SAIC® RTR-4™.....	54
Imaging System Software: EPIX Scanner, Logos Imaging System	57
General Purpose Software: Adobe® Photoshop® Elements	60
General Purpose Software: Adobe® Photoshop® (Full Release).....	64
Specialized Scientific Software: Media Cybernetics Image-Pro	66
Specialized Consumer Software: Tru-View PhotoFlair ®.....	67
Image Enhancement for Quantification of Deterioration	69
Introduction.....	69
Quantification of Deterioration	70
Image Enhancement for Three-Dimensional Analysis	75
Introduction.....	75
Stereo-optics (Three-dimensional Radioscopy).....	76
Determination of Size and Position Using a Single Radiograph.....	80
Calculations in Three Dimensions Using Two Radiographs.....	81
Photogrammetry.....	85
<i>Multiple perspectives and calculated dimensions</i>	<i>85</i>

<i>Software advances: digital imaging and computational algorithms</i>	86
<i>Photomodeler: An off the shelf software possibility</i>	87
<i>Recommendations for future research and applications in 3-D analysis</i>	91
Case Studies - Examples of Field Projects Using Digital Radioscopy	91
St. Anne’s Church, Prague – Examination of Medieval Roof Framing.....	91
St. Bernard’s Episcopal Church – Hidden Fasteners	93
New York State Capitol – Internal Construction and Failure Investigation	101
Summary	105
References:	108
Appendices	111
Presentations and publications discussing radioscopy by project staff.....	112
Radiation warning sign.....	113
X-ray setup form	114
Survey of state regulations regarding use of x-ray machines.....	115
State Radiation Control Programs.....	120

Introduction

The search for reliable means to investigate structures has coincided with advances in construction. As building technologies evolve, the search for better/more efficient investigative (structural investigation) methodologies also evolves. Most technologies used for structure inspection had their beginnings in other fields but were adapted to construction long after their discovery or development. X-rays are one such development.

Discovery of X-rays

In 1870 Sir William Crookes found that passing an electric current through a glass vacuum bottle with wires embedded at each end produced a purple light inside the bottle and a green glow outside (Wisehart, 1928). This phenomena was simply another unexplained scientific curiosity until Wilhelm Conrad Roentgen, at the University of Wurzburg in Germany, began experimenting with several types of vacuum tube, including the “Crookes tube” in the early 1890s (Nitske, 1971).

There are two common stories about the discovery of x-rays by Roentgen. The first is that while running experiments, Roentgen accidentally left a Crookes tube on and placed it on top of a pile of materials which included a book he had been reading. Inside the book was an antique metal key used as a bookmark. An unexposed photographic plate was under the book. After later use of the photographic plate outside and its subsequent development, the ghost image of the metal key was visible (Wisehart, 1928).

The second, more accepted, story places Roentgen in his darkened lab, using a Crookes tube, covered with a cardboard tube that blocked all visible light. In spite of the presence of the cardboard tube, when an electrical current was run through the Crookes tube, a barium-platinocyanide-coated screen began to glow across the room (Nitske, 1971; Brown, 2002). Roentgen found that when he held objects between the cardboard-covered tube and the screen, that varying amounts of energy were recorded on the screen, and in one image he saw the bones of his hand.

After the initial discovery, however it was made, it is known that Roentgen initiated seven weeks of detailed, meticulous experiments designed to validate his initial discovery and determine the nature of these previously unknown “x-rays” that could penetrate opaque matter. He discovered that x-rays cast shadows, like visible light, but questioned whether they obeyed the same reflection and refractions laws (Roentgen, 1896). He was able to record them on

both photographic plates and fluorescent screens (Nitske, 1971; Wiseman, 1928). These experiments, including the first human x-ray (a hand, reported to be his wife's, Figure 1) were done in isolation, with Roentgen sometimes even sleeping in his laboratory (Wisehart, 1928; Bleich, 1960).



Figure 1. X-ray of human hand, taken by Roentgen in 1895 or 1896, reported to be either his wife's hand (www.lixi.com/xray_history.htm) or that of Professor Albert von Kolliker, made at the first public lecture of the x-ray (Bleich, 1960).

Roentgen formally announced his discovery of x-rays in December of 1895. His first announcement was originally sent to the Wurzburg Physical-Medical Society (Roentgen, 1896). By January 1896, he made his first public presentation to the same organization and had also sent the report to colleagues across Europe. By mid-January, newspapers in the U.S. had reported on the new discovery, with headlines such as "New Light Sees Through Flesh to Bones" (University of Pennsylvania, 1993), and cartoons such as the one in Figure 2, reproduced from Life magazine (Life, 1896; Lang and Middleton, 1997).

The uses of this discovery quickly became obvious to the general public. Since the equipment necessary to create and record or measure the rays was easily available, it was rapidly put to use. For example, the two most familiar modern uses of x-rays that almost everyone has experienced are medical x-rays and baggage inspection at airports. Within a few months after the announcement of their discovery, x-rays were being used on human subjects to identify problems such as bone fractures and kidney stones. In June of 1896, only six months after the announcement of their discovery, x-rays were being routinely used by physicians to find and remove bullets from wounded soldiers (University of Pennsylvania, 1993). And as early as 1897, European Customs Inspectors were using x-ray inspection of baggage at the Brussels railroad station (Bossi et al,

1985). Innovative uses quickly followed, when in 1898 Dr. Charles Leonard produced radiographs of a Peruvian mummy (Lang and Middleton, 1997).



Figure 2. Cartoon from *Life Magazine*, February, 1896 issue, with caption: The New Roentgen Photography, “Look Pleasant Please”.

While credit is generally given to Roentgen for the discovery of x-rays, it is interesting to note that Nikola Tesla conducted experiments on visible and invisible rays long before Roentgen presented his findings in 1895 (Cheney, 1981). Research into Tesla’s work in the 1940s found that a photograph of Mark Twain taken by Tesla using a Geissler tube also showed the adjusting screw of the camera lens. This, in fact, was likely the first x-ray taken in the U.S.

In the U.S., Thomas Edison took up the investigation in an attempt to develop x-ray equipment that could be widely used. He eventually developed a hand-held fluoroscope but was unable to develop a commercial x-ray lamp, his true dream for this technology (Josephson, 1959). Other investigators quickly jumped on the bandwagon and throughout the early decades of the 20th Century, x-rays were being used widely not only for medical purposes, but also for a variety of industrial uses such as steel manufacture, foundry practices, railroading, and the production of electrical equipment. X-rays were even used to fit shoes, find grit in chocolates and sort fresh eggs (Wisheart, 1928; Bleich, 1960).

Unfortunately, the radiation hazard present in many of these uses, especially medical uses, was generally unrecognized at this time. Thomas Edison damaged his eyes from exposure to x-rays (Josephson, 1959). As late as 1928, a discussion of medical uses showed that often the patient was in front of an x-ray tube for extended periods while doctors watched the movements of the digestive organs or a beating heart (Wisheart, 1928). However, as early as 1896, Nikolas Tesla had lectured on safety when operating x-ray equipment (Cheney, 1981). He also reported his observations on the dangers of x-rays.

Today, the potential hazards associated with the use of x-ray technology are well known. Industrial applications are controlled so that radiation exposure is minimized, medical applications carefully monitor exposure of the patient, and all states have requirements that control the use of any radioactive substances or x-ray source. In spite of potential radiation hazards, uses of x-rays have continued to expand since their discovery. X-rays have been invaluable in solving esoteric problems, including analyzing ancient Egyptian artifacts and detecting forgers of currency and art (Lang and Middleton, 1997).

The Physics of X-Rays

What, exactly, was it that Roentgen discovered in 1895? These invisible rays that penetrated through solid matter had led to a great many science-fiction-type speculations. For instance, lead-lined underwear was developed to forestall peeping toms when the eventual x-ray glasses would be developed (University of Pennsylvania, 1993).

It turned out that x-rays are simply another form of electromagnetic radiation, similar to light and heat. But if these x-rays are simply electromagnetic radiation, why do they penetrate matter? The answer lies in an understanding of all forms of electromagnetic radiation.

In the 1860's, James Clerk Maxwell produced the four equations that define electrodynamics. These remarkable equations brought together for the first time the study of electricity, magnetism, and light. Maxwell showed that all types of electromagnetic radiation were simply mutually perpendicular, fluctuating electric and magnetic fields. This radiation is characterized by both a wavelength (λ) and a frequency (f), related to the speed of light in a vacuum as:

$$c = \lambda f$$

where c is equal to 3×10^8 meters/second. This equation shows that the wavelength of light is inversely proportional to its frequency. Figure 3 shows the types of electromagnetic radiation as both a function of their wavelength and frequency. Note that radio and infrared radiation have wavelengths longer than that of visible light with lower energy for individual photons, while x-rays and gamma rays have shorter wavelengths (and thus greater frequencies), and have greater amounts of photon energy.

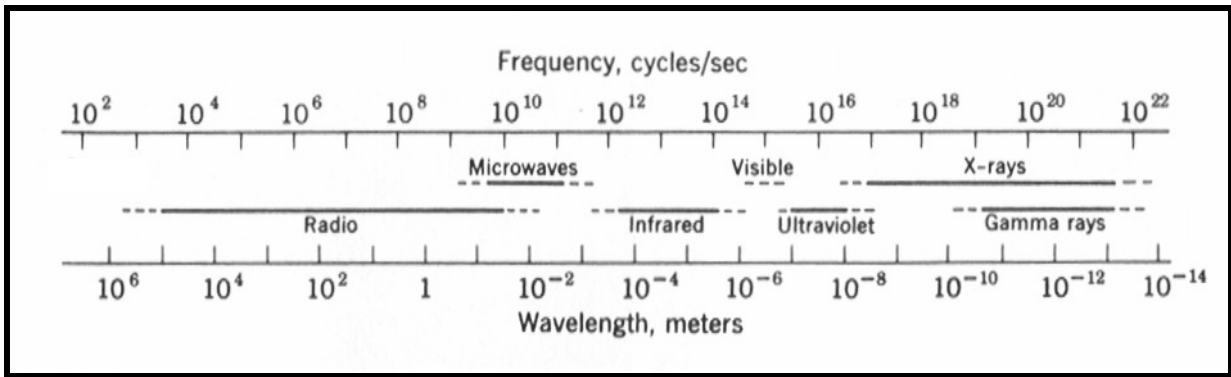


Figure 3. The electromagnetic spectrum, using logarithmic scales (from Halliday and Resnick, 1970).

This energy relationship is defined as:

$$E = h c / \lambda$$

where h is Planck's constant, and the energy (E) of individual photons is measured in electron-volts (eV). The smaller the wavelength (and thus greater the energy), the more likely the radiation is to penetrate matter. If you hold your hand up to a bright light, you can see some light coming through the edges, and they seem translucent. But even low energy x-rays easily penetrate human bodies, while high energy x-rays and gamma rays can only be stopped by several feet of concrete or a few inches of lead (EPA website). This differential absorption is what makes x-rays useful for investigations. X-rays of a given wavelength (or small range of wavelengths), may easily penetrate a wood beam, but are preferentially absorbed by the nails attaching the beam to the rest of a structure. Thus the final image (produced either on film or a fluorescent screen) will have light areas corresponding to less-dense material, where most of the energy is transmitted, and darker areas corresponding to heavier materials, where most of the energy is absorbed.

X-rays are subdivided by wavelength, with soft (or lower energy) x-rays having wavelengths around 1 to 10 Angstroms (one Angstrom is 10^{-10} meter) while very hard x-rays have a wavelength around 10^{-3} Angstroms. The x-rays used for this research are soft x-rays, produced at 150 kV, with wavelengths of highest intensity at about 0.13 Angstroms. This energy is approximately equivalent to that produced by medical x-ray equipment, which typically produces x-rays at 40 to 140 kV. As such, safety concerns using the x-ray source are minimized compared to radioactive sources of x-rays.

The intensity of a beam of x-ray photons is a measure of the energy per unit time per unit area produced by the beam of x-rays (for example in watts/square meter), and can be calculated in a variety of ways. The intensity of an x-ray

beam obeys an inverse-square law. That is, as the distance from the x-ray source is doubled, the intensity of the beam is reduced by a factor of four. This allows for simply increasing the distance between people and the x-ray source as a means of increasing safety when operating equipment in the field.

Closely related to the intensity of radiation is the idea of a radiation dose, or units of radiation exposure, usually defined as the energy deposition per gram of absorber (such as human tissue). Both the RAD (Radiation Absorbed Dose) and REM (Roentgen Equivalent Man) are units typically used in the U.S. to define appropriate limits for exposure to radiation. The RAD is equivalent to 100 ergs of energy per gram of absorber. The REM is equal to the RAD multiplied by QF (the Quality Factor). This factor accounts for the relative biological effectiveness of different types of radiation (including alpha and beta radiation, which are not electromagnetic radiation). The QF for x-rays is one, however, so the units are equivalent for our discussion.

How does this relate to someone using x-rays to investigate a structure? The Whole Body Occupational Dose limits for an adult are set by the Environmental Protection Agency (EPA) as 5 REM (5,000 milli-REMs or mREM) per year. For comparison, a typical adult living in Colorado (at an elevation between 5,000 and 6,000 feet), married, that takes at least 3 airline flights per year and watches TV receives a typical dosage of about 400-450 mREM per year (EPA website). A dental x-ray is usually 2 to 3 mREM, while the total exposure of each technician during this course of experiments totaled less than 15 mREM over 8 months. Monitoring radiation is discussed in the safety procedures section.

Portable X-ray Equipment

To produce the digital radiographs used in this research, two portable x-ray systems were used. These systems used the same x-ray source but had different imaging systems. One imaging system, the RTR-4TM imaging system from SAIC®, produces real-time digital radiographs, with technology somewhat equivalent to a digital camera. The other imager, the EPIX Digital Imaging System by Logos Imaging, uses a reusable plate which creates fluorescence when x-rays impinge on the surface, similar to x-ray film. This imager plate is then scanned for 3 to 7 minutes for the digital radiograph to be viewed. The x-ray source, the Golden Engineering XR200®, and both types of imagers are discussed in detail below.

XR200® X-ray Source

The source used for this study is an XR200® x-ray source, manufactured by Golden Engineering, Inc. This source is a pulsed source, producing x-ray pulses of short duration (60 nanoseconds each) and minimal dose (3.1 milliroentgens for each pulse at a distance of 12 inches from the front of the unit), with energy up to 150 kV. The aperture size is 1/8 inch (3 mm), and the beam produced by this source has a 40° beam angle, so that x-rays taken about two feet from the source have a spread equal to the width of the imager. For each x-ray, the number of pulses can be set from 1-99. One to two pulses are required to penetrate paper and four to twenty are typically used to penetrate most wood walls.

The battery-operated source is quite portable and easy to use in the confined spaces of historic buildings. It is 4.5 inches wide, 7.5 inches tall, and 12.5 inches wide, and weighs 12 pounds. It is powered by a 14.4 volt DeWalt® removable, rechargeable nickel-cadmium battery and can, therefore, be used in buildings with no source of electrical power. The base of the source unit has a threaded tripod mount that can be used with a standard photographic tripod.

Safety issues are always a concern when using x-rays. This unit has a variety of safety features. It should be understood that the unit itself is NOT radioactive! X-rays are only produced when pulses are generated, due to the introduction of an electrical potential across the vacuum tube (just as light is only produced when the electricity is turned on for a fluorescent fixture). The low dose of each pulse and the ability to create a specific number of pulses allow for an individual to work with the minimum amount of energy necessary to accomplish the investigation. Leakage from the unit while it is working is limited to 10 milliroentgens per 100 pulses on the sides of the unit, three inches from the center, and three milliroentgens per 100 pulses two inches behind the unit. Since x-ray radiation has an inverse-squared relationship between energy and distance, individuals standing in a safety zone more than 10 feet behind the unit when it is working are protected. The final safety feature is the key to the unit. The XR200® will only work when the key is inserted in the top. This allows the operator to always have the key in his or her possession so that the unit will not accidentally discharge while shots are being set up.

RTR-4™ Imager

The RTR-4™ portable digital x-ray imaging system (Figure 4) was manufactured by SAIC® (Science Applications International Corporation). This system is a fully digital imaging system that includes its own image modification tools. The system is composed of a control unit (which can be a laptop computer), the imager, and cables which connect the imager to the controller. The imager is a

compact, solid state camera with an 8.0- inch by 10.7-inch field of view. It measures 7 by 11.75 by 13.25 inches, and weighs 10 pounds. It is typically mounted on a tripod or placed directly against the surface of the object of interest, opposite from the source. As with all portable x-ray systems, access to both sides of the object of interest is required. The imager's electro-optical system captures the images and transmits them to the control unit, where they are stored as TIF images. Individual images are 304 kb in size, containing up to 65,535 (16-bit) pixels.



Figure 4. The RTR-4™ portable digital x-ray imaging system, manufactured by SAIC®, with the XR200® x-ray source, manufactured by Golden Engineering, Inc. in the foreground (photo from SAIC website: www.saic.com/products/security/rtr4n/rtr4n.html).

This imaging system generates digital radiographs in real time so that the images are essentially instantly available for viewing. It is easy to move the imager when the area of concern is not included in the original image. Similarly, it is easy to shift the imager along an object (say a beam or wall) to make sequential radiographs. The need for cables to connect the imager to the control unit can limit the ability to investigate hard-to-reach areas of a building (where it is not possible to extend the cables around a long wall for example). However, a cordless option, not used in this research, is available which could address this limitation.

The images, since they are TIF files, can be manipulated by any standard photographic-enhancement software. However, the control unit (or the software that is included for the laptop) includes a package that can also be used to enhance the images so that subtle details of the x-ray can be seen. This software includes not only the standard image-enhancement techniques (such as image sharpening and contrast stretching), but also features designed to assist

specifically with x-ray enhancement (such as edge detection algorithms and the ability to transmit all the grey tones of the x-ray into a full spectrum of colors).

EPIX Scanner and Imaging Plates

The second imaging system used in this research is the EPIX Digital Imaging System manufactured by Logos Imaging (Figure 5). This system is composed of the EPIX imaging plates, the EPIX scanner, and a laptop with software to import and save the scanned image. The imaging plates are reusable, photo-stimulatable phosphor imaging surfaces, either 8-inches by 10-inches, or 8-inches by 17-inches in size. To establish a reference point on the radiograph, a metal key should be taped to the plate cover to indicate the orientation of the plate against the object. The plates are composed of flexible plastic sheets coated with a very thin layer of tiny storage phosphor crystals bonded together. X-ray images are created on these imaging plates as the phosphor crystals capture the energy of x-rays passing through the object of study (Figure 6). This energy is stored in the crystals, and released by the process of scanning. However, the scanning process does not completely erase the image from the plate so the plates need exposure to light (usually about two minutes in the direct light) before they can be used again without seeing a ghost image from the previous shot. With care to keep the imaging plates stored out of the light and in their cases (to avoid scratching the coating), these plates are reusable indefinitely.



Figure 5. The EPIX Digital Imaging System manufactured by Logos Imaging (photo from Logos Imaging website: www.logosimaging.com).

The second component of the EPIX Digital Imaging System is the EPIX scanner. This machine, affectionately referred to as the “bread-maker”, is 15.5 inches high, 19.4 inches wide and 10.8 inches deep, and weighs 32 pounds. To mount the

imaging plates and insert them in the scanner, two carousels (one for each imaging plate size) are available. After exposure, the imaging plate is mounted on the cylindrical carousel (with care not to expose the photosensitive surface to much light) and inserted into the scanner. The scanner uses red laser light to cause the crystals to release their stored energy, which is released as blue light captured by the scanner. The scanning process can capture the image at either high or low resolution. The high resolution image, which takes about 7 minutes to process, is 300 DPI. The scanned image of an 8-inch by 17-inch plate at high resolution is about 24 MB. The low resolution image is half that and takes half the time to process. A newer version has been introduced since this research was conducted that cuts the processing time to 55 seconds. The laptop and software associated with the EPIX system capture the image as a TIF file. The EPIX software also allows for editing images.

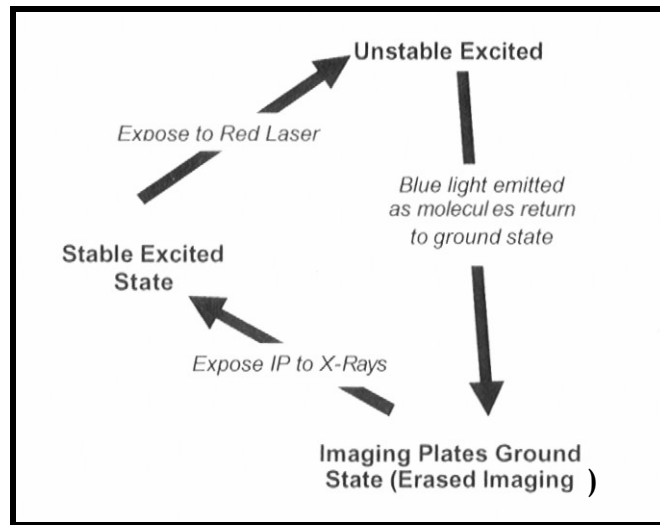


Figure 6. How storage phosphor imaging plates work (from Logos Imaging User Manual and Installation Guide, no date).

Comparisons Between the SAIC® and Logos Radioscopy Systems

These two imaging systems both produce high quality digital radiographs, are portable and have image editors which can improve and enhance digital image features as part of their software. Each also has advantages and disadvantages, depending on the application. With any radioscopy work, proper setup of the equipment in the field is paramount and key to generating useful images. The setup is also the most time-consuming aspect of field work. With setup being roughly the same for both systems (based on access and the logistics of the site), the following observations have been made when comparing the two systems.

The SAIC® system produces radiographs essentially in real time so more radiographs can be made in a short time relative to the Logos Imaging system,

with quick adjustments to maximize the imaged area. However, the resolution of the image is not as high as those using the Logos Imaging system. Also, the imager requires a source of power and placement of the relatively bulky imager with the necessary cables to the control unit can restrict its use in some locations.

The Logos Imaging system can be used in areas with no close source of power since the imaging plates are not connected to a control unit or the battery-operated source. The scanner and laptop controller can be located away from the setup, although this will increase the total processing time. The thin, flexible imaging plates inside their protective covers can usually be easily attached by means of thumbtacks or duct tape to relatively inaccessible areas. However, each shot requires that the imaging plate be attached on the back side of the object, exposed to x-rays, scanned, and then erased with strong light. This process is somewhat time-consuming and, therefore, allows for fewer radiographs to be generated in a given amount of time, relative to the SAIC system. However, with multiple image plates in use and a field assistant, this can be minimized. In many cases, a field assistant is beneficial simply because of overall productivity with setup, documenting setup and test parameters, and processing the images.

In general, if access to the back side of the object and location of power are not limitations in the field, and the contrast between materials being investigated is known to be good (say metal fasteners in a wood wall), the SAIC® system was found to be more efficient. If access to the back side of the object or power could be a limitation, or historic construction details are desired (with possibly minimal contrast between materials, such as mortise and tenon joints or wooden pegs used to join wood members), the Logos Imaging system was found to offer better resolution.

Safety Procedures

Although digital radioscapy is useful for examining structures without damaging them, radiation can damage living tissue. Generally, harmful effects are associated with radioactive sources or levels of exposure much greater than used with the equipment in this research. Nonetheless, prior to using the radioscapy equipment, it is important to understand the potential hazards to people.

Genetic effects, which are passed on to offspring, and/or somatic effects, which are experienced by the individual who is exposed are potential health risks. Somatic effects can be immediate and acute (sickness or death) under extreme exposure or delayed (the development of cancer or a decrease in lifespan).

Measurement units of radiation dosage are given in the table below. The severity of effects is a function of a number of factors, including:

- Cells can self repair and can keep pace with a certain amount of continuously administered radiation.
- Good physical condition may be a defense against radiation damage. Those in poor health are not as able to recover from radiation exposure.
- The type and energy of radiation controls the amount of damage. Beta particles and low energy x-rays will only damage the skin. High energy x-rays can penetrate deeper through the body and cause damage as they travel through tissue.
- The proportions of total dose and exposure time can have very different effects. It is safer to distribute a dose over time rather than through a single exposure. The concentrated one-time dose could be deadly, but spreading it over time can be better handled by the body. For example, “[i]f a person were to receive a dose of 500 Roentgens in one day, he would have less than a 50-percent chance of living. If this same dose were administered over a period of two months, the person would have a 90 percent chance of almost complete recovery.” (Field Radiography Employing Radiation Machines, Environmental Compliance & Health And Safety, Science Applications International Corporation (SAIC, no date, p. 5-6)

Table 1. Definitions Associated with Radiation Doses

<i>Gray (Gy):</i>	The SI unit of absorbed dose. One gray is equal to an absorbed dose of 1 joule/kilogram (100 RADS).
<i>Quality Factor (QF):</i>	The modifying factor that is used to derive dose equivalent (REM) from the absorbed dose (RAD). The QF for x-rays = 1.
<i>Radiation Absorbed Dose (RAD):</i>	The special unit of absorbed dose. One RAD is equal to an absorbed dose of 100 ergs/gram or 0.01 joule/kilogram (0.01 Gy).
<i>Roentgen Equivalent Man (REM):</i>	The special unit of any of the quantities expressed as dose equivalent. The dose equivalent in REMs is equal to the number of RADs multiplied by the QF (1 REM = 0.01 Sv).
<i>Sievert (Sv):</i>	The SI unit of any of the quantities expressed as dose equivalent. The dose equivalent in Sv is equal to the absorbed dose in Gy multiplied by the QF (1 Sv = 100 REM).

Site investigations using digital radiography require that a carefully organized safety plan be in place whether capturing images in the lab or in the field. This is especially important when individuals not associated with the investigation might be present, as with field work. The most important components of an adequate safety plan include:

- Operator training and radiation safety officer
- An individualized safety plan for the specific site
- Determination of safe distances
- Signage
- Source key protocol
- Monitoring for radiation exposure

Operator Training and Radiation Safety Officer

The operator must be familiar with not only the operation of the x-ray source but also the regulations of the state where the work is being conducted to comply with radiation safety requirements. Fortunately, most regulations are very similar so the learning curve is not significant once an operator understands the basic issues.

Training may be available through the company selling equipment, through state certifying agencies and contractors. A list of state requirements and training programs is available through: www.hsrdo.ornl.gov/nrc/ircertif.htm. The American Society of Nondestructive Testing (www.asnt.org/certification/irrsp/index.htm) also offers the Industrial Radiography and Radiation Safety Personnel training program.

At each job site, a radiation safety officer should be identified. This person should be trained in safe use of the equipment and should maintain the utilization and exposure records. He or she also serves as the contact for the state certifying agency. All operators of the equipment need to be trained to operate the equipment safely.

Safe Operation (Safe Distance, Signage, Source Key Protocol)

The safe operation of the equipment for a particular project should include:

- Defining the safe perimeter distance based on anticipated number of pulses and material being investigated
- Posting signage to warn the public in the immediate area
- Addressing line-of-site problems by using two people if the source and imager are not visible from one location

It is important to maintain a safe perimeter on both sides of the equipment and the item being examined. This is done by marking off the area with ropes or tape, using radiation safety cards and using a second person when both sides of the radioscapy testing are not in view. The second person will assure that the area behind the testing is clear of people. This is particularly important when doing field work where the other side of the area being examined is another room in which people may not be aware of the work being done.

Since the energy of the source decreases with increasing distance (the inverse square law), a safe perimeter around shot site can be determined based on the anticipated number of pulses required to generate an acceptable image. It is important to maintain a safe perimeter for all individuals not associated with the investigation (using signage or ropes) and to determine a safe distance from which shots can be taken by the operator. Radiation signs should always be posted around the area of the investigation. One example of such a sign is included in the appendix.

Records of each firing of the x-ray source need to be maintained including the number of pulses used, the distance and angle of the firing, boundaries and the type of shielding (if any) used. Some certifying agencies may want to inspect these records periodically. The records track the amount of exposure the operators may receive. The radioscapy form that Anthony & Associates, Inc. uses records the date, site, source number, test location, number of pulses, imager orientation, file name, photo number, and specific measurements (a sample set-up form is in the appendix).

The primary control of the XR200® source (used with both radioscapy systems) is a removable key that prevents firing the source without the key being inserted. As part of any safety plan, the key should always be in the operator's possession until the shot is completely set up. Only then should the immediate area be cleared, the key inserted and the shot taken, to avoid accidental discharge of the unit.

Monitoring for Radiation Exposure

Radiation exposure is obviously a concern when doing radioscopic examinations, and is the focus of the safety plan components identified above. Monitoring of radiation is important for both the operators and the site. Two types of monitoring devices were used during this investigation. The first were Pocket Ionization Chambers (PICs) from S. E. International, Inc., also known as pocket or pen dosimeters. They are used to determine exposure during individual x-ray operations. These 4.5-inch cylinders can clip on shirt pockets and are easy to use.

They read dosages up to 200 mREM and can be manually reset to zero for each x-ray session. They were also used to monitor for background radiation and any leakage near the source by positioning one immediately behind the source during the initial setup of each x-ray session. They are easily calibrated in the field and are typically read and recorded at the beginning and end of each session, at a minimum. Radiation dose limits are given in the table below.

Table 2. Employee Radiation Dose Limits

The dose limits for the following groups of individuals were addressed in a revised rule issued by the Nuclear Regulatory Commission in 1993.	
1.	Occupational Dose Limits for Adults
	Whole Body Dose Limits: 5.0 REM Total Effective Dose Equivalent/Year
	Organ Dose Limits: 5.0 REM/Year Stochastic, 50 REM/Year Non-stochastic
	Lens of the Eye: 15 REM/Year
	Extremities: 50 REM/Year
2.	Occupational Dose Limits for Minors
	The occupational dose limits for minors is 10% of the limits for adults.
3.	Dose Limits for the Fetus/Embryo
	0.5 REM, fairly uniformly distributed, over the period of gestation.
4.	Dose Limits for the Public-Uncontrolled Areas
	0.002 REM in any hour, 0.1 REM in any year.
(Source: SAIC, p.10-13)	

Long-term exposure to radiation was monitored using the more accurate Thermoluminescent Dosimeter badges (TLD badges), obtained from Landauer, Inc. TLD badges can be worn daily to monitor exposure. They should be provided to operators for use within controlled areas. Three types of TLD badges measure different types of rays:

- "K": For whole body exposures to x-rays, gamma rays, beta particles.
- "Z": For whole body exposures to neutrons, x-rays, gamma rays, beta particles.
- "U": For extremity exposures to x-rays, gamma rays, beta particles.

A new badge is provided for each individual every quarter and the old badge is returned, along with a control badge, for determination of cumulative dosage for

that quarter, year-to-date, and lifetime exposure (all in mREM). For smaller organizations, this service is also available on a bi-annual basis.

State Notification and Licensing Requirements

Portable radiology systems come under the purview of state regulatory bodies. Each state has a department, perhaps radiation safety or public health that sets the rules for operating the portable x-ray source. Most state regulations cover the operation of the source, not the operator (i.e., the operator need not be licensed). Although there is reciprocity between most states, one of the current limitations to widespread use of the portable x-ray systems for historic preservation is that each project requires that the operator must comply with the regulations for that state, usually accompanied with a fee for registration of the source. Some states require an inspection of the source before it can be used. Nonetheless, over the past decade, the ability to register the source in a state has become easier as procedures between states become more standardized and the use of the equipment becomes more widespread (usually for other applications, such as bomb detection and security work). Selected state contacts and radiation usage regulations are provided in the appendix.

Portable digital radiology generally comes under the heading of industrial radiography, defined below, in most states. State regulatory bodies may require: type of equipment, dates on the proposed work, purpose of the investigation, address, contact person with contact information, and unit licensing information. States may require also that equipment is registered with them prior to use. Prior notice may require a few days to two weeks. Some states may also require a copy of calibration certificates for the radiation survey equipment. Additional information on identifying the proper registration agency is given in the appendix.

Industrial radiography (IR) is the process of performing nondestructive testing of materials using radiation from a radioactive materials source or a radiation-producing machine. The potential for harmful radiation exposure to the industrial radiographer, to other workers, and to the general public exists if the radioactive material or x-ray machine is not handled properly. Statistics show that more radiation-related accidents occur in this industry than in any other. In an attempt to ensure that industrial radiographers are familiar with appropriate radiation safety procedures and thereby reduce the number of accidents, states and NRC have adopted regulations requiring industrial radiographers to attend a radiation safety course, complete a specified number of on-the-job training hours, and successfully complete a written examination prior to being certified. In order to facilitate the certification of industrial radiographers, 10 states and the American Society for Nondestructive Testing,

Inc. (ASNT) have nationally recognized certification programs. [Conference of Radiation Control Program Directors] CRCPD's G-34 Committee on Industrial Radiography is active in issues regarding IR certification. (Source: www.crcpd.org/IR.asp Page created 2/23/04)

Licensing

When purchasing portable low-energy x-ray equipment, regulations for licensing and operation vary by state. Initially, the manufacturer will notify the governing state's licensing authority to whom the equipment has been sold. It is the owner's responsibility to contact the proper state agency to learn the steps to register the equipment. Some information about certification and licensing is also provided with the equipment. Usually, registration with the state needs to be done within 30 days. An inspection of the equipment is also usually necessary. Many states provide a seal showing that it has been inspected.

The varied licensing and regulations use the *Code of Federal Regulations*, Title 10, Part 34, ("Licenses for Radiography and Radiation Safety Requirements for Radiographic Operations"), as well as guidance from the Atomic Energy Commission or U.S. Nuclear Regulatory Commission. Agreement states have agreed to provisions of the Atomic Energy Act of 1954.

Additional Resources on Regulations Governing Radiation Safety

The Conference of Radiation Control Program Directors (CRCPD) is a non-profit, non-governmental, professional organization of radiation professionals in state and local government who regulate the use of radiation sources. (CRCPD flyer 01/04 available on their website) This organization was established in 1968 with a two-fold purpose:

- To serve as a common forum for the many governmental radiation protection agencies to communicate with each other, and
- To promote uniform radiation protection regulations and activities. (CRCPD flyer 01/04)

Their website at www.crcpd.org provides links to state resources: "State Efforts: An Overview of What States Do" and Contacts for Radiation Control Fee Schedules. Their subcommittee called the G - 34 Committee on Industrial Radiography is working on recommendations to create a national industrial radiographer certification program. Currently, there are 10 states using the same certification process for industrial radiographers and /or radioactive materials.

The CRCPD website is useful as a quick place to check state contacts for information on regulations and certification programs. On their website there is a 50-state listing of the “State Radiation Control Programs: Industrial Radiographer Certification Contacts & Status”, updated in March of 2004. It provides a state contact with telephone and e-mail; provides the state’s status as an agreement or non-agreement state; states whether it is a radioactive material and/ or x-ray certifying entity; and finally provides notes for each state (please see table in the appendix). A December, 2005 update is available at: www.hsrp.doe.gov/nrc/rulemaking.htm

American Society for Nondestructive Testing (ASNT) is recognized by CRCPD as an independent certifying program. At www.asnt.org/certification/irrsp/cp-irrsp-1a.pdf is an overview on the requirements to get Industrial Radiography Radiation Safety Personnel certification. Forty hours of training and 120 hours of experience are required to take the examination.

Training

Most states want to know that the operator has received training in operating the x-ray equipment. Some require a training card from a state or supplier recommended trainer.

Survey of States

Phone surveys were done with Alabama, Colorado, New Jersey, New York, Oregon, and Virginia. The summaries of the findings describing the regulatory requirements for use of this equipment for historic preservation research are provided in the appendix. The summary identifies the governing agency, who to contact, what is required to bring radiography equipment into that state, and if there is reciprocity or the ability to use licensing from your home state.

Previous Use of X-rays in Historic Buildings

While medical and industrial uses of x-rays were rapidly developed once they were discovered, their use has not been widespread in the historic preservation community. Examination of structures with traditional x-ray technology using film and high-energy x-ray sources has been done for quite some time. However, due to safety concerns and the high costs involved, its use has been quite limited in historic preservation. As opposed to traditional film x-ray technology, use of digital real-time x-ray technology for structure investigation is quite recent.

X-rays emitted from traditional high-energy electromagnetic radiation sources are capable of penetrating most materials used for building construction. Depending on the material properties of the object being inspected, a photographic image is produced which reflects the density, thickness, energy absorption and chemical properties of the material. Digital, real-time x-ray technology offers significant advantages for assessment of historic structures over traditional x-ray techniques.

Real-time radiography, or radioscopy, originated in the late 1800s. Termed fluoroscopy, it provided a two-dimensional image of an object of interest immediately on a screen. Because of its portable nature and ability to produce "real-time" images, radioscopy, unlike film x-ray techniques, allows for easy manipulation of the test material during inspection, thereby allowing for better examination. Fluoroscopy had two primary disadvantages which limited its use: although somewhat portable there were safety concerns with the x-ray source and there was no means to store the image for later processing. Digital radioscopy does not have these disadvantages; advances in the technology make it safer to operate and it has the ability to store images. Perhaps, though, the most useful feature is the ability to post-process the x-ray image by zooming in on particular details and changing contrast, brightness or position.

Prior to the development of digital radioscopy, investigators had used similar low-energy portable x-ray sources for examining historic structures. Hart (1974) used x-ray analysis to examine the Narbonne house in Salem, Massachusetts. This house, the main portion of which was built in 1675, is described as "one of the few substantially unaltered half-houses of 17th C. Massachusetts" (Hart, 1974). The goals of the examination were to determine the presence and configuration of wall bracing, possibly identify original window framing, and determine whether some of the framing had once been an exterior wall.

Hart used a portable x-ray generator and Polaroid film in the field to conduct the examination. The examination successfully identified the configuration of hidden structural braces. Further, the technique showed the type of fasteners used (both cut and hand-wrought nails), types of wooden members present (irregular split lath, hoist and mortise shapes) and that the wood had no signs of decay. By examining exterior walls Hart was able to determine that no original window framing was present. The question of whether some of the framing had once been part of an exterior wall was inconclusive due to limited access with the x-ray equipment and modifications to the structure.

An additional question addressed by Hart's research was the timing of the gambrel addition to the half-house. On the basis of its style, the addition would likely date from the 1720s or later. However, cut nails found in the examination

show that the addition (or its attachment to the main house) could not be earlier than 1790, and the shape of the ceiling lath would date it to no earlier than 1820. One problem encountered by Hart (1974) was that the test was conducted during December, which made it necessary to use heat lamps to warm the film and processor to prevent inferior results. In spite of such difficulties, further work was conducted on x-ray inspection.

Hart (1975) published another article on x-ray examination of historic structures and listed the following features for an ideal nondestructive system for probing historic structures, most of which were not fully available until the development of digital radiology:

- Portability
- Easy operation
- Safety
- Easily interpreted results
- Results easily stored and retrievable
- Ability to penetrate all types of material encountered in buildings
- Low cost

In spite of the lack of many of those features at the time, Hart stated numerous advantages to the use of x-rays for structural examination:

- The ability to identify the physical condition of the wood
- The ability to do a structural examination of the building pattern
- The ability to identify types of building elements (studs, lath, nails)
- The ability to identify construction details for historical dating purposes

X-ray examinations of the House of Seven Gables (built in 1668) and other historic buildings were described by Wrenn (1976). Based on work conducted by Hart, Wrenn outlined the merits of using x-rays to assess the structural condition of wood in historic buildings. The ability to determine material conditions and construction details without disturbing the fabric of the structure was seen as the primary benefit. For example, Hart found decay in a summer beam and evidence of a ceiling repair in the House of Seven Gables; identified old mortise and tenon joints from a chestnut beam removed from a house in Bethlehem, Connecticut; exposed the decorative detail of a chair rail molding in the First Harrison Gray Otis house in Boston, Massachusetts that had been obscured by multiple layers of heavy lead paint; and identified an earlier repair to a stair landing in the Codman House of Lincoln, Massachusetts.

Wrenn (1976) noted that the technique was limited by the inability to take an x-ray straight through an object and get a clear image. He stated that the lack of depth found in an individual x-ray can be problematic.

Interest in the construction of the Delorme dome at Thomas Jefferson's Monticello led to an x-ray examination described by Harnsberger (1981). Jefferson had left no joinery details in his notes, just the cryptic comment that the dome was to be constructed "in Delorme's manner". This method of construction involved laminating two thicknesses of wood in short curved segments to create structural ribs for arches and domes. In his original book, Delorme described the details of the joinery using mortise, tenon, and wooden pegs. However, these sophisticated carpentry techniques may have been too complex for construction in late 18th century rural Virginia. It was impossible to know how the dome was constructed without removing original material from either the plastered interior of the roofing, so an x-ray investigation was found to be the most effective method to identify details of this historic building.

Polaroid film was used to record images taken through the domed roof (Harnsberger, 1981). A portable x-ray emitter (source) was mounted on a tripod near the dome ceiling while a receiver was placed above the exterior of the dome. Multiple x-rays were taken initially to determine the correct exposure to penetrate the wood, plaster, and lead-coated copper roof. Then x-rays were taken to "prospect" for a vertical rib. Once one was found, it was x-rayed in multiple frames from the top oculus to the base of the dome. When the x-rays identified a horizontal purlin, it was also x-rayed in multiple frames from its connection with the original rib to the next rib.

Harnsberger's x-ray work revealed an unexpected pattern to the rib construction. Instead of two thicknesses of wood, the inspection found four thicknesses of oak boards for each rib, each board attached to the adjacent one with short nails, and the whole assembly held together with longer nails. The purlins were toenailed to each rib using a wooden cleat, which was nailed just below the purlin. Unfortunately, wall thickness and construction details did not allow for an examination of the connection of the ribs either to the top oculus or the base. However, the examination did allow for an interpretation of Jefferson's use of Delorme's innovative timber framing system, using simpler nailing techniques available to local carpenters to replace the more complex joinery described by Delorme.

A discussion of other radiography uses in conservation is presented in the book by Lang and Middleton (1997). Few examples of application to wood are given but use of radioscopy on cultural materials and art show many potential applications to wood. For example, stereo-radiography provides three-

dimensional images of objects and showed promise for mapping the configuration of hidden joints in wood structures and artifacts (Halmshaw, 1995). Real-time digital imaging using radioscopy is ideally suited to this application.

Radiography has been used to determine the location or extent of deterioration in wood due to insects or decay. Frames of historic artwork have been examined with x-rays to show the presence of wood rot and insect damage (Lang and Middleton, 1997). The success of traditional x-ray imaging for this application shows promise for digital radioscopy once the capabilities and limitations of the technology have been more fully explored. That, in part, is the purpose of this research.

In 1996, Anthony conducted his initial investigation of portable real-time x-ray equipment to determine its applicability to timber structures. The investigation focused on the ability of the x-rays to penetrate wood and provide useful images that could be stored for detailed analysis. Starting in 1996 fieldwork has been conducted that identified technical and logistical issues which need to be addressed before this technology can gain widespread acceptance in the forensic engineering community. Some of those issues have been addressed in this research.

One means of introducing some of the issues that have been addressed in this research is by presenting a summary of a few projects where digital radioscopy was used by one of the authors (Ronald W. Anthony) prior to conducting this research. The purpose of giving these summaries to the reader is to bring some sense of the real-world problems for which radioscopy was found to have capabilities and limitations. It is these capabilities and limitations that drove the experimental design of this research.

Investigation of Metal Fasteners in Timber - Built-Up Timber Trusses

Concerns about load-carrying capacity led to an examination of connections in trusses in large military warehouses built prior to 1950. The original structural framing in the buildings consists of timber frames with built-up timber trusses as roof supports. Cracks present in some of the truss chords, diagonals and verticals initiated the investigation to verify whether any metal fasteners exist in the connections between wood members that make up the trusses.

A key question regarding structural integrity of the warehouses was whether metal fasteners were present in the connections in the built-up timber trusses. Although drawings of repairs to one warehouse were found that indicated split ring connectors were present, it was not known whether this joint detail had

been used in other warehouses. Therefore, digital radiography was used to examine the connections in selected warehouses to determine the presence of split rings; their size, number and condition; and the condition of the surrounding wood.

A test configuration for the bottom chord with a single-bolted connection is shown in Figure 7. This configuration was used for similar connections between horizontal truss chords and vertical and diagonal web members.

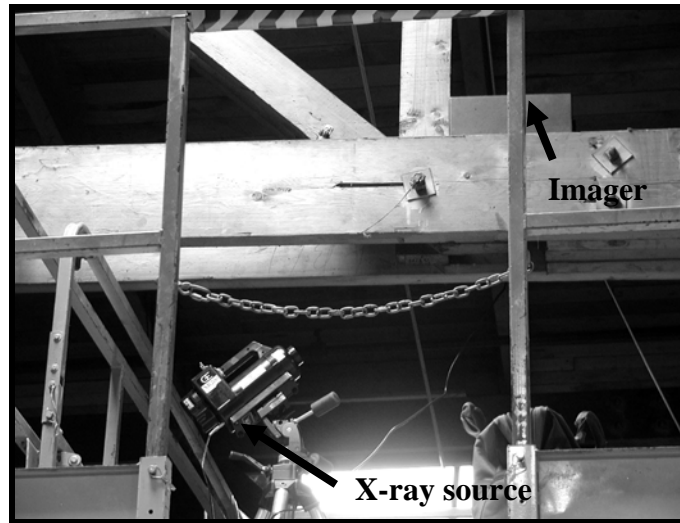


Figure 7. Test configuration for digital radiography of bottom chord with a single-bolted connection.

The radiograph resulting from the single-bolted connection is shown in Figure 8. Four split ring connectors are visible in the radiograph. Although a scale is shown in Figure 8 (and in other radiographs), direct measurement of a component on the radiograph is not precise. Radioscopy essentially projects a three-dimensional object onto a two-dimensional image, resulting in somewhat distorted sizes. Precise dimensions can be obtained using stereo-radioscopy and by measuring the distances between the x-ray source, the imager and the object of interest.

The bolt, visible in Figure 8, showed no evidence of corrosion as determined by observing the smooth, parallel edges of the bolt. The connections in the roof trusses used 4-inch split ring connectors. Joints with diagonal web members used four split rings while splices in bottom chords used only two. As was observed on the bolts, the radiographs showed that the split rings are in good condition and do not exhibit signs of corrosion or failure. Further, based on the radiographs, the wood adjacent to the fasteners is in good condition and has not deteriorated.

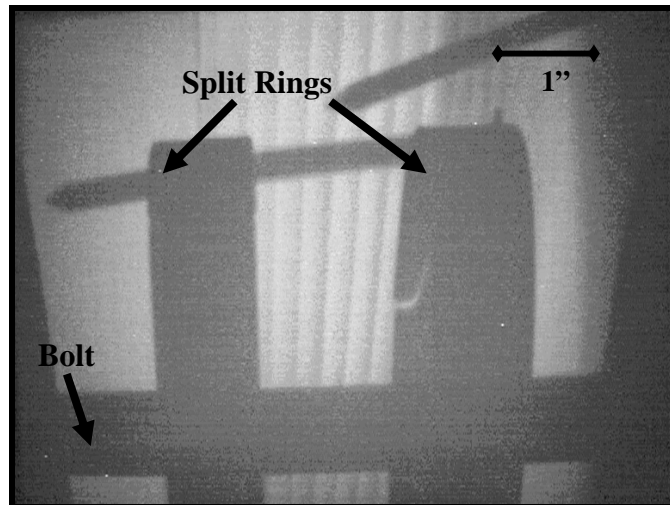


Figure 8. Radiograph of bottom truss chord, view from below.

Figure 9 shows the bottom chord of a repaired truss. The accompanying radiograph, given in Figure 10, shows that no split ring connectors were used in the repair. Further, the reason for the repair can be seen as a vertical fracture in one of the timbers. The head of the bolt securing the repair timber to the original truss chord is also visible in the radiograph.



Figure 9. Imager attached to repaired bottom truss chord.

This investigation was successful in identifying fasteners and the cause of a repair but raised several questions about how to best use the technology. The number of pulses that should be used, the optimum distance from the source to the object (the truss) and logistics of the setup (since the truss was accessible from a moveable lift with insufficient platform space for the operator to remain during firing of the source) were considerations for improving efficiency while in the field. All pointed to the need for limited lab testing to understand the

technological constraints as well as acquiring as much information about the object of interest and identifying access limitations before traveling to the field.

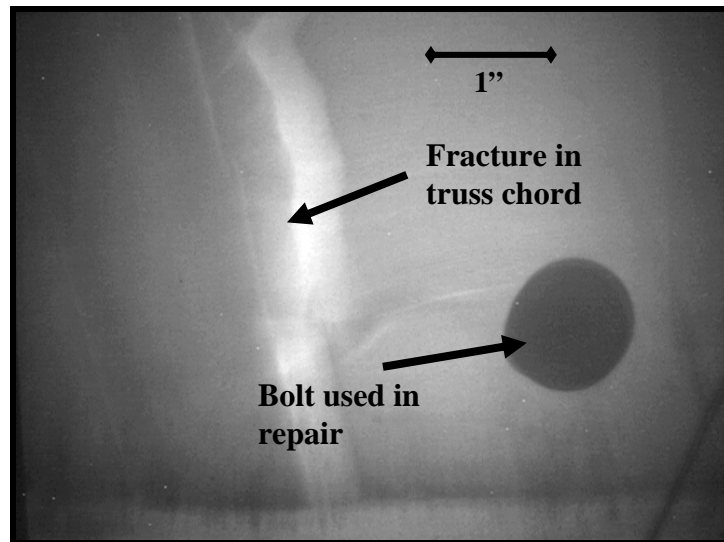


Figure 10. Radiograph of repair to bottom truss chord, side view. Note the fracture in the original timber (bright area).

Investigation of Metal Fasteners in Timber-Iron Rods Embedded in Beams

In 1997 the balcony on Pavilion I at Thomas Jefferson's Academical Village (Figure 11) at the University of Virginia collapsed. The cause of the failure was determined to be a corroded iron rod. Four rods supported the balcony from above. The ends of the rods were embedded in timber beams and not accessible for visual inspection.

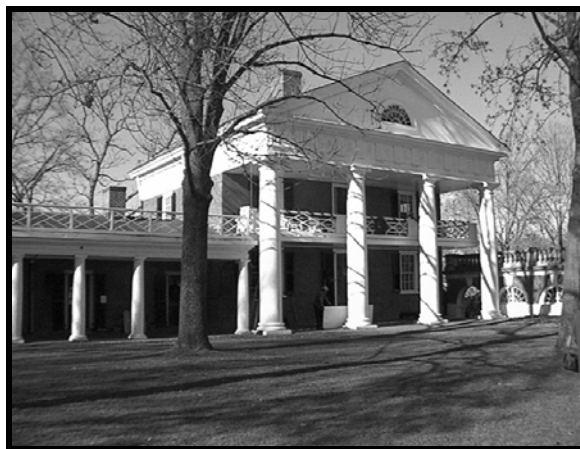


Figure 11. Pavilion I at the University of Virginia, after repair.

Post failure, digital radioscopy was used to determine whether corrosion of the iron rods could be detected. Figure 12 shows an iron rod embedded in a timber

beam in the same configuration used on Pavilion I. The rod was shown to have minimal surface corrosion as evidenced by the reduced cross section of the rod within the beam. The remaining cross section of the rod could be measured during post-processing of the radiograph data stored on a computer. Note the lack of a void in the wood surrounding the rod; a condition that might be expected if the corrosion was due to the presence of moisture.

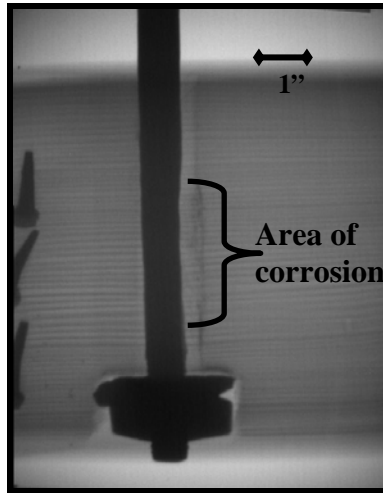


Figure 12. Radiograph of a corroded rod embedded in a timber beam.

This project reinforced the ability to distinguish materials with different energy absorption properties (iron versus timber). It did raise issues about whether deterioration of the wood could be accurately detected. Further, the presence of a “hot spot” at the center of the radiographs raised questions about information that may be hidden because of the higher level of transmitted energy at the center of the imager. The ability to transmit x-rays through steel plates and still detect either the presence of metal fasteners or details in the wood was verified but showed that significantly higher pulses were required to penetrate the steel plates.

Investigation of Metal Fasteners in Timber – Failure of Double Shear Joints

Digital radiography was used in a laboratory study to evaluate joints subjected to double shear loading, as if under seismic loading. The specimens were tested in the laboratory in accordance with ASTM D 5652 (1995) procedures. Radioscopy provided the means of assessing the failure mode of both nails and bolts without dismantling the joints. An example of double shear tests after failure is shown in Figure 13. While inspecting joints in a structure after a seismic event would be more cumbersome than imaging test specimens in the laboratory, the brief study verified that radioscopy could be used to aid in assessing seismic damage to historic structures.

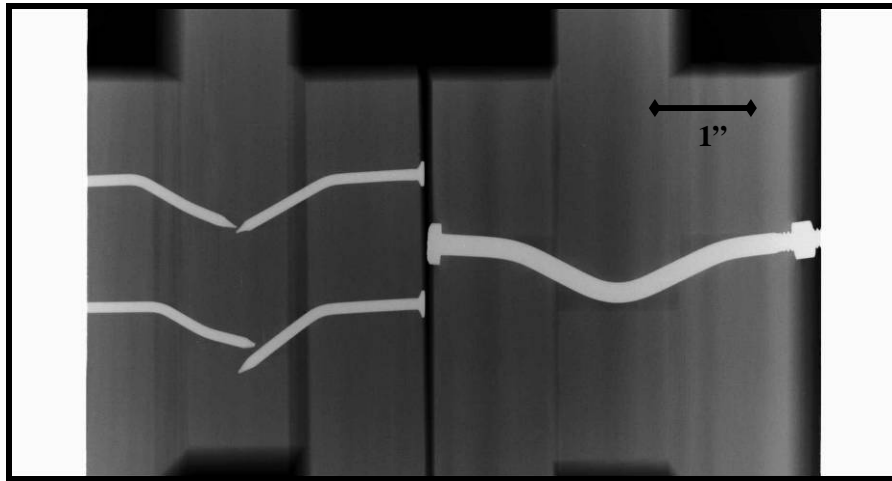


Figure 13. Radiograph of double shear tests of nailed and bolted joints (inverted grayscale).

Investigation of Deterioration – Simulated Termite Damage

Termite activity can result in catastrophic damage in timber structures. Infrared thermography and acoustic nondestructive methods have been used to detect termite activity but no suitable technique has yet been established to quantify the loss of material in a structural timber (Gilberg et al, 2003). Knowledge of the remaining sound cross section is crucial for determining load-carrying capacity and structural safety. Laboratory work was conducted to determine the feasibility of using digital radioscopy to quantify termite damage.

Quantifying deterioration can be accomplished using imaging processing techniques to distinguish subtle differences in measured x-ray intensity. Transmitted x-ray energy is recorded as intensity. Greater intensity measured at a given point implies less wood substance to absorb the x-ray energy. The loss of wood substance can be due to deterioration. By comparing the measured intensities on a radiograph, the extent of deterioration in wood members can be quantified.

Figure 14 shows a timber with simulated termite damage. Holes were drilled into the timber to generate profiles of known cross section. Radiographs taken of the test section were initially examined visually to determine whether variations in intensity due to the different volume of wood at each plane could be distinguished. The radiograph, shown in Figure 15, reveals that it is difficult to visually distinguish subtle differences in intensity. However, using digital imaging techniques it may be possible to identify differences in intensity that correspond to the remaining cross section at each plane. The current research, discussed later, examines existing data processing techniques and image

processing methods for the analysis of radiographs of termite-damaged wood that explore this possibility.



Figure 14. Simulated termite damage in timber.

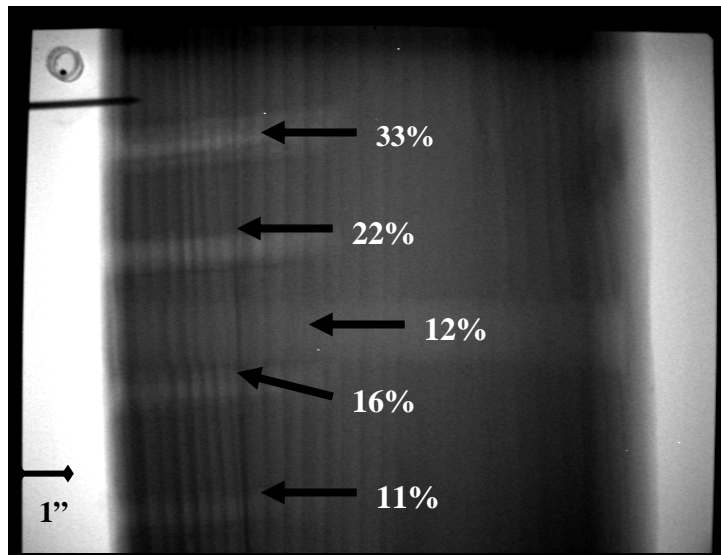


Figure 15. Radiograph of simulated termite damage showing measured loss of cross section at various locations.

This work emphasized the need for image enhancement if the goal is to quantify the extent of section loss due to termite attack. Since termites leave abrupt changes in the wood (either the wood is solid or missing), quantifying termite damage conceivably could be easier than detecting the gradual transition from solid wood to a void that is associated with decay fungi.

Noting the transmitted energy on a pixel-by-pixel basis could provide the means for detecting where a void was most severe but none of the available software

packages (including those that come with the radiology systems) have that capability today. The ability to colorize the image seemed to show promise but required a reference (sound wood) to allow for assigning a loss of section when viewed on a radiograph.

Investigating and Imaging Construction Details Non-Intrusively

In order to improve our knowledge of how most effectively to use x-ray equipment to assess the interior construction of walls and to produce radiographs that display the most information, laboratory radiographs were taken with a variety of setups. These were used to identify the most appropriate approach to address many situations confronting the preservationist.

To produce radiographs that display interior details of a given wall most effectively, multiple factors must be taken into consideration. These can broadly be grouped into three categories: the geometry of the setup, using the x-ray to optimize contrast and minimize distortion, and image enhancement. The first two factors can be employed to generate the most informative radiograph possible with the equipment available and the latter can be used to improve the radiograph to see subtle features or identify the relative position and size of components of the wall system.

Geometry

The geometry of the setup can dramatically influence the quality of the radiograph. To understand why, it is important to understand how components within a wall (the “object” of an x-ray, when discussed below) generate an image on a radiograph. If you think of the x-ray source as a light, then the image on a radiograph is the shadow cast by the object. All the characteristics of edge sharpness, size and distortion discussed below can be observed by standing in the bright light from a window and casting shadows on the wall opposite the light source.

The edge sharpness, or “fuzziness”, of a radiograph is partially controlled by geometry. If you have ever been in a room or outside with multiple overhead lights, you probably noticed that you cast multiple shadows. One large light source creates a shadow with fuzzy edges, in part because every portion of the light source is creating a shadow. Thus, the size of the light source can influence the sharpness of the image cast. On an x-ray source, this light source is the aperture. The smaller the aperture, the better. The XR200 has an aperture of 1/8 inch (3 mm), which minimizes the fuzziness effect. Given that the source aperture is small, but not a point, the multiple shadow problem can be improved

by reducing the distance between the object and the imager and increasing the distance from the source to the object. However, as the distance from the source increases, more pulses are required to penetrate the object due to the inverse square law. In essence, an optimum distance from source to object exists for every setup. However, without knowing all of the parameters or having unlimited time in the field, it is necessary to establish guidelines that can be used as a starting point for the field work.

Minimizing the distance between the object and the imager is important for several reasons. The closer the object is to the imager, the smaller the image of the projected object is on the radiograph, as it approaches its actual size (Figure 16). Because of the shadow effect at the edges due to the aperture size and diffusion of the x-rays, the object edges appear sharpest (less fuzzy) when the imager is closest to the object. Finally, by moving the imager farther from the object, the intensity of the x-ray is diminished (the inverse square law). All three of these effects can be seen in Figures 16 and 17.

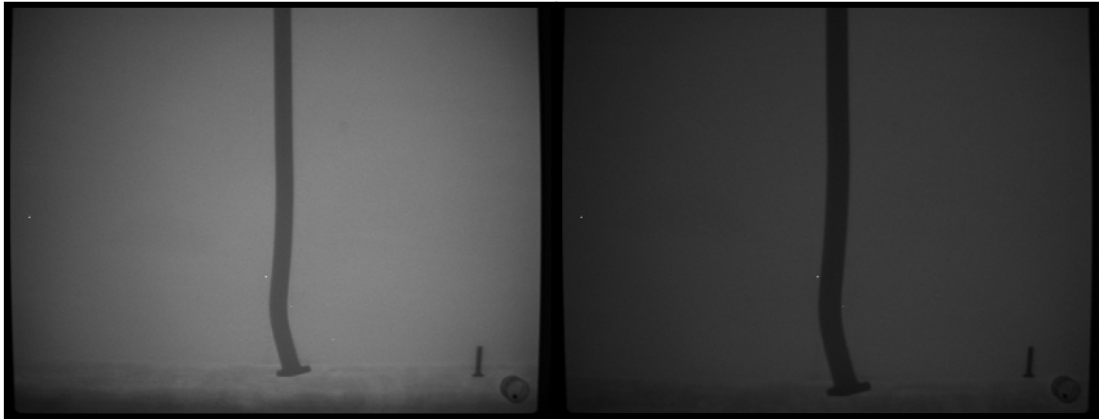


Figure 16. A 6-inch thick timber with a spike, x-rayed at 24 inches from the source using 50 pulses. Image on the left taken with the imager against the back of the timber while the image on the right was taken with the imager 8 inches behind the timber. Note the change in size of the spike and decreased intensity of the x-ray beam. The two objects in the lower right corner of the radiograph show the orientation of the imager.

If the object is perpendicular to the line between the source and the center of the imager, its shape will show little, if any, distortion (as in the middle screw in Figure 18), but if it is at an angle (such as the screws on the right and left in Figure 18) the portion of the screw closest to the source will appear larger, creating distortion. The net effect is that the image appears to the observer as if one is looking at it from the direction of the source (i.e., the screw on the right below has the bottom coming toward the observer).

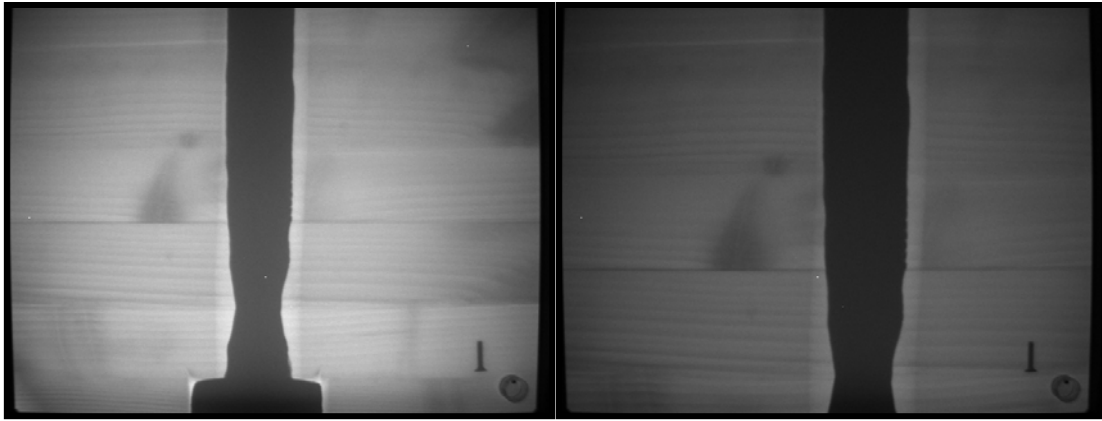


Figure 17. Rod embedded in 5-inch glued-laminated beam, x-rayed at 24 inches from the source using 32 pulses. Image on the left taken with the imager against the back of the beam while the image on the right was taken with the imager 8 inches behind the beam. Note decreased clarity of edges, especially the wood grain.

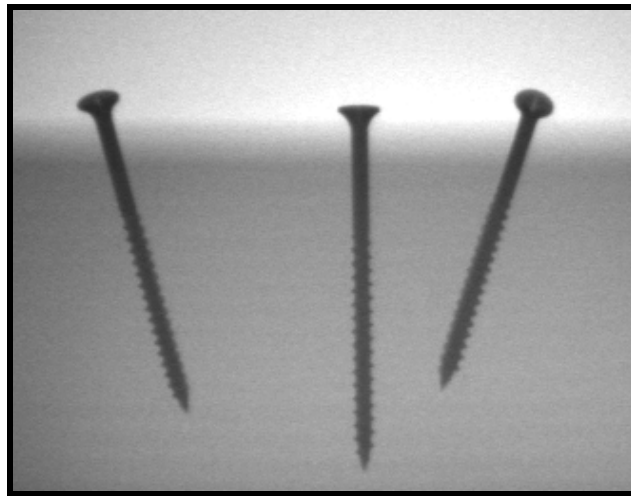


Figure 18. Three screws inserted into a 4-inch x 4-inch block at different angles.

Other changes in geometry, such as having the source and imager not perpendicular to one another, can create different kinds of distortion. The three images in Figure 19 demonstrate that as well. Using the same setup as in Figure 12, a 1/2-inch metal grid was attached to the outer face of the 4-inch by 4-inch wood block. Then, with the source at 24 inches from the block and perpendicular to it, the center radiograph was taken. The radiographs on the left and right in Figure 19 were taken with the source moved 6.5 inches to the left and right, respectively, and angled back toward the center of the block (always pointed towards the center screw). Note that the offset angles create a different sense of whether the screws are angled (the image on the left looks almost as though the screws are simply different sizes). Further, their arrangement relative

to one another appears to be different, even though the relative position of the screws within the block is unchanged.

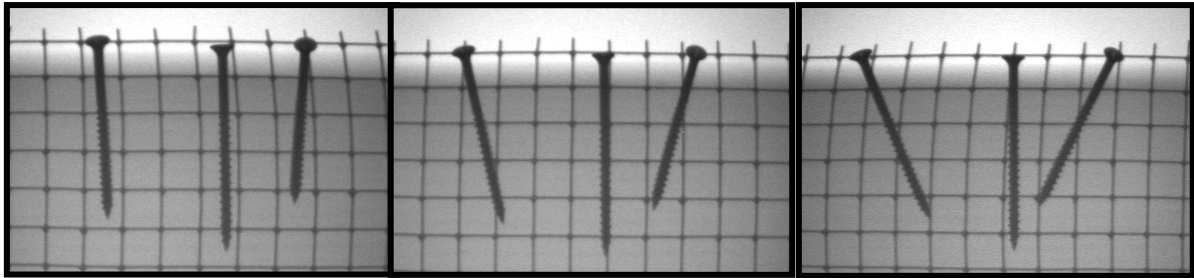


Figure 19. Three radiographs of three angled screws with a metal grid on the face of the block. Radiographs were taken with the source angled left of center, perpendicular to the board (no offset angle), and angled right of center.

As the distance between the source and object increases, the energy of the pulses per unit area penetrating the object decreases as the area of the beam increases. As such, there is an optimum distance to place the source from the object to maximize resolution and coverage of the object. To address this, objects of different thickness were x-rayed at distances of 12, 24 and 36 inches between the source and the object (in all cases, the imager was placed directly against the back side of the object to maximize contrast). A six-inch thick block of wood with an embedded spike was x-rayed at these distances, using 10 pulses (pulse number is discussed below).

As seen in Figure 20, the radiograph taken at 12 inches illuminates only the central portion of the imager. The details at the edges of the object (and imager) are not visible. The radiograph taken at 24 inches illuminates the entire imager surface (although the central portion is most exposed), while at 36 inches, the radiograph becomes grainy and has lower contrast. It is also much darker before post-processing due to the reduced energy of the x-ray beam with increased distance from the object). For most building inspection applications using these systems, the optimum source-to-object distance ranges from 18 inches to 24 inches.

From the above discussion, it is clear that the optimum conditions for creating clear radiographs are when the source, object, and imager are in parallel planes and positioned perpendicular along a single line of site. The imager should be placed directly on the back side of the object, thereby minimizing the distance between object and imager and maximizing contrast on the radiograph. Contrast is discussed below. The optimum spacing between source and object, when the object is a wall, is typically between 18 and 24 inches. This spacing allows the x-ray beam to fill the imager completely without losing detail along the sides and minimizing the number of pulses necessary to penetrate the wall.



Figure 20. A six-inch thick block with embedded spike, x-rayed at 12, 24, and 36 inches between the source and the block, respectively. All radiographs have been adjusted for brightness and contrast to improve viewing in the report.

Producing Contrast

After geometric concerns are addressed, generating high-quality images requires an understanding of the final contrast produced in a radiograph. This is a function of the composition of the materials to be examined, primarily the density and thickness. Contrast is also affected by the type of radiation used to penetrate the object and scattering of the beam. With the equipment used in this research, the investigation was limited to studying the appropriate number of pulses to use for a variety of situations. The limitation was because the 150 kV source produced x-rays over a fixed range of wavelengths.

A series of tests were run using individual blocks and test walls with different numbers of pulses, placing the source 24 inches from the object. Figure 21 shows the results of over and under exposure. At 10 pulses, little of the wood grain or the boundaries between boards are visible, while at 50 pulses, only the rod has not been “washed out” in the center of the radiograph due to over exposure.

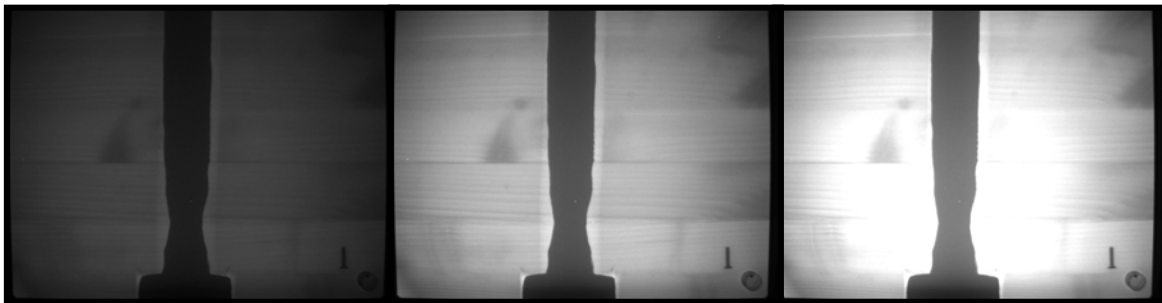


Figure 21. Steel rod in 5-inch glued-laminated timber with the source 24 inches from the timber. Shots with 10, 32 and 50 pulses, respectively (no image enhancement).

It could be argued that with post-processing, under exposure is not a problem. However, under-exposed radiographs can display loss of detail after post-processing. The six-inch block with an embedded spike, x-rayed using 2, 10, and 24 pulses is shown in Figure 22. With additional pulses comes clarity and definition of the difference between the wood block and the spike. Further, the wood features at the bottom of the radiograph are enhanced. All these x-rays were under-exposed and then post-processed.

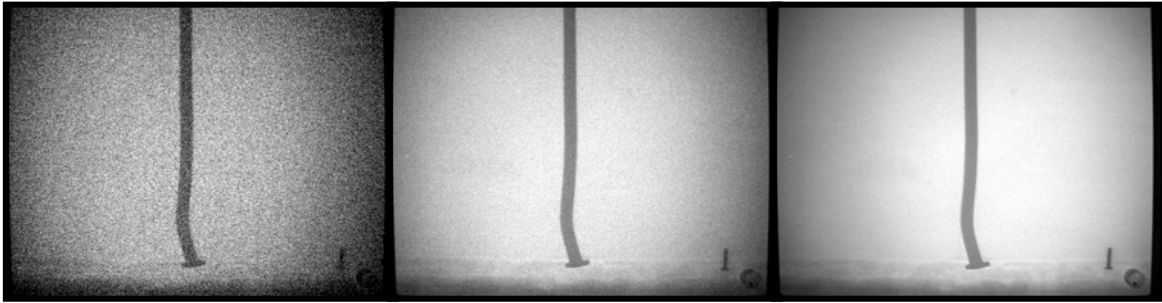


Figure 22. A six-inch thick block with an embedded spike, x-rayed using 2, 10, and 24 pulses respectively, at a distance of 24 inches from the source. All radiographs adjusted for brightness and contrast.

To determine a reasonable number of pulses for solid timber of varying thicknesses, a 10-inch-thick timber was notched into a stepped block with $\frac{3}{4}$, $\frac{1}{2}$ and $\frac{1}{4}$ of the original thickness (7.5, 5 and 2.5 inches thick, respectively). The block was x-rayed using between 16 and 100 pulses. Figure 23 presents three of these radiographs, showing the relative brightness and contrast for the various thicknesses of the stepped block.

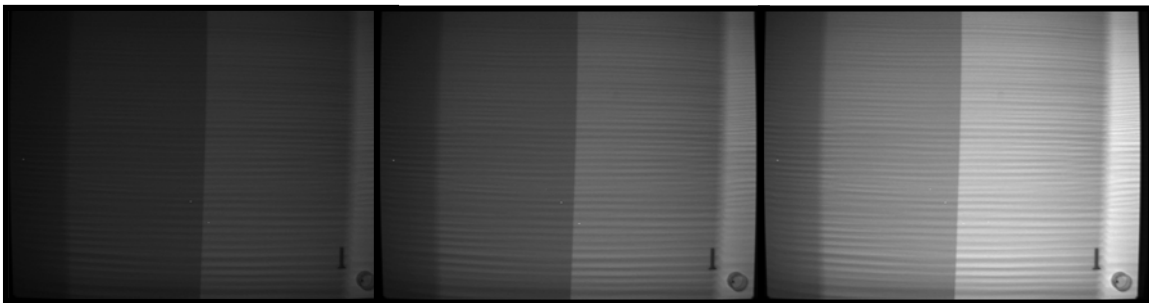


Figure 23. Stepped wood block, x-rayed at 24 inches, using 24, 50, and 100 pulses (no image enhancement). Thickness reduces from 10 inches to 2.5 inches from left to right of each image.

To determine a reasonable number of pulses for a typical wall constructed of 2-inch x 6-inch lumber and containing a variety of fasteners, a test wall was built. The addition of exterior and interior sheathing and siding were added to determine the number of pulses were required to penetrate the added features.

Figure 24 shows examples of some of the radiographs taken at 24 inches from the source to the wall surface, using a range of pulses. This wall had sheetrock on the interior and cedar siding over oriented strandboard on the exterior. Although not traditional historic materials, these materials were used because of the ease of changing the layup of the wall for different tests.

Using 16 to 24 pulses, the wall components are clear in the radiograph - all the screws, nails, metal clips and wires are visible; the wood grain in the 2 x 6 studs is clear, and even the overlap in the cedar siding is visible. At 8 pulses, some of these features are difficult to see, while at 40 pulses, features in the center of the radiograph are lost due to over exposure.

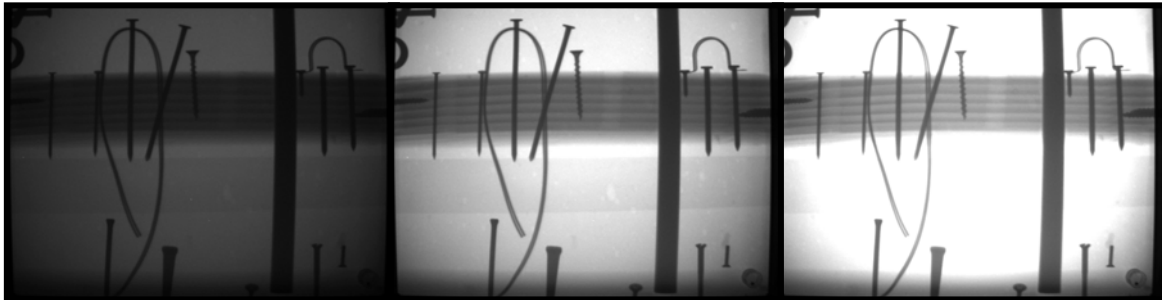


Figure 24. Radiographs of test wall with sheetrock interior and cedar exterior, 8, 24 and 40 pulses, respectively, no image enhancement.

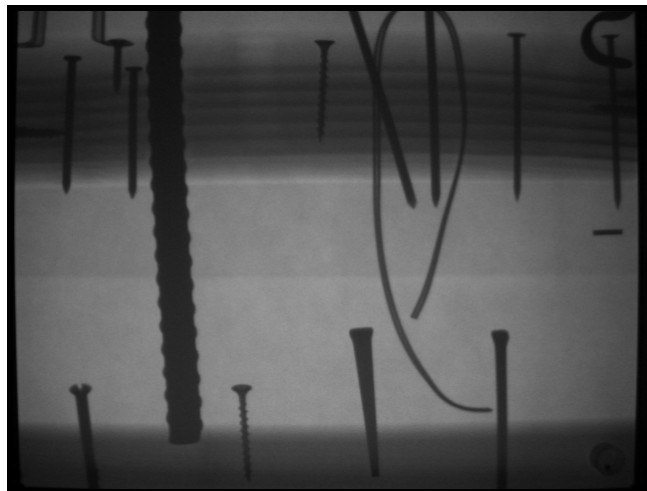


Figure 25. Radiograph of test wall with oriented strand board (OSB) and cedar siding, 10 pulses, no image enhancement.

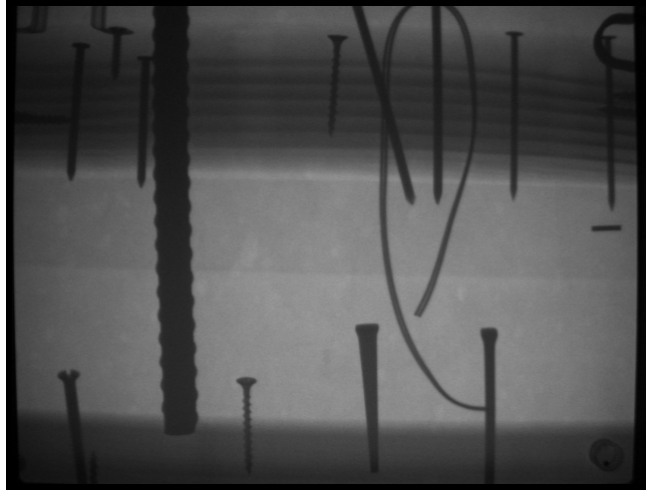


Figure 26. Radiograph of test wall with OSB and cedar siding, sheetrock interior, 15 pulses, no image enhancement.

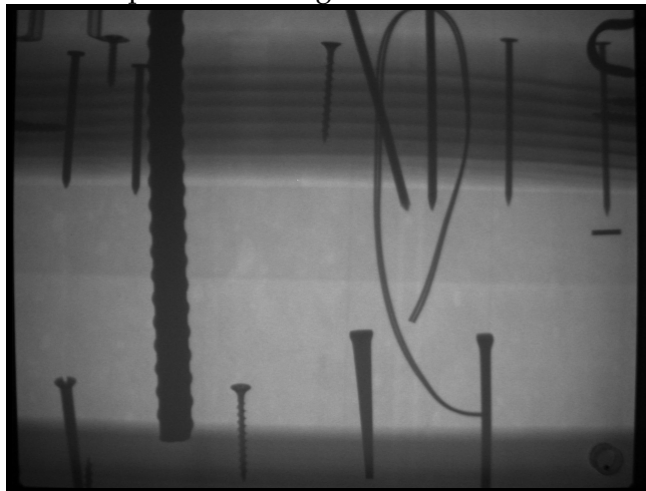


Figure 27. Radiograph of test wall with OSB and cedar siding, sheetrock and wood bead board paneling on the interior, 20 pulses, no image enhancement.

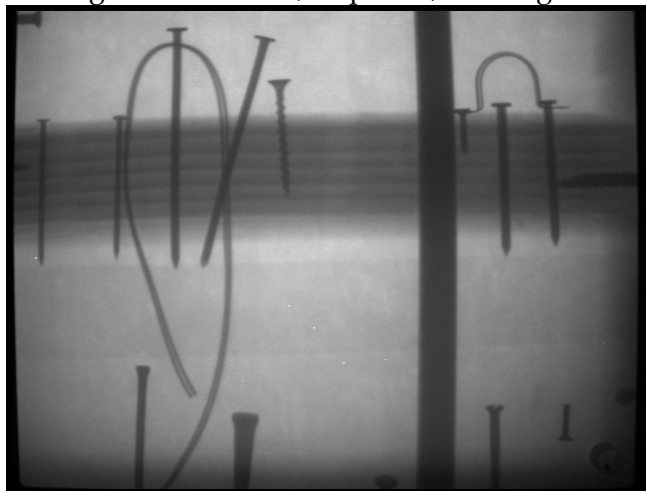


Figure 28. Radiograph of test wall with cedar siding, sheetrock and 1/2-inch-thick limestone veneer interior, 80 pulses, no image enhancement.

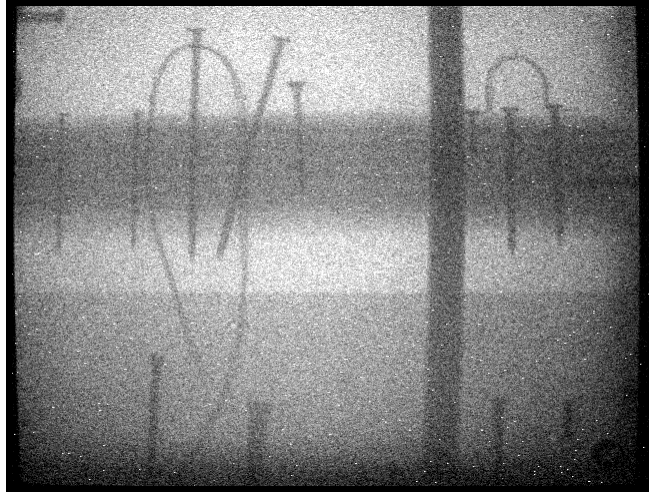


Figure 29. Radiograph of test wall with 6-inch limestone block facade, sheetrock interior, 300 pulses, adjusted for brightness and contrast.

In summary, the optimum number of pulses for most wood-frame wall constructions ranges from 6 to 30, depending on depth and wall components, unless masonry finishes are present. With a typical wood-frame wall, ranging in depth from 6 to 12 inches, initial radiographs can be taken using 10 pulses. An examination of the resulting radiograph will allow the operator to appropriately select the optimum number of pulses for the situation.

To more accurately refine the number of pulses needed, an examination of the histogram will help. The histogram is a graph showing the distribution of frequencies in an image. If the histogram is compressed to left, more pulses are required to produce optimum contrast. If it is compressed to right, use fewer.

Identifying the Location and Condition of Fasteners and Connections

Once a radiograph is generated to optimize contrast, the internal components of walls, individual timbers, or other structures can be examined in more detail. Identifying the location and condition of metal connections in a wall made predominately of wood is relatively straightforward because of the high contrast between the two materials. Wood connections, such as mortise and tenon joints, dovetail joints or wooden pegs, are more subtle features that may require image enhancement techniques to visualize on the radiograph.

Metal Connections

In many of the examples given above, metal fasteners were evident in the radiographs. Because of the high contrast between the metal and the

surrounding wood, inclusion of metal fasteners allowed for comparison of radiographs using different pulses, distance and wall construction. In fact, much of the research to examine fasteners coincided with the work discussed above. For purposes of illustrating the effectiveness of using radiography to locate and examine fasteners, a brief discussion follows.

Split ring connectors were shown in Figure 8, iron rods in Figures 12 and 17, nails and bolts in Figure 13, and screws in Figure 18. Nail types can be determined from the radiographs, which can be useful in identifying historic fabric or at least dating the period of construction. Hand-forged nails, cut nails, rosehead nails, and common wire nails are all easily distinguished in a proper radiograph. Thread patterns can be determined for screws, bolts and reinforcing rod.

Of equal significance to the historian or architect and perhaps greater significance to the structural engineer is the condition of the fasteners. Corrosion is often hidden within the timber and can lead to catastrophic failure. As is visible in the iron rod embedded in timber in the radiograph shown in Figure 17, the loss of diameter of the rod due to corrosion can be estimated.

Also useful for structural considerations, the connector spacing can be established when none of the fasteners are exposed. Figure 30 shows the nailing pattern in a granary crib wall. Using stacked lumber as the structural walls, no nails, bolts, or rods were visible that would indicate how the walls were connected. A simple radiograph quickly revealed the spacing of nails. Based on the known thickness of the wall, it was also possible to determine the length and diameter of the nails.

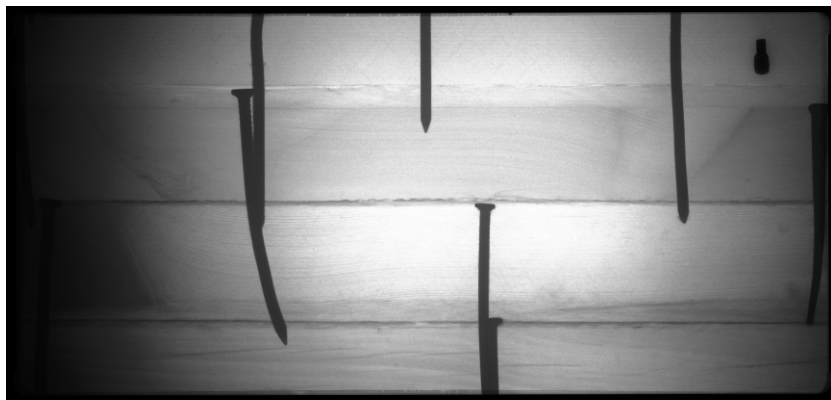


Figure 30. Radiograph of a stacked-lumber granary crib wall showing nail type and spacing. Note individual laminations of the stacked crib wall.

Examples of how radiography was used to locate and identify metal fasteners are given in the case studies section of the report.

Wood Connections

Easily locating and determining the condition of metal fasteners embedded in wood is possible, in part, due to the different densities of wood and metal. For wood connections, such as mortise and tenon joints, the interpretation of the radiographs is more challenging.

Laboratory and field research conducted on mortise and tenon joints showed that differences in the grain orientation of the mortise and tenon can be seen on a radiograph. A cross-hatched pattern is typically visible where the two pieces of wood overlap as the tenon penetrates the mortise.

Figure 31 shows the x-ray source in position to provide an image of a mortise and tenon joint in the field. Visible moisture stains raised concerns about the condition of this joint. Since this joint was between timbers with good access on both sides of the joint and, thus, it was easy to shoot perpendicular to the face of the timber, it was an excellent candidate for examining an all-wood joint. The radiograph of the joint is shown in Figure 32.



Figure 31. Mortise and tenon joint showing placement of x-ray source.

Note the light spot near the center of the radiograph, corresponding to a improperly drilled hole through the tenon. Figure 33 is an enhanced version of the radiograph that better illustrates the cross-hatch pattern indicative of two pieces of wood with the grain perpendicular to one another. Further image enhancement was able to show the wood grain in the beam with the mortise, verifying that the mis-drilled hole was in the tenon. There is more discussion of image enhancement techniques in a later section of the report.



Figure 32. Radiograph showing peg and improperly drilled hole in the tenon.

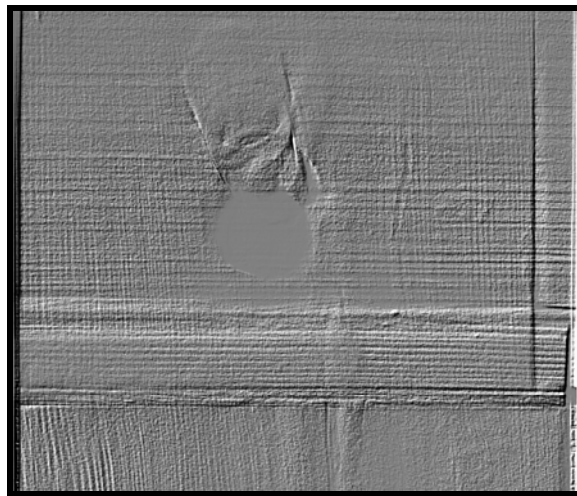


Figure 33. Radiograph shown in Figure 32, using image enhancement to better illustrate the wood grain of the tenon and the beam with the mortise.

The images shown above demonstrate the ability to “visualize” a mortise and tenon joint when it is possible to place the source and imager perpendicular to the face of the joint. Since many field situations do not provide such easy access, a mortise and tenon joint was evaluated in the lab to determine the effect of an angled alignment with the face of the joint. The timbers making up the joint were 6 inches by 5 3/8 inches and secured with two timber pegs.

The initial setup was similar to that described above with the source and imager perpendicular to the face of the joint (Figure 34). With the imager placed directly behind the joint, the radiograph shown in Figure 35 is generated. The size of the tenon, relative to the mortise, is readily visible, as are the knots in the beam and the pegs securing the joint.



Figure 34. Mortise and tenon joint.

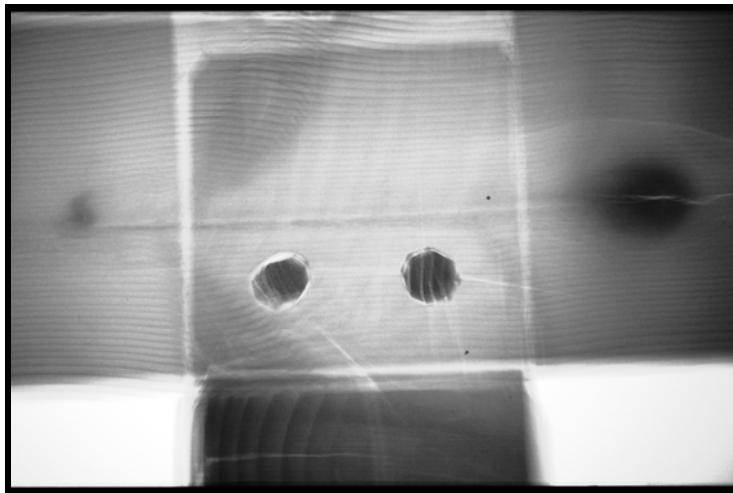


Figure 35. Radiograph of the mortise and tenon joint shown in Figure 34, as viewed from the back of the joint.

So how does the image change if it is not possible to be aligned directly with the joint, as would be the case if it was necessary to place the setup so as to examine a joint on top of a timber-frame wall? Visually, the joint would have the appearance shown in Figure 36. The corresponding radiograph is shown in Figure 37.

Although the images in Figures 35 and 37 are of the same joint, the affect of orientation of the setup is immediately apparent. Laid side-by-side, it would be impossible to know that the two radiographs were of the same joint. This reinforces the findings discussed in the geometry section regarding the significance of the setup. It also conveys the importance of documenting the position of the setup relative to a point of reference on the object (in this case, the joint). Photographs and a sketch showing distances and orientation of the setup

are critically important for accurately interpreting the radiographs after the field work is completed.



Figure 36. Mortise and tenon joint viewed at an angle from below the joint.



Figure 37. Radiograph of the mortise and tenon joint shown in Figure 36, as viewed from the back of the joint.

Identifying Wood Deterioration

The effect of decay, termites and mechanical damage in timber is often difficult to assess without extensive destructive tests. This phase of the research focused on the suitability of digital radioscopy for identifying internal deterioration in wood. Decayed timbers and logs and termite-damaged studs served as the research materials.

To assess whether the relative extent of deterioration could be determined visually, the wooden stepped block that was described in the Producing Contrast

section was used. The block, shown in Figure 38, represents a uniform increase in material at 25, 50, 75 and 100 percent of the thickness. The radiograph in Figure 39 does show increasing brightness from left to right as the thickness of the block decreases. Because the length of the block is greater than the length of the imager, only the edges of the thickest and thinnest sections of the block are visible in the radiograph.



Figure 38. Stepped block cut with 100, 75, 50, and 25 percent of the original block thickness.

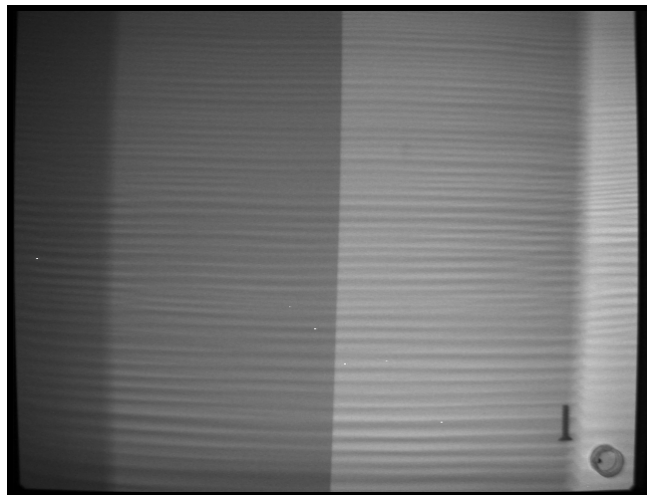


Figure 39. Radiograph of the stepped block with 100 percent thickness on the left, progressing to 25 percent thickness on the right.

Since the relative brightness is a function of the setup (distance from source to object and number of pulses), it is difficult to quantify the loss of thickness based simply on the grayscale image. Colorizing the image results in similar distinction, ranging from yellow for the section that is 100 percent of the block thickness, to green, then blue. For this image, the two thinnest sections of the block cannot readily be distinguished. Quantifying the loss of material in this

non-deteriorated block is not possible visually from either of the radiographs. With that knowledge in mind, examining decayed wood, which does not have the benefit of uniform boundaries between the different thicknesses of wood, is even more difficult.

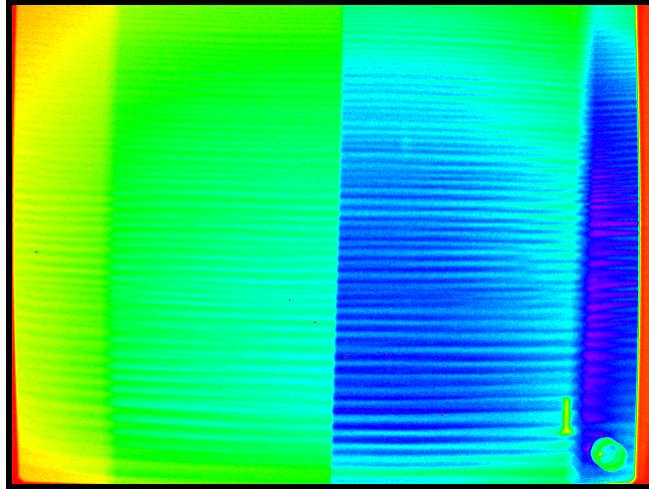


Figure 40. Colorized radiograph of the stepped block with 100 percent thickness on the left, progressing to 25 percent thickness on the right.

A decayed timber removed near the base of an old ice house served as an excellent object for radioscopy because one side was intact with no visible signs of deterioration (Figure 41). However, the back face was completely deteriorated and the thickness at any location could be measured (Figure 42).

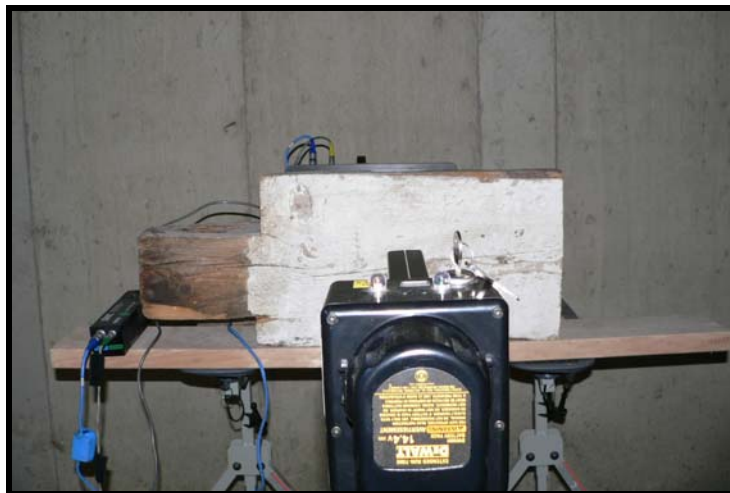


Figure 41. X-ray source focused on the solid face of a decayed timber.

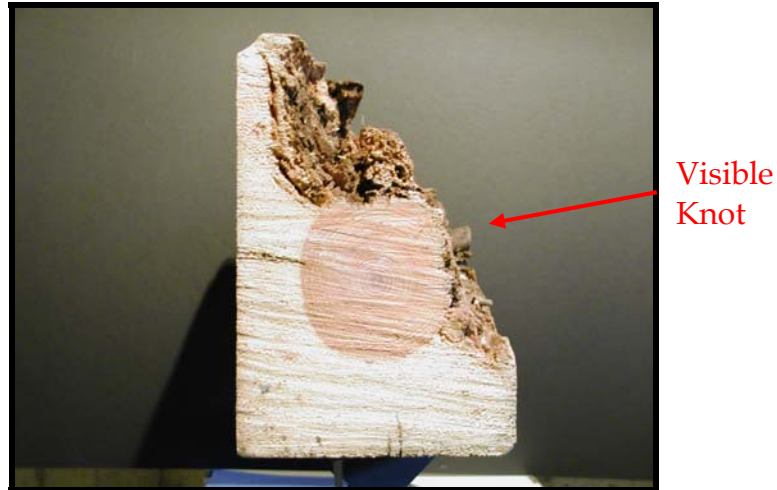


Figure 42. Cross section of the decayed timber. Note the location of the visible knot.

The radiograph as viewed from the face of the timber is shown in Figure 43. Note that in addition to the visible knot there are knots above and below the visible knot that are not visible on the photograph of the timber profile. Of more importance is that the radiograph is darkest at the bottom of the image where the timber is solid and lightest at the top of the image where the void is the most extensive. We can conclude from this image that there is less material at the top of the timber than at the bottom; however, we cannot yet determine how much material is missing.

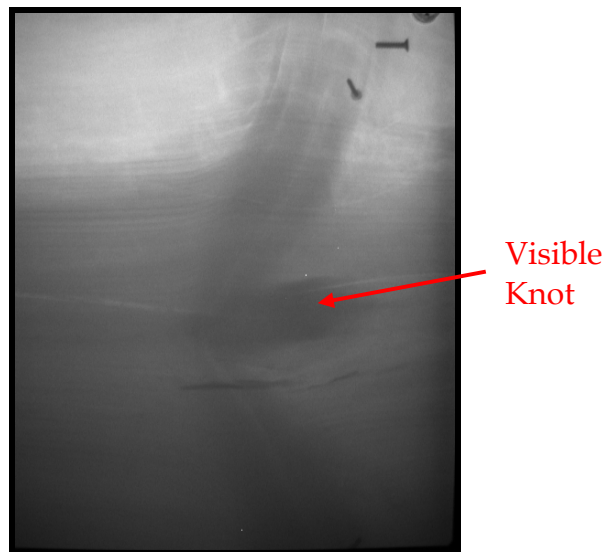


Figure 43. Radiograph of the decayed timber shown in Figure 42.

Colorizing the radiograph in Figure 43 makes it more obvious that the amount (thickness) of wood is not uniform from top to bottom. As discussed regarding the stepped block, the enhanced image still does not give us the means to quantify the loss of material, although the presence of decay is obvious.

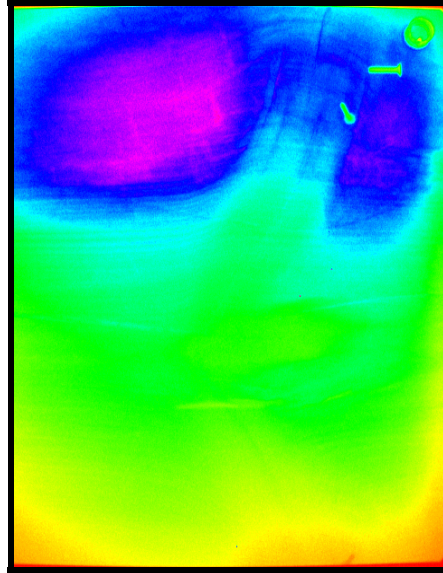


Figure 44. Colorized radiograph of the decayed timber shown in Figure 42.

Similar research was conducted on termite-damaged wood. A stud with termite galleries (Figure 45) was placed into the test wall with wood paneling on the interior of the wall and OSB sheathing on the exterior of the wall. The radiograph of the termite-damaged stud is shown in Figure 46. Note the similarity between the non-uniform color pattern in the radiograph of the decayed timber and the stud. Since termite galleries tend to be very irregular along the length of an affected piece of lumber, the color pattern is more ragged for the stud than the decayed timber. This allows us to differentiate between

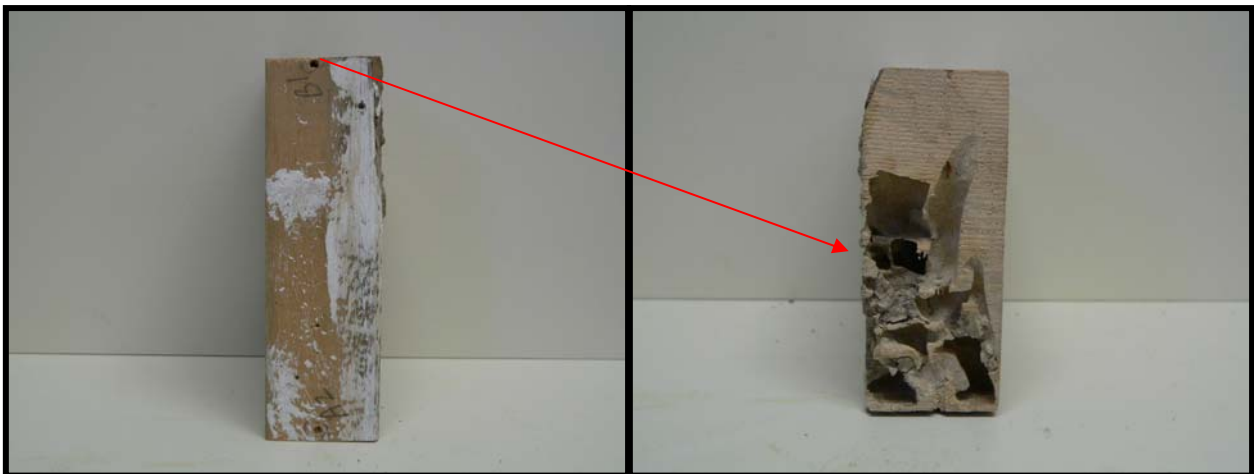


Figure 45. Section of a stud with termite damage, showing side view on left (with no visible damage) and the corresponding end view on right (showing termite damage). The arrow shows which end view is displayed.

hidden damage caused by decay fungi versus termite or other insects. With the enhanced image in Figure 46 it is interesting that the vertical cut lines in the bead board paneling are visible once colorized.

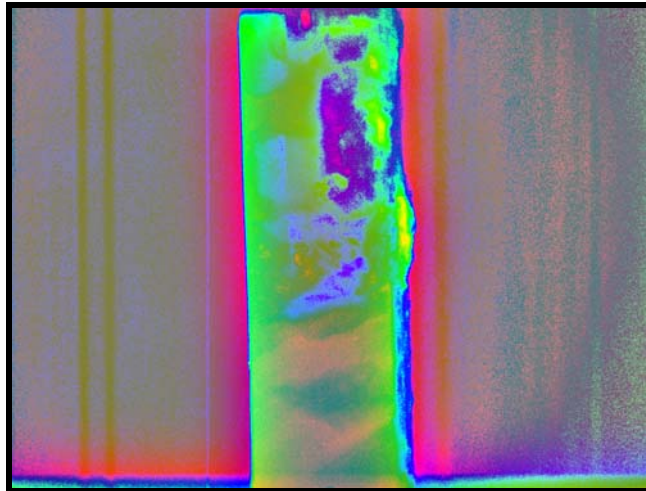


Figure 46. Colorized radiograph of a termite-damaged stud in a wood-frame wall (side view).

Many historic structures are of log construction. A solid log section is shown in Figure 47. Because the log is round, the most effective system to use was the Logos Imaging system with its flexible imaging plates. The plate was wrapped around the circumference of the log and secured with duct tape. Other than the plates being curved to conform to the shape of the log (to maximize contrast), the setup was similar to those used for the rest of the research.



Figure 47. Solid log section.

The radiograph of the solid log shows uniformity in the grain of the log throughout most of the image (Figure 48). As with the decayed timber discussed above, the dark areas are knots. Figure 49 shows a section of the log with an

internal void. The radiograph of the section with the void has an absence of grain, as characterized by the light areas in center of the radiograph where no wood remains (Figure 50). The lighter area without visible grain is characteristic of internal voids in any wood members. As with the solid section, the dark areas of the image are knots. Decayed wood can also sometimes be seen as a mottled pattern on the radiograph (see Figures 43 and 50).

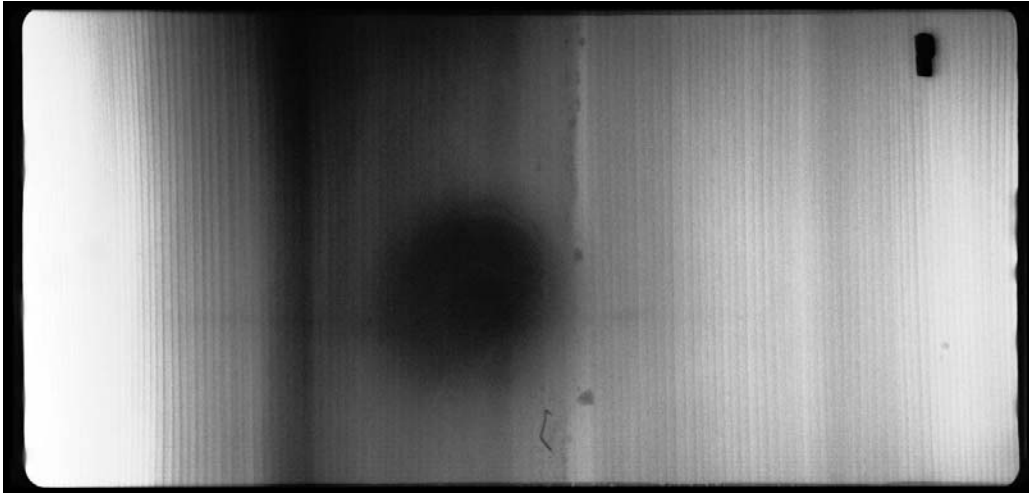


Figure 48. Radiograph of solid log section.



Figure 49. Decayed log section.



Figure 50. Radiograph of decayed log section.

In summary, decayed wood can often be identified in a radiograph when it displays the following features:

- Lighter color(s) due to reduced cross section
- A transition from non-decayed wood with intact grain pattern visible on the radiograph to the lack of a visible grain pattern in the decayed area
- A generally mottled appearance in the lighter decayed area

Additionally, wood that has been attacked by insects will also show lighter areas corresponding to a loss of material. The boundaries between undamaged and damaged wood are more abrupt than for decayed wood and tend to display a ragged or tunneled pattern.

Clearly, viewing raw radiographs can be useful for identifying the presence of deteriorated wood. As is discussed next, image enhancement and post-processing can help to quantify the extent of damage from a digital radiograph.

General Image Enhancement

Introduction

As demonstrated in the previous discussion, one major difference between laboratory radioscopy and field radioscopy is the increased uncertainty in establishing an informative and useful image in the field. Situation-dependent placement of both the imager and source introduces a greater possibility for improper spatial relationships. Hence, while traditional film radiography has been used with some success in the nondestructive evaluation (NDE) of historic buildings, this approach has been limited by the inability to field calibrate the placement of equipment.

One major advantage of digital radioscopy is the increased ability to field calibrate imaging. Whether the feedback is immediate (live imaging) or requires a field-based processor, the increased capability to modify spatial relationships opens new opportunities for the building investigator. In addition to the advantages presented by field calibration, rapid in-field feedback also allows the investigator the opportunity to analyze a situation, then identify and diagnose material and assembly-related issues at a broad level. While such near instantaneous diagnosis is sufficiently valuable to merit its use, digital radioscopy affords an additional level of usefulness through the very way it stores information.

Familiar to users of digital photography is the ease with which images can be edited for special effects. Digital radiographs afford the same opportunities in that, like digital photographs, information is stored as some gradient of color value in an individual cell (i.e., pixel) positioned adjacent to other such cells. This assignment of color value and position results in a bitmap. An advantage of a bitmap image is in being able to readily analyze and control the image on a pixel-by-pixel basis. However, bitmap graphics (also known as raster graphics) are resolution dependent, that is, they contain a fixed number of pixels. As a result, they lose detail and appear jagged when viewed at too large a scale on screen, or in print. In contrast, vector graphics are made up of lines and curves defined by mathematical objects (i.e., vectors). Vector graphics are resolution independent, and *with adequate information* can be positioned in three dimensional space, as opposed to the 'flatness' of raster images.

Digital radiographs are records of the total and cumulative amount of radiation passing onto the imager at that specific point. Whether film or a digital imager, this information is recorded as a 'color' along a continuous gradient. A simple grayscale gradient records total density where black is 'high' and white is 'low.'

Post-processing can be used to enhance the distinction by emphasizing various parts of the gradient. The resulting graphic output can be enhanced grayscale or a color image used for the purpose of improving visual analysis.

Additionally, while the radiographic images themselves are not three-dimensional, post-processing multiple radiographs taken from different perspectives can be used for purposes of optical or digital photogrammetry. This ability to measure relative position can be used to create vector objects that can indicate three-dimensional spatial position.

As suggested above, the possibilities of the post-processing and manipulation of digital photographs are recognized in the practice of conventional photography and are being applied in a variety of professional fields. For example, both digital enhancement of images and photogrammetry are being used in forensic automobile accident investigation. Enhancement of radiographic images is becoming more widely applied in industrial NDE applications. While such applications are different than those in this study, we began with a proposition that raw image radiographs might be made more useful in the diagnosis of building conditions and assemblies.

We identified two common and significant obstacles faced by building investigators in which field radioscopy might assist: wood deterioration and the location of hidden objects. Specifically, wood deterioration is often marked by a loss of material density. Radiographic imaging was assumed to be a likely means of detecting this loss of density. Hidden objects, often mechanical fasteners, are of a density different than the surrounding material. Hence, they are, as demonstrated earlier, clearly distinguishable from the surrounding building fabric.

Of the variety of traditional and modern building materials we chose to investigate wood (timber) because it is both widely used and subject to material degradation (e.g., decay and insect damage) and frequently joined with metallic (i.e., higher density) fasteners (e.g., screws, nails, spikes). While we believe our research into wood is not the limit of the applicability of radioscopy building evaluation, successful implementation with this material can afford a useful first pass for feasibility.

A radiographic image is a cumulative recording of the amount of radiation reaching the imager. As this is cumulative, the line (i.e., orientation) of x-rays from source to imager is of great importance. Although radiographic images appear similar to photographs, the optics involved are significantly different. Hence, both the positioning of the imager and the source relative to the building component being analyzed are of utmost importance. Successfully positioning

the imager near (and close to parallel to) the principal plane of the object of interest results in the crispest and most accurate imagery. Unfortunately in field imaging ideal setups are difficult to achieve. However, even without exact positioning radiographs usually convey some sense of difference between denser and less dense areas. Denser areas are darker (less cumulative radiation) and less dense areas lighter (more penetration, and hence, exposure.) In addition to appearing photograph-like the radiographer can subject this raw imagery to further analysis, with the knowledge that the degree of exposure (degree of grayness) is a recording of density.

Unlike with film radiographs digital image enhancement can manipulate the relationships between adjacent areas of an image. Accomplished by a variety of algorithms, such mathematical transformations done on a pixel-by-pixel basis can achieve powerful visual affects when viewed at a larger scale. Such manipulation has become a standard practice in digital photography. A variety of software for specialized scientific applications, general professional use and amateur photography has been developed. While each of these has its position in the marketplace, the more specialized programs are generally more powerful, although sometimes at the price of being narrowly tailored to specific uses.

As part of this study we chose to make a first-pass review of the usefulness of a leading professional image manipulation software, Adobe® Photoshop®; a specialized scientific software package, Image-Pro Express; and a specialized consumer photograph enhancement package based on NASA developed technology, Tru-View PhotoFlair®. Our exploratory manipulations focused on three areas: 1) enhancing image legibility, 2) eliminating 'hot spots' resulting from the original image capture and 3) identifying (and ideally, quantifying) loss of density.

In general, the main limitations of digital x-rays are the "fuzziness" of the images and the information limitations of grayscale analysis. Fuzziness can be the result of several factors. However, in general, there are several geometric considerations the radiographer needs to address. While good relative positioning of source, object and imager is the best method of reducing unsharpness, a variety of field conditions, including awkward access, uncertainty about the position of hidden objects, and multiple objects in different positions (and at different angles) relative to source and imager, can all contribute to fuzziness and the need for post-processing.

Since radiographs are a measure of total radiation, the grayscale as a measure of intensity is appropriate. Although the interpretation of grayscale radiographs (as for example, determining loss of density) can be enhanced, some distinctions, such as hue, cannot be interpreted from a grayscale image. Hot spots in

radiography are the result of field positioning that too narrowly focuses the x-rays relative to the imager. Again, better positioning in image capture might effectively address this issue, but in some cases it was assumed that post-processing might be able to correct for a hotspot.

Several off-the-shelf software packages were investigated, including the two that were provided with the imaging system software. The software packages varied greatly in their available features for addressing visual enhancement. However, each is equipped with digital image filtering, an algorithmic means of transforming the image. Specific image processing techniques include:

- histogram equalization: in this method the image is modified by using an automatic, mathematically derived algorithm that causes darker regions in an image to appear brighter.
- high-pass filtering: in this method the edge features are highlighted. This makes it easier to see the finer detail in the image and eliminates some of the impact of illumination changes.
- unsharp masking: in this method the high-pass filtered image is added back to the original image to enhance the edge detail while keeping the original image context.
- autolevels: autolevels uses a single user-defined parameter to enhance images. In some applications autolevels produces good results for illumination changes.
- multi-scale retinex: this algorithm performs a pixel-by-pixel analysis in the context of surrounding pixels, enhancing both contrast and edge definition.

To compare the software packages, images from the same set of objects were manipulated using each package. The first object was one with three groups of materials with different levels of x-ray absorption. This test wall, referred to as the complex wall, included a selection of different metal fasteners (maximum absorption of x-rays), wooden studs (moderate absorption), and thin outer clapboard (low absorption). The goal of enhancing this image was to improve discernment of the entire image, with no level of absorption being distorted. Within this complex wall was also a much more subtle feature, a strip of plastic that was not visible on the original radiograph. A second goal was to determine whether image enhancement could “detect” this subtle feature. The second object, framing lumber in a test wall, was one with very little contrast – all the components were wood. We attempted to manipulate the image from the wood-frame wall so that all subtle details of wood grain, various wood members, and splits and cracks were discernable.

Imaging System Software: SAIC® RTR-4™

The SAIC® image editing package allows for normal image manipulation methods typically associated with all photographic packages: sharpening, smoothing, adjusting brightness and contrast, and histogram stretching. Additionally, the grayscale image can be colorized (providing a broader range of tones in the final image) or inverted (with dark and light areas inverted), and filters that help identify edges (edge enhance, emboss) are present.

The features that were particularly helpful in improving the complex wall radiograph (Figure 51) were the manual contrast stretch (not the automatic stretch), the rainbow palette, the image sharpen (moderate), the edge detect and emboss features. The first two of these were under the Display Menu, and while they improved visualization of detail, they were not saved in the final TIF file, so they could not easily be imported to other software. The contrast stretch feature was particularly helpful in that manual manipulation of the histogram allowed for more detailed investigation of both lighter and darker areas of the image. While both lighter and darker areas could be better defined, they could not all be improved at the same time. The histogram equalize feature performed similarly (see the improved definition of the overlapping clapboard in the lighter areas of Figure 52). It was not as versatile as the manual contrast stretch.

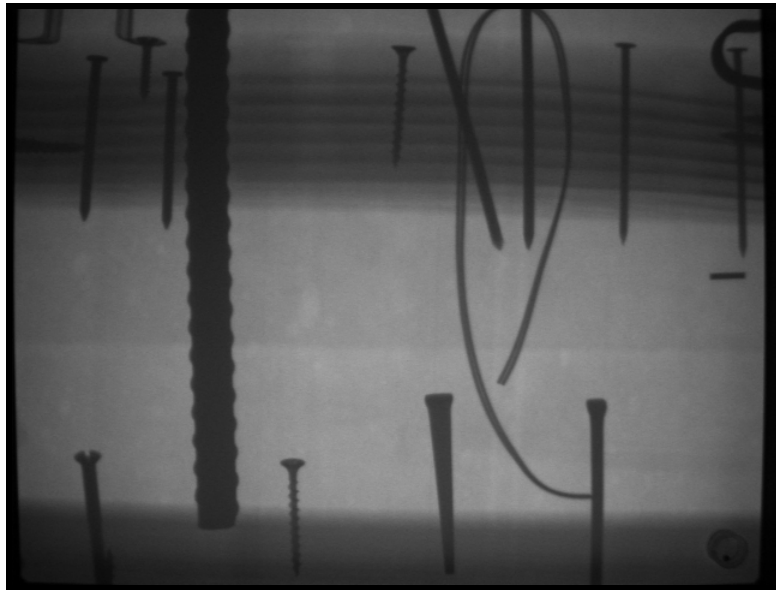


Figure 51. Original radiograph of the complex wall, unmodified.

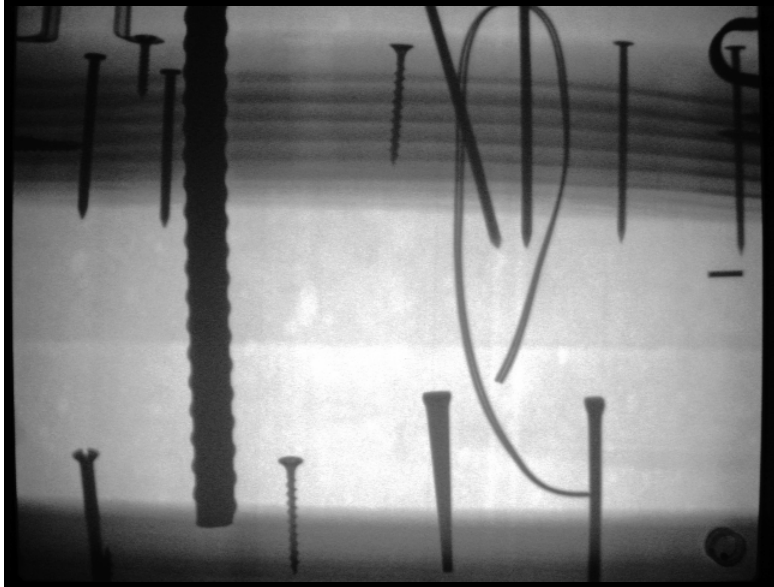


Figure 52. Modified radiograph of the complex wall, using the histogram equalize feature from the SAIC® imaging editing package.

The emboss and edge detect features (Figures 53 and 54) were useful to emphasize the contrast between the wood studs and the metal fasteners, with the emboss feature providing slightly more detail. The emboss feature also helped to make the radiograph appear three dimensional, or have depth of field, giving the metal fasteners the appearance of being raised, and even emphasizing the overlapping clapboard on the outside of the wall, and the wood grain in the studs.

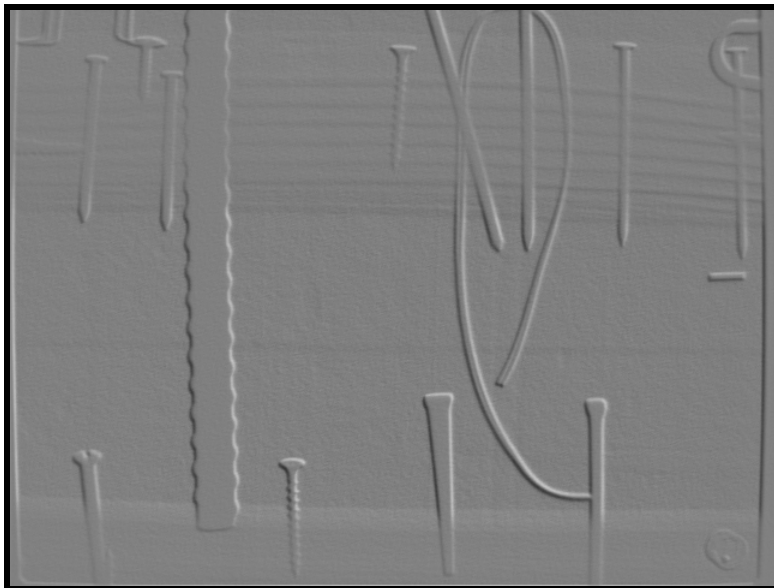


Figure 53. Modified radiograph of the complex wall, using the emboss feature. from the SAIC® imaging editing package.

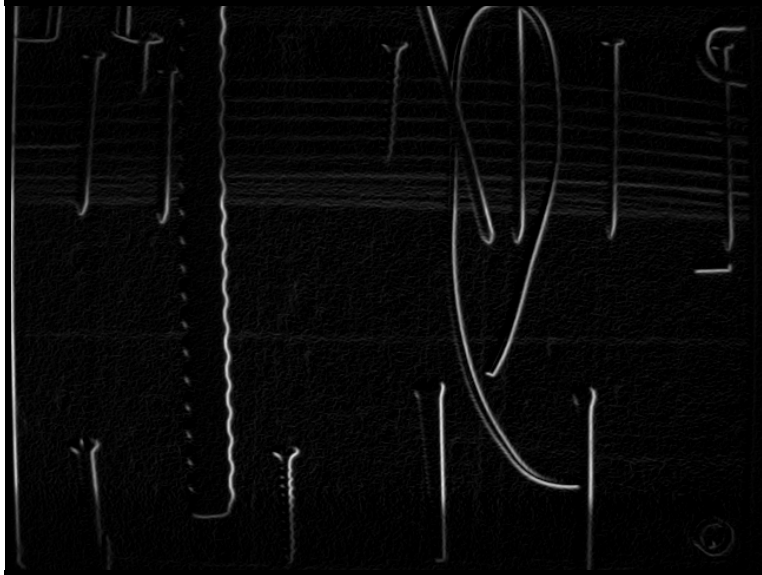


Figure 54. Modified radiograph of the complex wall, using the edge detect feature from the SAIC® imaging editing package.

Modifications to the radiograph of the wood-frame wall were more disappointing (Figure 55). Because of the small range of contrast, the rainbow palette feature merely changed the grey tones to a fixed color. The greatest improvement was when the contrast stretch feature (either automatic or manual) was used, but since this could not be saved as an image, it is not presented in the report. The histogram equalizer improved the contrast, but created a grainy texture while emphasizing the hot spot of radiation from the source (Figure 56). The emboss and edge detect features only emphasized a little of the wood grain without providing additional detail.

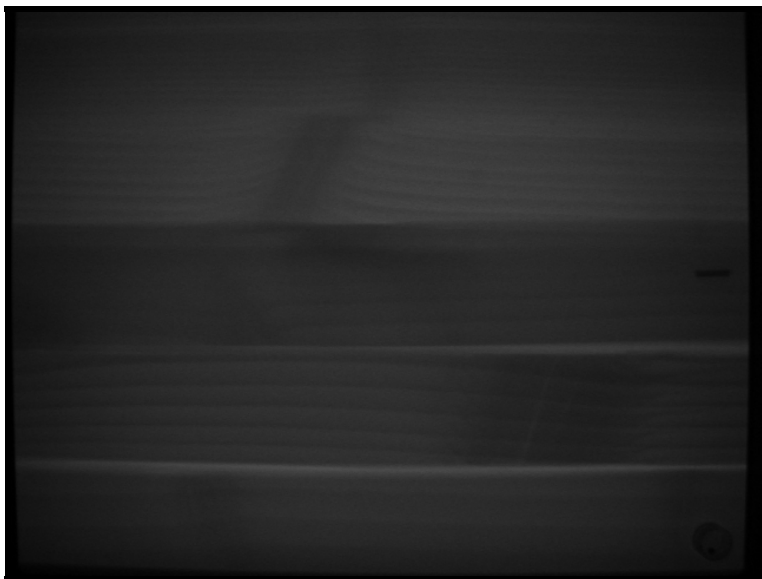


Figure 55. Original radiograph of the wooden wall, unmodified



Figure 56. Modified radiograph of the wooden wall, using the histogram equalizer from the SAIC® imaging editing package.

Imaging System Software: EPIX Scanner, Logos Imaging System

The Logos Imaging System software has components similar to the SAIC® System. One-button features include the invert, equalize, sharpen, smooth, emboss, despeckle, outline and colorize features. Manual features that allow the user some control over the final image included an image enhancement feature that allowed brightness, contrast and gamma to be manipulated separately in the final image. Finally, the histogram function was similar to the manual contrast stretch available in the SAIC® package. Both improve the range of grey tones shown on the radiograph, darkening ones that are too light, and lightening those that are too dark

The colorized radiograph is shown in Figure 57. Because the range of grey tones is replaced with a full palette of colors, visualization of some features is enhanced. Note the horizontal nail edge on the upper left hand portion of the radiograph which was difficult to see in the previous radiographs.

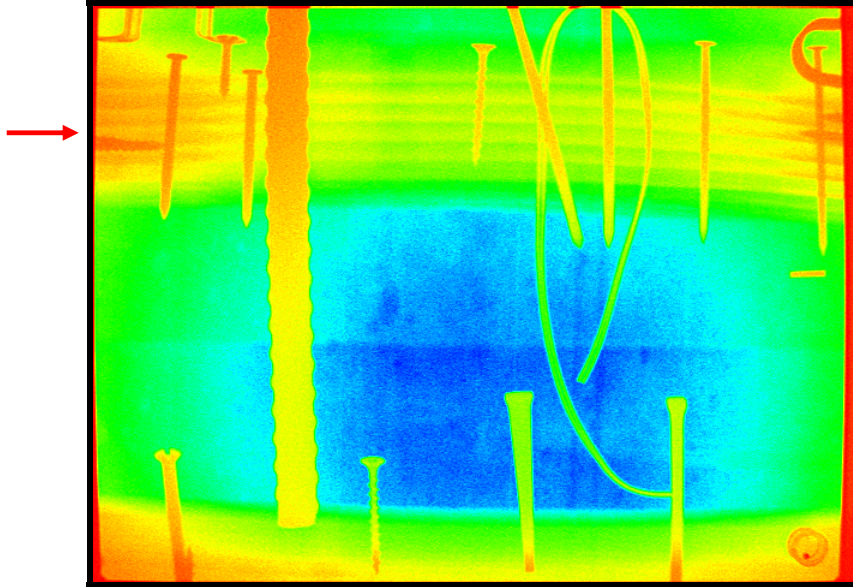


Figure 57. Modified radiograph of the complex wall, using the sharpen and colorize features from the Logos Imaging software.

The emboss features are similar for both systems (see Figures 53 and 58). But the outline feature of Logos, while similar to the edge detect feature of SAIC® (see Figure 59) shows more details of the metal components (compare Figures 54 and 59).

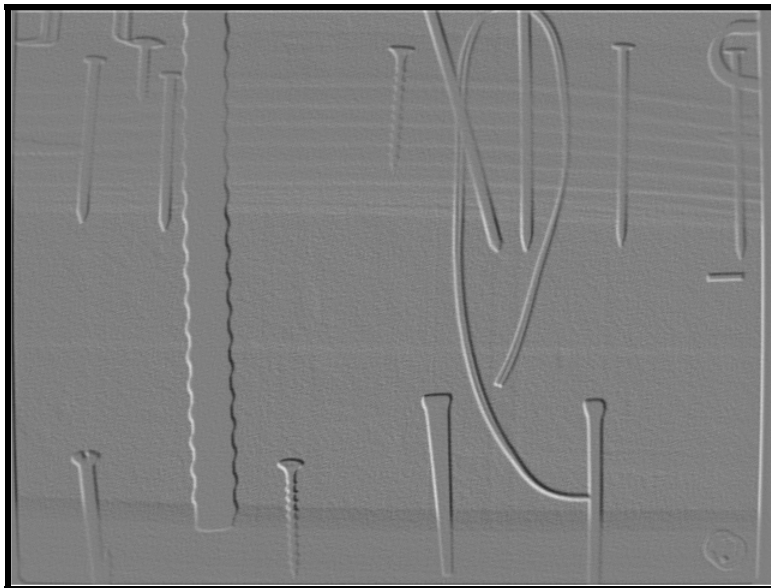


Figure 58. Modified radiograph of the complex wall, using the sharpen and emboss features from the Logos Imaging software.

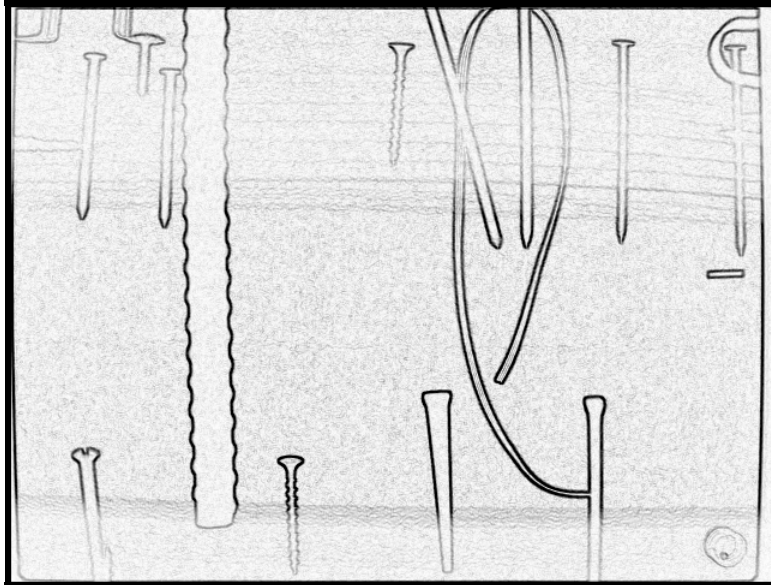


Figure 59. Modified radiograph of the complex wall, using the sharpen and outline features from the Logos Imaging software.

The radiograph of the wooden wall is shown colorized in Figure 60. The range of tones in the colorized version emphasizes the wood grain, but also displays the hot spot effect from the source. Figure 61 and 62 contrast the automatic equalize and manual histogram functions available in the Logos system. The manual adjustment of the histogram creates more even tones throughout the radiograph, partially eliminating the hot spot effect, and allowing more of the peripheral details to be seen.

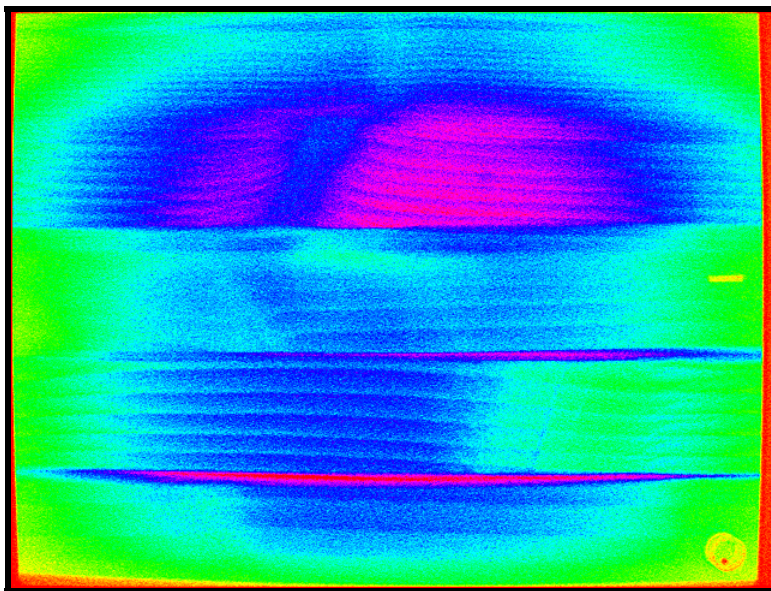


Figure 60. Modified radiograph of the wooden wall, using the colorize feature from the Logos Imaging software.



Figure 61. Modified radiograph of the wooden wall, using the equalize feature from the Logos Imaging software.

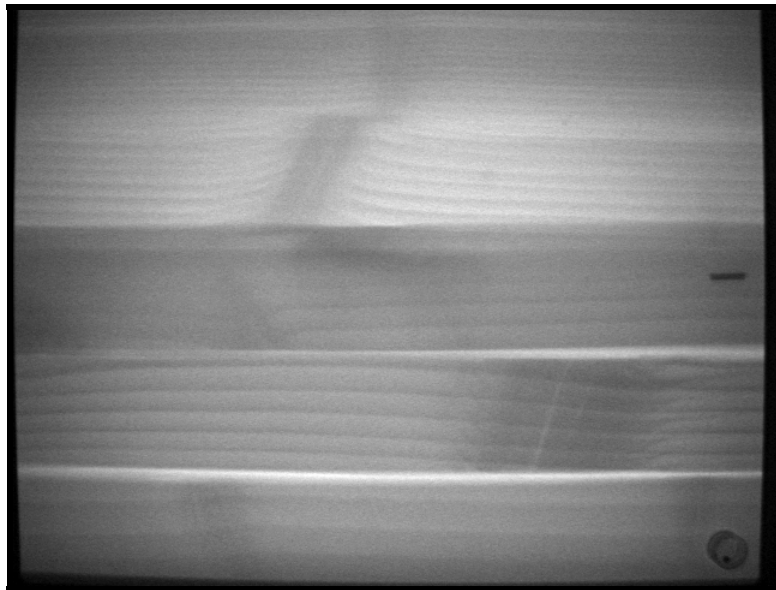


Figure 62. Modified radiograph of the wooden wall, using the histogram feature from the Logos Imaging software.

General Purpose Software: Adobe® Photoshop® Elements

In addition to the two proprietary software packages that came with the radioscopy systems, several commercially available photographic enhancement packages were investigated, including Adobe® Photoshop®, Adobe® Photoshop® Elements and Jasc Paint Shop Pro®8. These packages, for the most part, contain the same image modification techniques found in the packages available with the x-ray systems. However, some features of Adobe®

Photoshop® (Full Package & Elements) provide more flexibility while using a particular type of image modification, allowing for the identification of more subtle features.

Adobe® Photoshop® has an extensive array of features and is widely considered to be the standard in digital photograph manipulation software. Hence, we chose to use Photoshop® as our “base case” software for attempting to manipulate our radiographs. In general, we found it to be the most versatile, but at the price of a fairly steep learning curve for the infrequent user or one not familiar with the terminology of digital photography and optics. However, as a result of our first-pass analysis we also found that Photoshop® was able to varying degrees successfully address each of our three manipulation objectives: 1) enhancing image legibility, 2) identifying loss of density, and 3) eliminating hot spots.

Photoshop® affords a full palette of image adjustments and filters capable of enhancing legibility. Of these, contrast adjustment, histogram manipulation, unsharp mask, hipass filtering, and auto levels were all useful under differing specific conditions and sometimes in combination. We first reviewed these concepts using the more user-friendly PS Elements, and then in more depth using the full package version of Photoshop®.

Regarding image legibility, the unsharp mask command (Figure 63) allows the user to vary the amount feature (high values work best), radius (low to moderate values work best), and threshold (values close to zero work best) values while viewing the final result. This allows for more focused sharpening techniques which can further emphasize boundaries between different components of the wall.

The emboss feature also allows for flexibility, where sun angle (direction of illumination), height (low, between 5 and 20 works best) and amount (use higher values) creates a greater distinction between features. Compare Figure 64 to the emboss feature used in Figures 53 and 58. A similar filter, bas relief, can also enhance subtle differences in the images, allowing manipulation of the detail (use high end values), smoothness (low end values), and light direction.

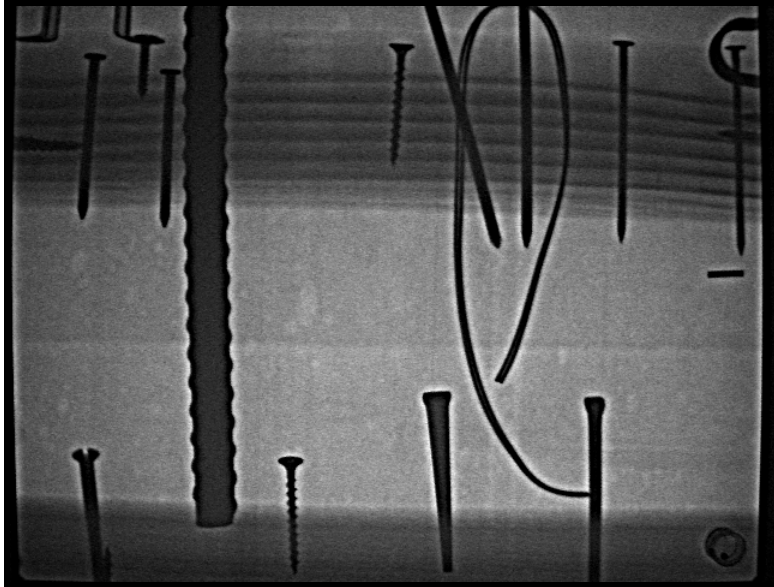


Figure 63. Modified radiograph of the complex wall, using the unsharp mask command in Adobe® Photoshop® Elements.

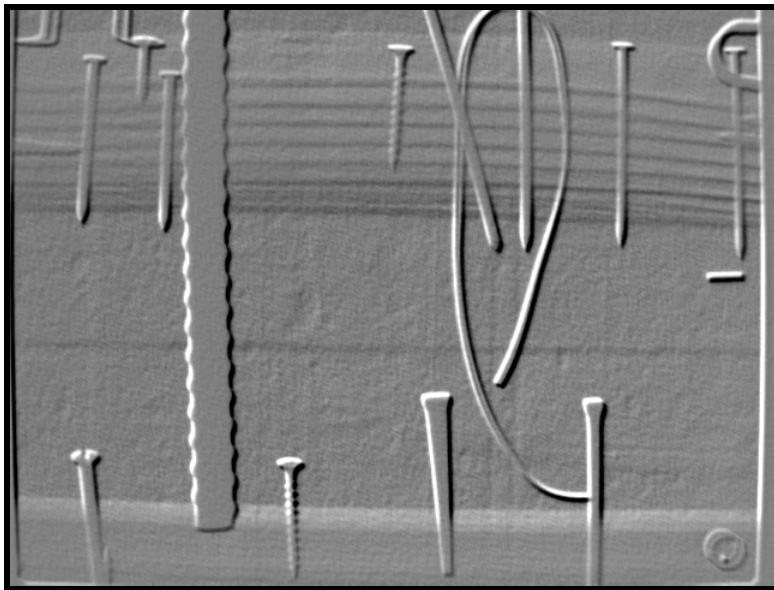


Figure 64. Modified radiograph of the complex wall, using the emboss command in Adobe® Photoshop® Elements.

The glowing edge filter, found under the stylize heading in filters, also works much better than the edge detect features found above, since edge width (use low to moderate), brightness (use a high value) and smoothness (use a low value) can all be adjusted on the screen while viewing the initial and final result. Compare Figure 65 with Figures 54 and 59 above. There is even a hint of the plastic strip on the right side of the radiograph, as there was with the bas relief filter.

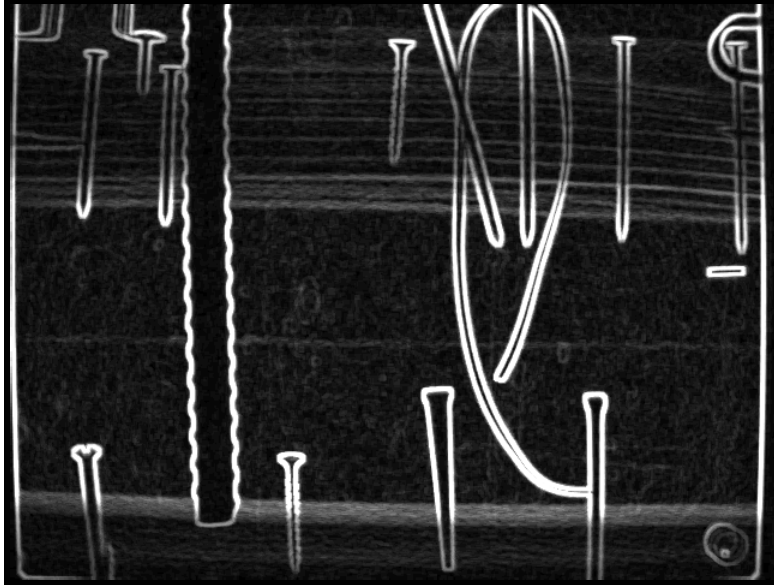


Figure 65. Modified radiograph of the complex wall, using the glowing edges filter in Adobe® Photoshop® Elements.

The wooden wall was not as dramatically improved using the filters. The best definition of both gaps between the boards and wood grain was found using the unsharp mask filter (Figure 66) and the emboss filter (Figure 67). Compare these to Figure 55, the original radiograph.

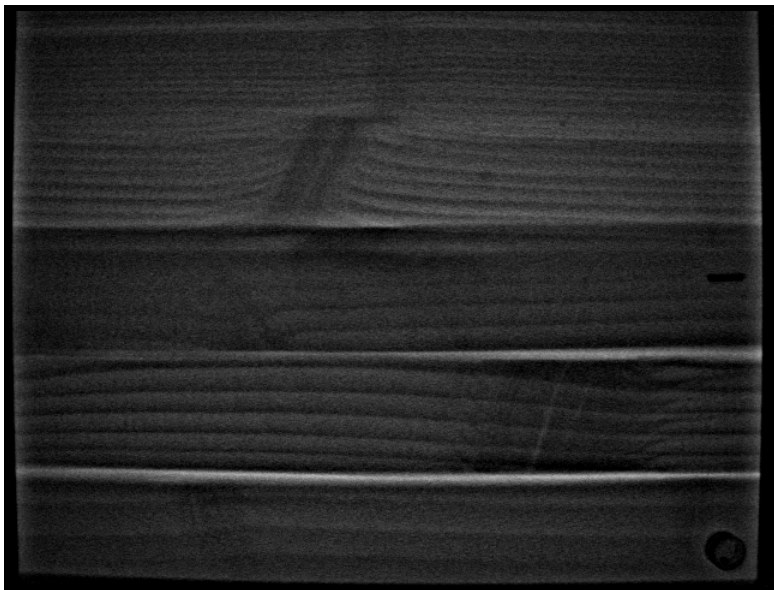


Figure 66. Modified radiograph of the wooden wall, using the unsharp mask command in Adobe® Photoshop® Elements.

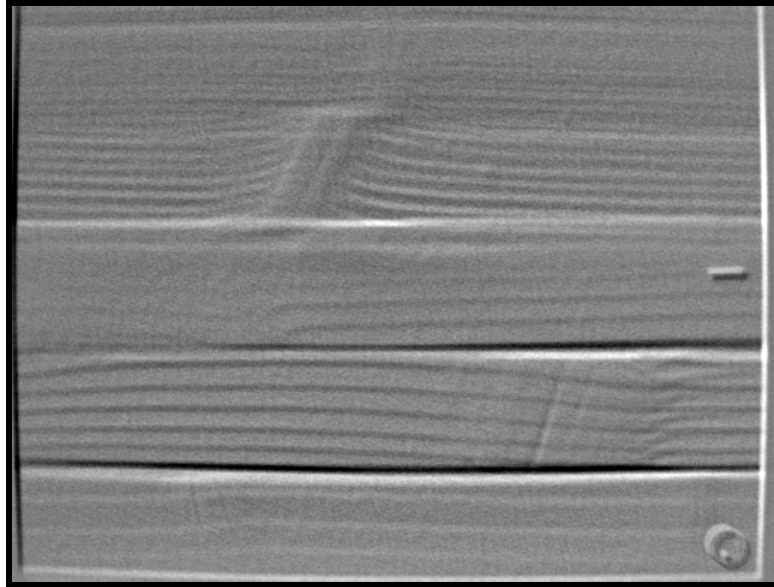


Figure 67. Modified radiograph of the wooden wall, using the emboss filter in Adobe® Photoshop® Elements.

General Purpose Software: Adobe® Photoshop® (Full Release)

The strength of the full release version of Adobe® Photoshop® (and in many cases Adobe® Photoshop® Elements) is that each of the various image adjustments and filters is controllable, with most of the manipulations of an auto-preview window in which variables might be adjusted before committing to processing the entire image (Figure 68). The high degree of flexibility and choice of tools makes working with Photoshop® powerful, but also very demanding in terms of expertise and time. The primary use of the software is in the graphics

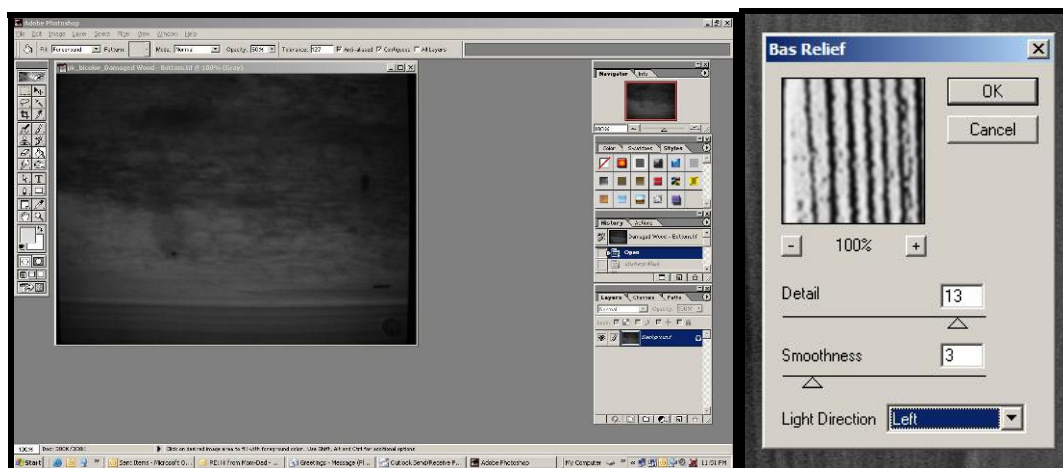


Figure 68. Adobe® Photoshop® screen with radiograph prior to manipulation and typical preview pop-up.

industry, where knowledgeable technicians can maximize the potential of this software. For the digital radiographer, several commands are worth noting and further experimentation.

- *Contrast and Brightness* control are the easiest to use of the image adjustments. (Figure 69) They proved effective for slight corrections of over- or under-exposure. However, they did little to actually enhance the sharpness or focus of the images.
- *Levels, Curves, and Autolevels*, under the Image Adjust menu (Figure 69) provide means for controlling histogram equalization, and hence allow for 'highlighting' different parts of the grayscale. The first two commands are manual but interactive; and the third automatic.

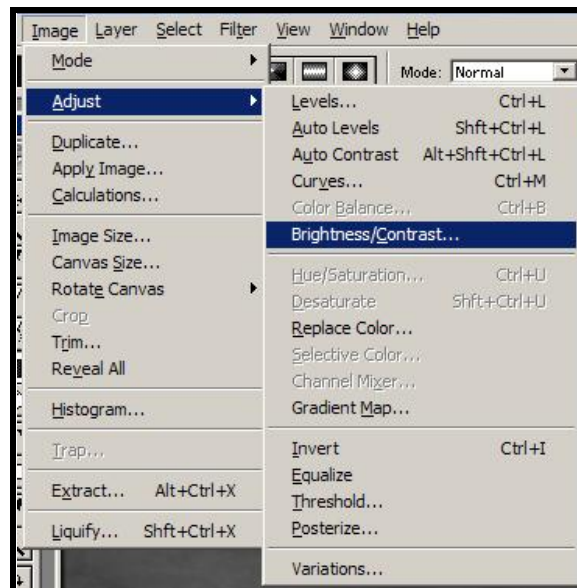


Figure 69. Image adjustment commands in Adobe® Photoshop® (Version 6.1).

In addition to image adjustments, Adobe® Photoshop® provides several filters worth noting.

- *Bas relief* (located in the menu under Filter/Sketch) proved to be an effective way to “raise” wood grain from an otherwise flat image Figure 70b.
- *Unsharp mask* (located in the menu under Filter/Sharpen) is an effective means of both heightening contrast and increasing edge definition as suggested by Figure 70c. The radiograph in this image depicts is of the wooden wall.

While the three-dimensional effect such filtering creates is a pseudo-representation, it makes the resulting image more intelligible to the viewer.

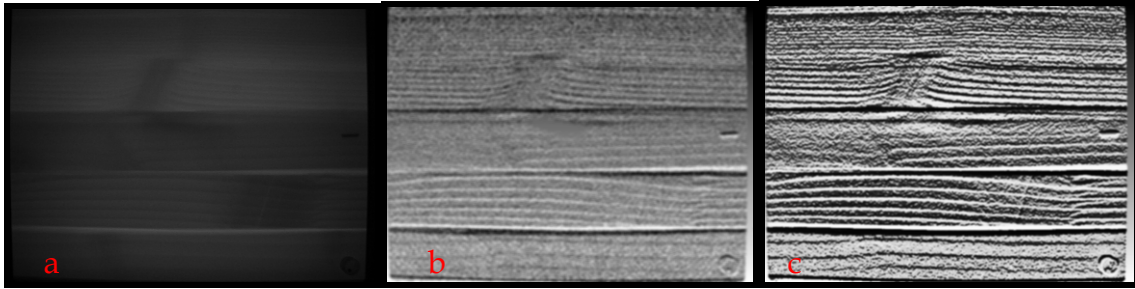


Figure 70. Progressive filtering of the wooden wall using Adobe® Photoshop®, with the original radiograph (a), the contrast corrected with bas relief (b) and bas relief with unsharp mask (c).

Our second area of concern was the control of hotspots resulting from the relative positioning of source, object, and imager. Adobe® Photoshop® provides a means for visually correcting the contrast problem (Figure 71). The application of a radial gradient mask proved to be an effective way of removing the hotspot. The process involves creating a new Photoshop® layer that masks the central portion of the image. The size of the mask and the degree of transparency are interactively controlled by the operator. This process is roughly the equivalent of a “dodge” in the printing of traditional photographs. The image with a corrected hotspot may then be subjected to further image adjustments and/or filtering. However, it remains preferable to attempt to limit hotspots during image capture.

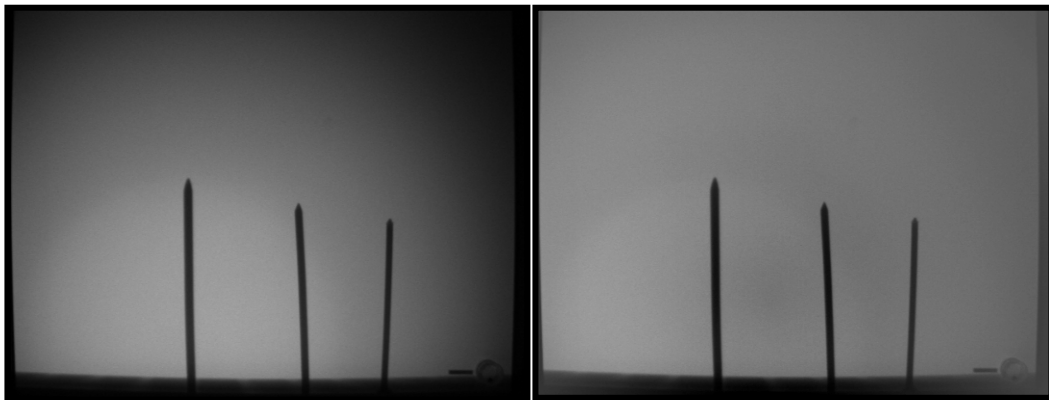


Figure 71. Sample hotspot correction using a radial gradient mask in Adobe® Photoshop®

Specialized Scientific Software: Media Cybernetics Image-Pro

The [Media Cybernetics](http://www.mediacy.com) (<http://www.mediacy.com>) Image-Pro family of software provides utilities for acquiring, analyzing, measuring and communicating information in “various scientific, medical, and industrial applications.” The strength of this family of products is in their vertical integration of processes from acquisition to report preparation. However, for

our purposes, most of these features proved unnecessary. We used the most basic version of this program, Image-Pro Express, with the intent of determining whether its orientation to the scientific applications increased its functionality for this study's x-ray analysis as compared to Adobe® Photoshop®.

Like Photoshop®, Image-Pro includes a variety of enhancement filters. The high-pass, unsharp mask, and histogram equalization filters performed similarly to their equivalents in Photoshop®. There are also several features, of which the descriptions and interface are more clearly related to the needs of the scientific researcher, rather than the photographic editor. For example, the flatten command reduces the intensity variations in the background pixels. However, its description explains that equalizing background variations is often done to prepare an image for a count/size measurement or other analytic operation “if its objects are difficult to isolate because the background contains pixels of the same intensity as the objects of interest.” This command proved useful in removing background noise, but it must be noted that the same effect could be achieved with Photoshop®, albeit with less of an explanation.

We speculated that Image-Pro's conversion to color bitmaps from grayscale followed by color enhancement might also provide a more comfortable interface. While this might be true for some users the use of pseudo-color was not substantially improved over that attainable with Photoshop®. However, we must also note that as with Photoshop® a more thorough investigation into this feature is warranted. In summary, Image-Pro's orientation to the scientist provides a sometimes more intelligible interface, and a variety of features that would be useful in some scientific applications (e.g., microscopy) we generally found that this program provided little advantage over Adobe® Photoshop® for interpretation of radiographs in historic preservation.

Specialized Consumer Software: Tru-View PhotoFlair®

PhotoFlair® by Tru-View Imaging Company, is the commercially licensed version of the NASA developed Retinex image processing algorithm. Similar to some respects to the filters and levels of Photoshop®, the retinex algorithm specifically improves dynamic range compression and sharpness of images. The patented technology has been applied to accident investigation, medical imaging, as well as general photography. Based on preliminary investigations, researchers from Tru-View and the NASA Langley Research Center reported promising results in the enhancement of medical x-rays, mammograms, and CT scans (Rahman *et al*, 2001). Given the similarities of these applications to our own interests we further evaluated this software.

PhotoFlair® is available as both a stand-alone program and as a plug-in for Photoshop®. It proved to contain a very easy and quick-to-use enhancement feature. The ability to substantially improve images with one-click was convincing. Figure 72 displays the effect of the algorithm on the complex-wall image. Applying the manipulation requires a single selection of an icon on the toolbar (left arrow). The resulting image (right) shows greater contrast and sharpness. This allowed for immediately identifying the two screws (right arrow) that were difficult to detect in the original image. The program also allows for adjustment to the automatic adjustments, and alternate calibrations can be saved for future use.

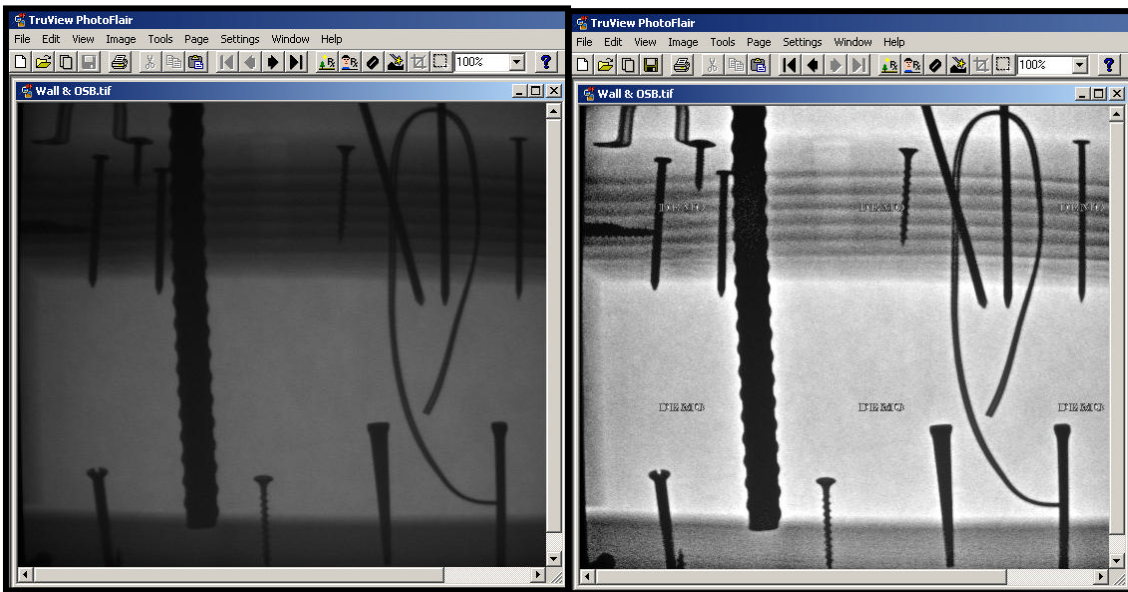


Figure 72. Example of the one-click algorithm in PhotoFlair®.

The two image enhancement packages available with the imaging systems provided most important features that allow for basic image improvement. Under most circumstances, they would be able to address problems associated with digital image capture. Several features, including emboss and colorize commands, were quite valuable in identifying subtle features found in individual radiographs. Of the other photo enhancement packages investigated, Adobe® Photoshop® proved the most versatile, with Adobe® Photoshop® Elements being the cheapest, easiest to use, and requiring little in the way of a learning curve. For purposes of historic preservation, the Adobe® Photoshop® Full Release added little to Elements. PhotoFlair® was found to offer a quick, easy improvement with one button, and could be added to Adobe® Photoshop® as a plug in .

Image Measurement for Quantification of Deterioration

Introduction

Wood is widely used for structural purposes. Its strength gives it the ability to transmit loads. Structural analysis of the material is based on several factors, including the cross-sectional area of individual members. Members that have lost cross-sectional area through decay or removal (e.g., drill holes, notches) may be compromised based on both the extent of the reduction and its location in the load transmitting assembly. Radioscopy is a way of assisting the field investigator in identifying and possibly quantifying such loss. The ability to do so can contribute to subsequent analysis and recommendations for remediation.

The visual analysis and representation of decay in wood proved to be more challenging. Figure 73a depicts higher density wood (with more solid wood) as darker, and lower density (with more decayed wood) as lighter, but without much contrast. Simple contrast manipulation, using Adobe® Photoshop® (Figure 73b) yielded an erroneous pattern (possibly due to the hotspot problem previously discussed). However, an unsharp mask (Figure 74) combined with overlaying a color mask (Figure 73c) based on substituting a transparent mask of contrasting pseudo-colors makes the image somewhat more intelligible. The drawback of this approach was the necessity of multiple transformations, and the time and effort required in each. Clearly, a better approach was needed.

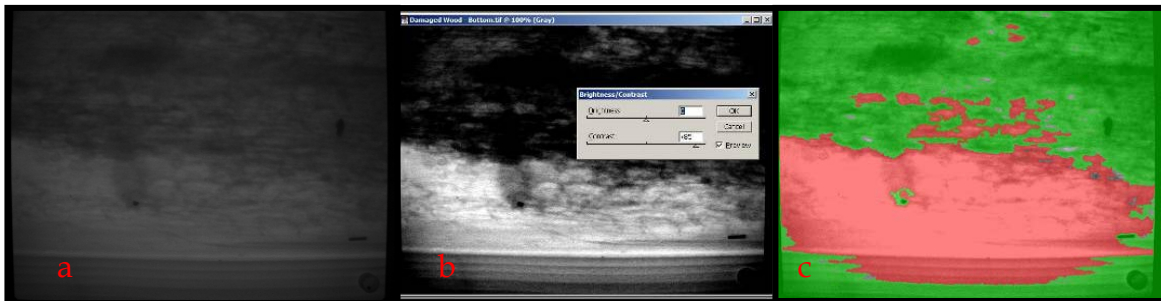


Figure 73. Decay analysis showing the original radiograph on the left, contrast manipulation in the center and a bi-color mask on the right, all image enhancement using Adobe® Photoshop®.

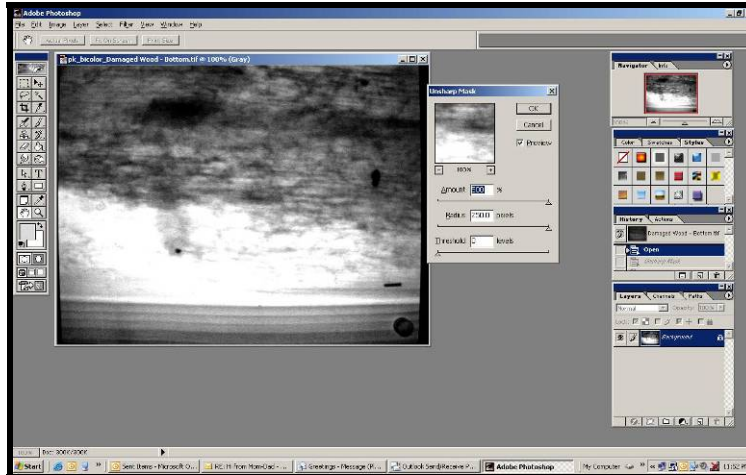


Figure 74. Screen shot from Figure 73 with the unsharp mask feature being applied using Adobe® Photoshop®.

Quantification of Deterioration

In the earlier discussion of deterioration we showed that it was relatively easy to identify the presence of deterioration and loss of section. In an effort to try to quantify loss of section due to decay or insect damage, it was decided to begin with a simple case, the stepped block seen in Figure 39. This was a known situation with discrete boundaries separating the sections, which ranged in thickness from 10 inches to 2.5 inches. Radiographs were taken using a standard source-to-object distance of 24 inches. Successive radiographs were taken with different pulse numbers, ranging from 16 to 100.

To find a user-friendly method to quantify the range of tones in these radiographs, we elected to use a readily available software package, Adobe® Photoshop® Elements. This package (along with most other photographic-enhancement software) has a histogram function that identifies the range of tones in a radiograph by graphing the number of pixels at each color intensity level (which are grey tones only for the radiograph). The number of pixels is represented on the vertical axis and the horizontal axis ranges from the darkest values (at zero) to the brightest values (255 for this package). For a given radiograph, the thickest section (10 inches) thus had the lowest range of histogram values, while for a specific thickness, the mean histogram value increased as the number of pulses increased.

One of the advantages of using the histogram function to quantify decay is that it can be used with the Rectangular Marquee Tool. Without selecting any portion of the radiograph, the histogram function displays the histogram of the entire radiograph. But each section can be outlined with the Rectangular Marquee Tool, and then the histogram function can be employed. For each radiograph,

this was done, using the entire section at 100, 75, 50 and 25 percent of the initial cross section, and taking the mean and median values for each histogram. The results are displayed in Figure 75.

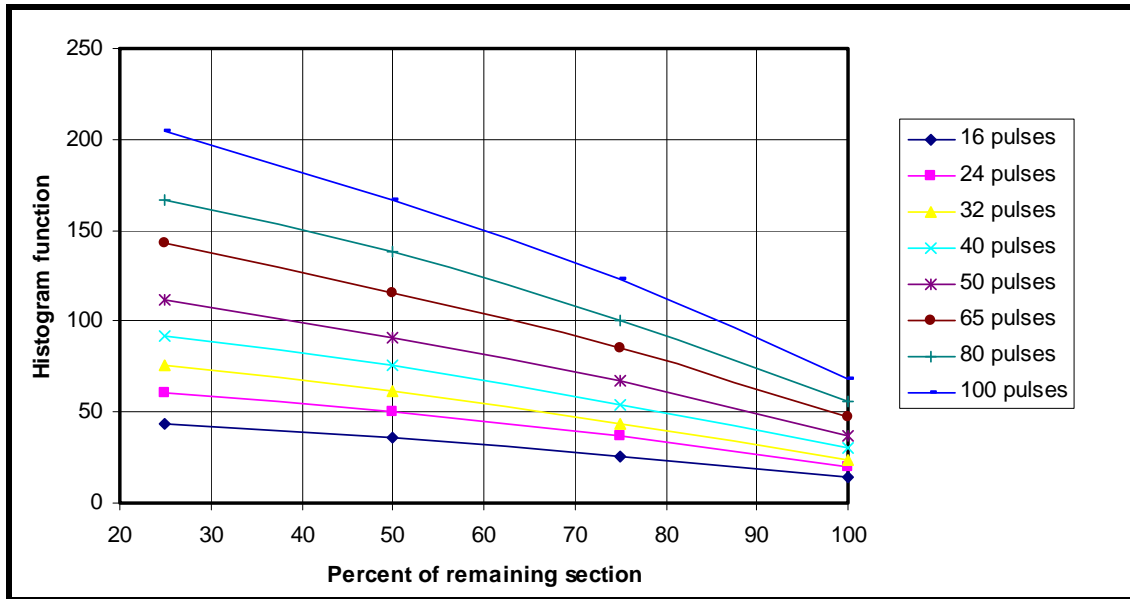


Figure 75. Graph of histogram function (from Adobe® Photoshop®Elements) versus percent of remaining section for stepped-block radiographs.

This established that there was an excellent correlation (R^2 values were all 0.99 or above) between the mean value and the percent of remaining cross section at each pulse level. However, this information was useful only for one species, using one particular setup and only for these thicknesses. It was felt that in a typical field situation, a more realistic method to determine loss of section might include an identification of intact wood versus decayed wood and a comparison between them. To this end, the ratio of the median histogram value for sound wood (the 10-inch section) to the median histogram value for other thicknesses was calculated, and plotted against the percent of remaining section. This is shown in Figure 76.

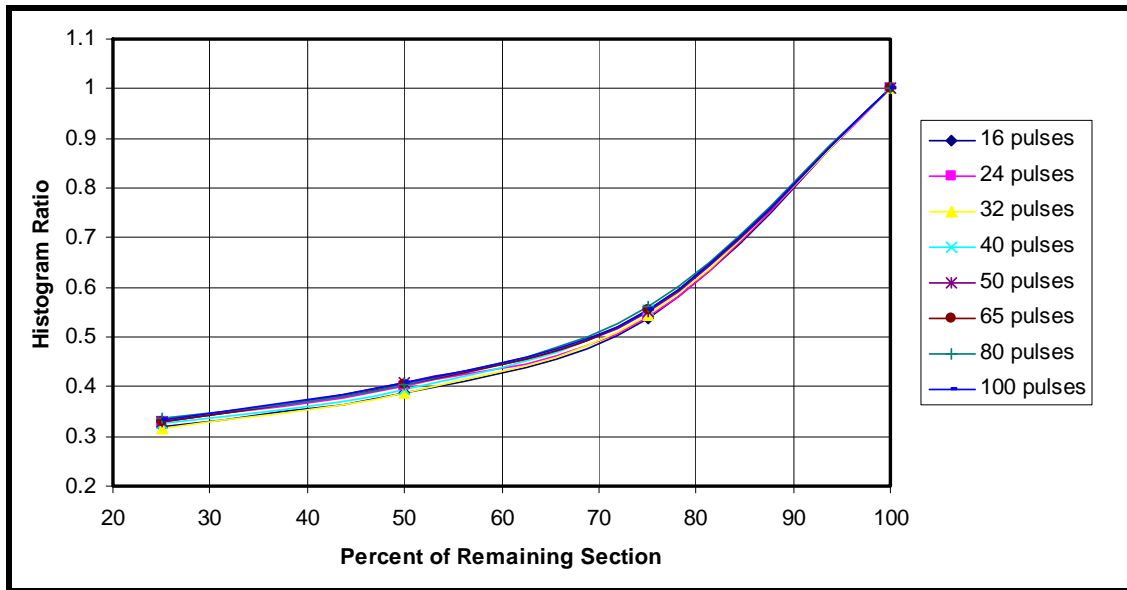


Figure 76. Graph of histogram ratio (from Adobe® Photoshop® Elements) versus percent of remaining section for stepped-block radiographs.

The plots of the histogram function, when using the ratio of the reading at 100 percent to the reading taken at 75, 50 and 25 percent all collapsed to essentially one function. This is important in that the number of pulses are not a factor when trying to determine loss of section in a timber as long as ratios are used, rather than raw values.

However, there were questions about the applicability of this graph to other situations. The primary concern was for the hot spot effect. This effect is clearly visible in Figure 40, the colorized version of the stepped block. It was also apparent when the histogram function was used on smaller sub-sections across a portion of the radiograph representing only one thickness, with higher values found closer to the center of the hot spot. It is possible that the graph above might be more linear, since the 10-inch section and 2.5-inch section of the step block were on the outer edges of the radiograph, and hence had median histogram values that were lower than would be expected if they were in the center of the radiograph due to the hot spot.

To address this problem, the radiographs were examined visually, to determine the probable center of the hot spot. It was then decided to use only the top 15 percent of the 7.5-inch and 5-inch sections, which appeared to have approximately the same relationship to the center of the hot spot as the entire portion of the 10-inch and 2.5-inch sections. To make this a relatively uniform measurement, the grid function was superimposed on the radiograph prior to measurement. The results of this analysis are shown in Figure 77. While there is still some curvature in the graph, it does appear to partially correct for the hot

spot problem, with all histogram ratios following approximately the same trend line. To completely eliminate the hot spot problem, additional investigation would be required. The masking of the hot spot discussed above would not necessarily correct the histogram appropriately.

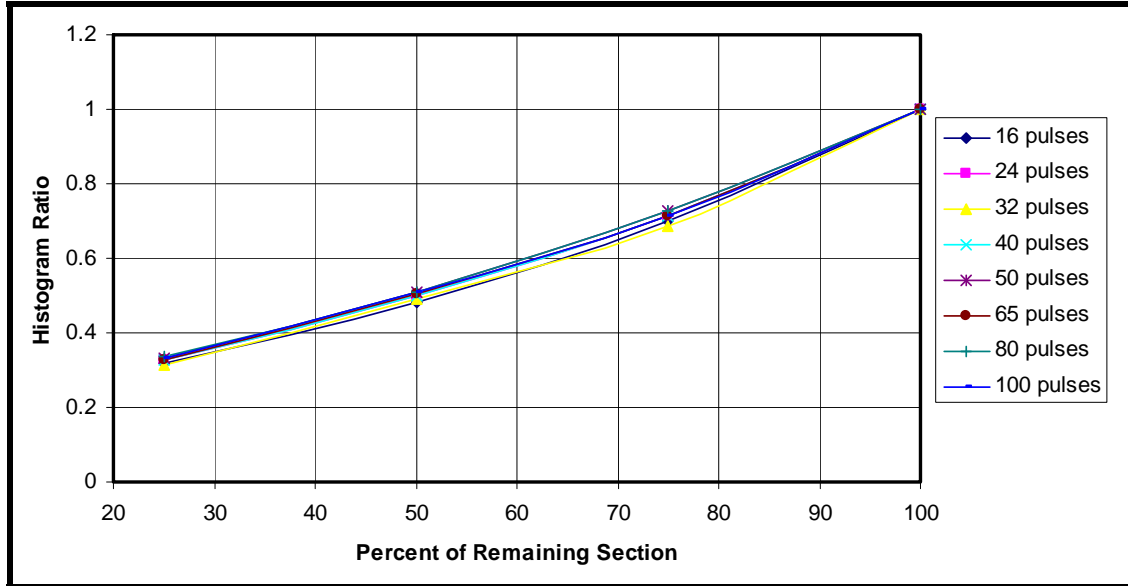


Figure 77. Graph of the corrected histogram ratio (from Adobe® Photoshop® Elements) versus percent of remaining section for stepped-block radiographs.

To validate the potential relationship, several radiographs were used. For the initial set of radiographs, another ratio was calculated. This was the ratio of the median histogram values for the 7.5-inch and 5-inch sections, using only small sub-sections of each near the center of the radiograph (and thus the center of the hot spot). This ratio, which represents 1/3 loss of section if the whole timber was 7.5 inches thick, was done for all radiographs taken, with pulse values ranging from 16 to 100. As expected, there was a very small range of values, with the average value shown in Figure 78 (labeled 67% Average), plotted against the averages of all the lines plotted in Figure 77. Further, measurements were taken on the radiograph of the decayed log in Figure 43, and of the timber with simulated termite damage, shown in Figures 14 and 15 (labeled TD 1 to TD 4).

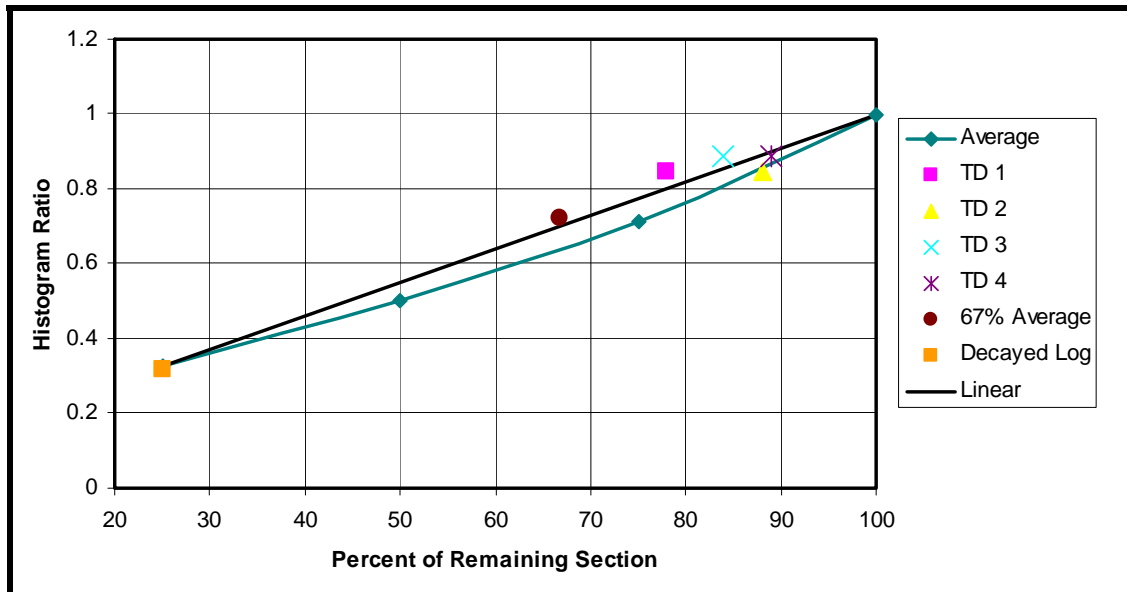


Figure 78. Graph of average corrected histogram ratio (for all pulses) versus percent of remaining section for radiograph of the stepped block, with additional points described in the text.

Finally, a linear function, showing what might be the effect if the hot spot problem was completely eliminated was plotted as the heavy black line on Figure 78. The equation for this line is:

$$HR = 0.009 RS\% + 0.1023$$

Where:

- HR is the histogram ratio (the median value of the histogram for “intact” wood divided by the median value of the histogram for “damaged” wood)
- RS% is the percent of remaining section

Rearranged to solve for the percent of remaining section, the equation is:

$$RS\% = (111 \times HR) - 11$$

This research implies that a simple histogram function might be reliable to estimate loss of section, if small adjacent sections (within the same area of the hot spot) were used to compare intact to damaged wood. However, it would require more research to identify the impact of setup geometry, different species, different x-ray systems, different software packages, and other miscellaneous factors on the ratio. The final equation might prove to be simply the histogram ratio multiplied by 100 percent.

Image Enhancement for Three-Dimensional Analysis

Introduction

The ability to determine the position of hidden objects within an assembly is highly desirable but can be elusive. While several types of nondestructive evaluation (e.g., impulse radar, impact echo, electromagnetic detection) are somewhat capable of discriminating between masses of differing density or composition, none provides an intuitively legible pictorial representation.¹ The promise of radiography lies in the fact that unlike the highly mediated data readouts of sonic methods (Figure 79) and the imprecise feedback of electromagnetic devices, radioscopic data “displays” spatial relationships between objects of differing density.



Figure 79. Raw radar data readout (Photo from U.S. Army Construction Engineering Research Lab).

It is this property of naturalistic imagery that motivates the desire to better identify and understand the relative position of the masses of differing density. Optical and cognitive abilities allow humans to rapidly and successfully distinguish discrete forms and to perceive depth of field and relative distance.

¹ In a study of the use of various NDE technologies in the investigation of the New York State Capital researchers concluded “Of the NDE techniques employed on this heavy masonry building, radar proved to be the most successful for imaging hidden structure and conditions. Next, in order of success, were impact echo, ultrasonic pulse velocity, spectral analysis of surface waves, and infrared thermography. Electromagnetic detection was very useful, but its scope is limited to buildings that contain some iron or steel and to locations where framing members are isolated from pipes, conduits, and other metal features. Fiber optics was found to be of minimal use in this type of building because of the limited areas where voids were present.” Radioscopy was not part of their study. The case was documented by the U.S. National Park Service Technical Preservation Services, and published as Preservation Tech Note #4 (<http://www.cr.nps.gov/hps/tps/technotes/PTN40/NYStateCap.htm>).

The question the authors asked was how can radiographs allow for, and support, this innate ability?"

Determining spatial relations between areas of varying density can be achieved optically or by calculation. Preliminary investigation into both approaches was undertaken for this study. *Stereoscopic photo-interpretation* is based on geometrically constructing camera angles so as to allow for stereo-viewing of the combined image. The technique is widely applied to visual media other than radiographs in applications as diverse as the child's hand-held "View-Master" stereoscope to equipment for the interpretation of aerial photography. *Photogrammetry* - "the art and science of making measurements from photographs" - when based on multiple images, can further the geometrical analysis through the application of mathematical algorithms.

In the scope of this study, the research team concluded that gross spatial relationships of objects of varying density can be distinguished through both stereo-optics and algorithmic modeling. However, given the difficulty of geometrically precise field setup of equipment, and the imprecision and error inherent in measuring and inputting indistinct radiographic "shadows" into a model, the human eye and brain appear to be the most efficient way of making judgments about spatial relations at this time. Improvements in either field setup or post-processing may tip the scale. This possibility warrants additional research.

Stereo-optics (Three-dimensional Radioscopy)

The simplest way to determine the three-dimensional (3-D) structure of the interior of a wall is to use some type of stereo viewing. This can be accomplished with two radiographs taken of the same area from different angles. The equipment necessary ranges from nothing (you can train your eyes to view two adjacent stereo photos in 3-D) to expensive computer programs. The most basic type of equipment is a pocket stereoscope (which can be purchased at companies like Forestry Suppliers, ASC Scientific or Ward's for about \$30).

Depth perception and 3-D viewing occur when your brain integrates and interprets the images received from each eye. The visual cues that allow this to occur include relative size, linear perspective, shade, shadows, and increasing fuzziness with distance. But physiological processes are even more important. Binocular divergence, which is the difference between the images that each eye receives of a particular object is closely tied to convergence, which is the angle made by the two lines-of-site of the eyes. Binocular disparity and convergence are the most important features used in stereo viewing of photographs, aerial photos, and radiographs.

The first stereoscopic viewer was invented by Sir Charles Wheatstone in 1838, shortly after the invention of photography. Simple devices to view stereo photos of vacation spots or exotic locals were common in the early 20th century, and these can still be purchased at toy stores today.

Equipment has been developed for use in mapping, interpreting aerial photographs, and viewing remote images produced by satellites. The most direct approach to simple viewing ranges from the inexpensive pocket stereoscope mentioned above, which uses only two convex lenses on a collapsible stand to much more complex models that use lenses, prisms and/or mirrors. With increasing complexity comes increasing cost, but greater ease of stereo viewing. In the last several decades, stereo plotting systems have been developed, and have become increasingly automated (Heipke, 1995). But these systems are primarily used for photography and are probably “overkill” for radioscopy.

Numerous sites are available online that contain additional information on the basics of stereo viewing. The Canada Centre for Remote Sensing has a site that provides an excellent overview of stereoscopic viewing:

http://www.ccrs.nrcan.gc.ca/ccrs/learn/tutorials/stereosc/chap1/chapter1_1_e.html

Gale Rhodes, of the Department of Chemistry, University of Southern Maine has created a site that discusses stereo viewing of photographs and computer screens using no equipment, only the unaided eye:

<http://www.usm.maine.edu/~rhodes/0Help/StereoView.html>

Other helpful sites affiliated with either universities or government organizations give some details on viewing stereo photographs, usually aerial photographs and their interpretation. However, the same principles can be applied to the viewing of stereo pairs of radiographs. These sites have helpful information on the use of pocket stereoscopes and 3-D visualization. They include:

<http://www.crssa.rutgers.edu/courses/airphoto/airphoto7/sld001.htm>

http://rst.gsfc.nasa.gov/Sect11/Sect11_3.html

<http://www.fes.uwaterloo.ca/crs/geog165/api.htm>

The radiographs taken in this investigation were typically taken in a plane 24 inches from the object and offset 3 to 6 inches to the left and right of the target area, as see in Figure 80. The images are then taken of the same target area, but from different angles. Sequential radiographs can also be taken along the length of a wall and viewed as stereo pairs, but the area of stereo viewing will be limited to the area of overlap of subsequent radiographs.

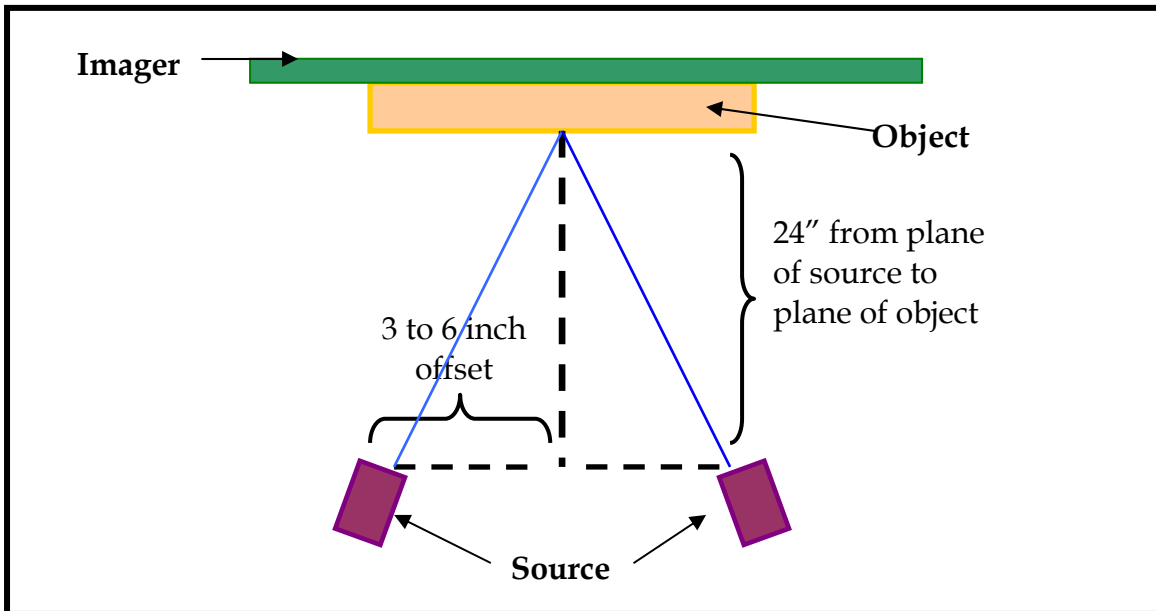


Figure 80. Placement of source and object for creation of stereo pairs.

When using a pocket stereoscope to view stereo pairs of radiographs, it is easiest to have printed copies of the radiographs to work with. They should be lined up adjacent to one another, with the radiograph taken to the left of the target site on the left side, and the one taken to the right on the right, so the radiographs have the same relationship as do your eyes to the target area. They should also have the same orientation (in the viewing plane, one radiograph should not be “crooked” or tilted at an angle relative to the other). If they are tilted because of the geometry of the x-rayed object, simply rotate one radiograph so that the tilt is eliminated. Find an area in the center of the radiograph that is the same location, and line this point up on both radiographs so that the points have the same separation as the distance between your pupils (it should be about 3 inches). Set the pocket stereoscope up above these two points, with the center of the lenses separated by the same distance. Look down through the stereoscope as if looking off to infinity, and you should see the image in three dimensions.

When looking at stereo pairs, whether of aerial photographs, normal photographs, or radiographs, some vertical exaggeration can occur. This means that the dimension perpendicular to the viewing plane is exaggerated. It is termed vertical exaggeration because it is usually an issue when viewing aerial photos. This exaggeration occurs because the ratio of the distance between successive photographs and the distance above which they are taken is different than the ratio of the distance between the viewer's eyes and the distance to the photos or radiographs.

Normally, when viewing aerial photos, this vertical exaggeration creates the illusion of steeper mountains, taller trees, etc. While this does help with viewing in 3-D, it must be accounted for in mapping exercises. With a radiograph, the dimension which is exaggerated is the depth of the wall. Again, this helps to see the relative position of nails, screws and other fasteners, but it must be taken into consideration when used to accurately locate items in a wall.

Below are two stereo pairs that can be viewed with a pocket stereoscope. Figure 81 shows two radiographs of three screws in a 4-inch by 4-inch wood block. These were taken with the source 20 inches from the object, offset three inches to the right and left (see Figure 80 above). When viewed in 3-D, the bottom of the screw on the right is angled sharply toward the viewer, the screw in the middle is relatively vertical, and the bottom of the one on the left is angled to the right and away from the viewer. Make sure you can see this in 3-D before trying Figure 82, which is more complex.

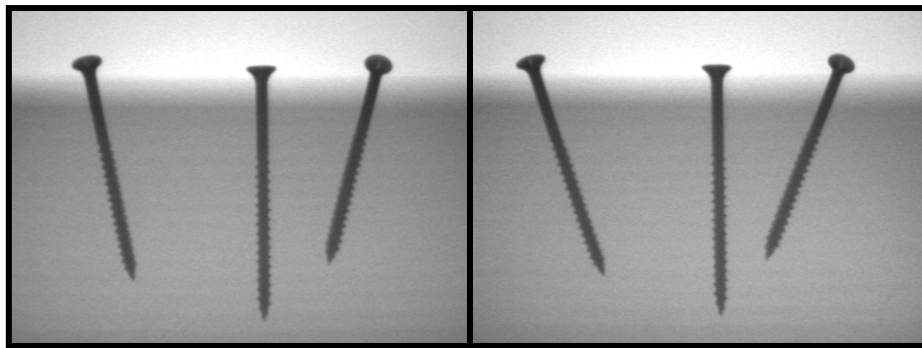


Figure 81. Stereo pair of three screws in a 4-inch by 4-inch block.

Figure 82 shows two radiographs of the complex wall. They were taken with the source 23 inches from the object, with a 3 inch offset. In this figure you should see the bottom nails tilted, the center two away from the viewer and the outer two toward the viewer, the large rebar is roughly in the center of the wall, in front of the horizontal blocking, and the loop of wire is behind two large nails, but in front of the blocking.

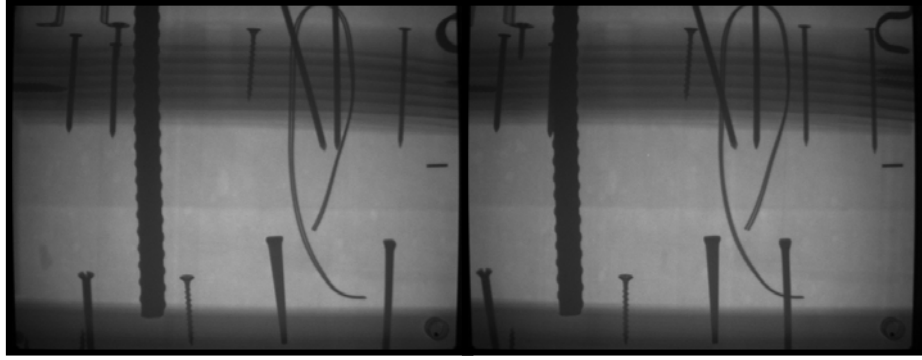


Figure 82. Stereo pair of complex wall

Determination of Size and Position Using a Single Radiograph

Occasionally the size of wall components and their location within a wall can be determined by using some simple geometric principles (discussed in the section on Geometry above). Because a radiograph is essentially a shadow cast on the imager, the closer the object is to the imager, the smaller it is and the closer it approximates its actual size. When viewing a radiograph, the view always appears as if from the source side of the object, unless you mirror image the radiograph. If the image has multiple nails of the same size and orientation, the smaller nails are to the “back” of the wall (closer to the imager), while the larger ones are closer to the front (the source side). A large threaded rod with bolts on both ends at an angle through the wall would have its thickest end towards the source. These observations sometimes allow an appreciation of the relative locations of wall components without calculations or stereo viewing.

When this simple approach is not sufficient, the relationship between object size and image size, which is a function of the relative distance between the source and imager and the source and object can be used. It is defined as:

$$S_O / S_I = D_{SO} / D_{SI}$$

where:

S_O is the size of the object,

S_I is the size of the image,

D_{SO} is the distance from the source to the imager, and

D_{SI} is the distance from the source to the object

If the object size is known (a standard size nail or screw, for example), its location within the wall can be determined by calculating D_{SO} , and subtracting it from D_{SI} to obtain the distance inside the wall from the imager:

$$D_{SO} = (S_O / S_I) D_{SI}$$

If the object size is unknown, a range of possible sizes can be obtained by measuring the distance from the source to the front of the object (D_{SF}), since:

$$S_O = (D_X / D_{SI}) S_I$$

If D_X is equal to D_{SI} (the object is adjacent to the imager) the size of object and image are identical. This is the largest possible actual size for the object. If D_X is equal to D_{SF} , this establishes the smallest possible actual size for the object.

These relationships work best if the object and imager are parallel to one another and perpendicular to the face of the object. With small components such as nails, using the long axis as a reference size will only work if the nail is parallel to the sides of the wall and the imager. For equidimensional objects (the maximum diameter of a round bolt head, for example), this works well.

More complex mathematical relationships of multiple wall components can be incorporated using two adjacent radiographs taken with the same source-to-image and source-to-object distances. This requires establishing common reference points.

Calculations in Three Dimensions Using Two Radiographs

While fairly simple estimates of location and/or size can be made using one radiograph (if the setup distances are known), more accurate calculations can be made using two radiographs that are taken by moving the source parallel to the plane of the object while keeping the imager stationary. These trigonometric calculations are well established both for radiographs and photography (and have been widely used for things such as topographic mapping, using aerial photography). The information in this section has been taken from an excellent reference on x-ray photogrammetry by Bertil Hallert (1970).

The optimum setup to collect radiographs that can be easily used to make these calculations is to set the source so that it shoots perpendicular to the plane of the object. If the first image is taken on the left of the target area, and then the source is moved to the right for the second image (without moving the imager), the conditions are met for using the relationships defined in Figure 83. Other, more complex calculations for different geometric positioning can be found in Hallert (1970).

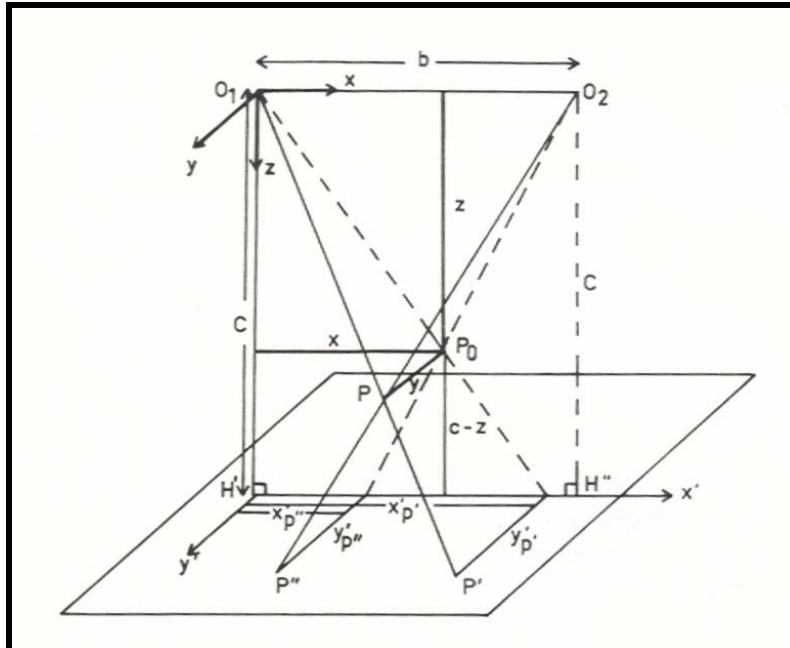


Figure 83. Definition diagram for using stereo radiographs to determine points in three-dimensional space (from Hallert, 1970).

The following parameters can then be measured and/or calculated:

- O_1 is the location of the source for the left-hand image.
- H' is the location of the center of the beam from the source (the center of the hot spot seen on the radiograph), called the Principle Point.
- c is the distance between O_1 and H' , referred to as the principle distance.
- b is the distance that the source is moved parallel to the plane of the object, referred to as the base.
- P' and P'' are the locations of the true point P on the two radiographs, left and right respectively.
- The x - and y -coordinates for P' and P'' (x', y' and x'', y'') are measured using the left and right radiographs, with the location of H' as the origin.

After the radiographs have been taken, the measurement of x - and y -coordinates for each point of interest can be facilitated (when using digital radiographs) by using the grid system and ruler found on most image-enhancement software. It is important to note that H' has the same absolute location on both radiographs, even though the location of the hot spot has shifted on the right-hand radiograph. It is also important to note, when measuring the x - and y -coordinates on a computer, that the correct image size is used. After measurements are completed, the following formulas are used to determine the true x , y , and z coordinates of each point:

$$z = (b c) / (b + x' - x'')$$

$$x = (b / (b + x' - x'')) x'$$

$$y_1 = (b / (b + x' - x'')) y'$$

$$y_2 = (b / (b + x' - x'')) y''$$

The two different ways to calculate y are important, because they allow for an estimate of the accuracy of the method. The difference between y_1 and y_2 is called y -parallax, and its value allows the investigator to determine how reliable this method is in a particular situation. Fuzziness of the radiograph, inconsistencies in measurement, and problems with the setup all can contribute to problems with these calculations.

To assist in using this technique, a set of sample calculations have been made using a setup with three nails. The radiographs of the three nails are shown in Figure 85. The images have a true size of 10.5 inches long by 8 inches high, and the nails are 3.5 inches long, with their head hidden in the board beneath them. The imager was placed directly behind the three nails and 24 inches from the source. The source was moved horizontally 6 inches for the second radiograph. The locations of the coordinate system for each radiograph are shown in red. All measurements (in inches) and calculations are shown in Table 3.

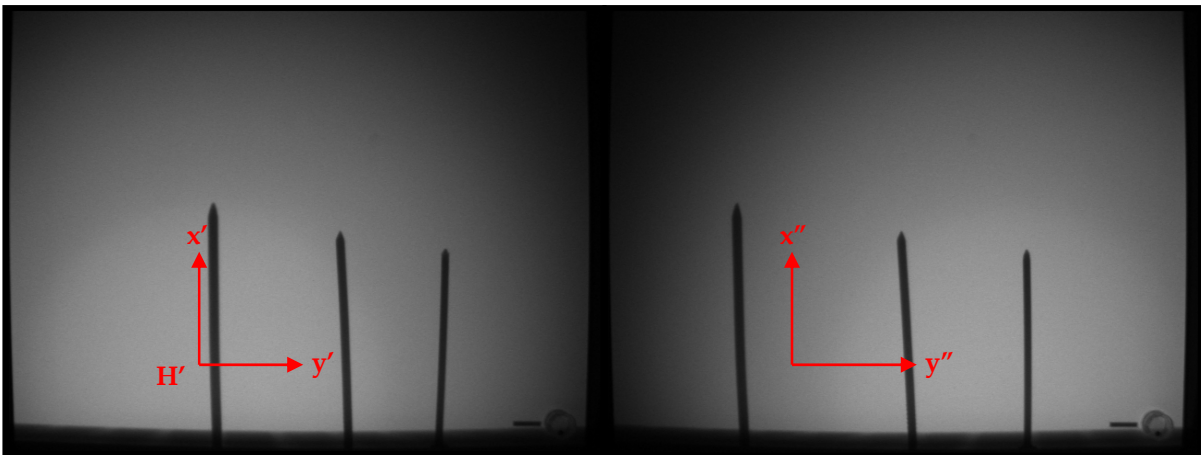


Figure 84. Two radiographs of three nails, taken with the source moved six inches from left to right, parallel to the plane of the imager.

For each of the three nails the points at the top and base were measured. The head of each nail was in the board underneath, so the full length of the nails could not be measured. It can be seen from the above calculations that the nail on the right is closest to the imager (which would be located at a z -coordinate of 24). The nails are spaced roughly two inches apart. The length of the nails (calculated using the true end points in three dimensions), is close to the

expected exposed length of about 3.25 inches. The y-parallax is very small (the maximum value was 0.03 inch), indicating that these measurements are reliable for identifying the location and size of the nails.

Table 3. Determination of coordinates for radiographs of three nails.

Point	x'	y'	x''	y''	z	x	y ₁	y ₂	Nail Length
Top of Left Nail	0.02	3.03	-1.33	3.00	19.59	0.01	2.48	2.45	3.36
Base of Left Nail	0.08	-1.08	-1.25	-1.08	19.64	0.07	-0.89	-0.89	
Top of Middle Nail	2.30	2.50	1.62	2.50	21.55	2.06	2.24	2.24	3.26
Base of Middle Nail	2.43	-1.10	1.83	-1.08	21.82	2.21	-1.00	-0.98	
Top of Right Nail	4.17	2.18	3.92	2.17	23.04	4.00	2.10	2.08	3.16
Base of Right Nail	4.08	-1.08	3.90	-1.08	23.29	3.96	-1.05	-1.05	

A second test of the equations was done using the three angled screws shown in Figure 81. These screws had a slightly more complex placement than the three nails in Figure 84. The calculations for these are shown in Table 4. They show the three screws are placed close to the imager (z values between 21 and 24); the left screw has the bottom point back toward the imager; the middle screw is nearly vertical and the right screw has the bottom pointing toward the source. The lengths of all three screws are estimated at 3 inches.

Table 4. Determination of coordinates for radiographs of three screws.

Point	x'	y'	x''	y''	z	x	y ₁	y ₂	Screw Length
Top of Left Screw	-1.37	1.63	-2.05	1.58	21.55	-1.23	1.47	1.42	2.97
Base of Left Screw	-0.92	-1.12	-1.17	-1.10	23.04	-0.88	-1.07	-1.06	
Top of Middle Screw	0.77	1.58	0.32	1.57	22.33	0.71	1.47	1.46	2.96
Base of Middle Screw	0.83	-1.60	0.35	-1.65	22.21	0.77	-1.48	-1.53	
Top of Right Screw	2.18	1.63	1.92	1.62	22.98	2.09	1.56	1.55	2.89
Base of Right Screw	1.72	-0.88	0.98	-0.92	21.39	1.53	-0.79	-0.82	

Photogrammetry

Research into the integration of radiography and photogrammetry reached its apogee by 1980. Before the maturation of current medical imaging technologies (e.g., computed tomography scanning, magnetic resonance imaging) x-ray photogrammetry was a viable area of medical research. By 1970, Hallert published X-Ray Photogrammetry: Basic Geometry and Quality in what became the standard for understanding the transference and transformation of “optical” principles to the projective geometry of radiographs. A medical text, it focused on the geometrical relations of bone replacements and reconstructions (e.g., knees, hips, jaws) and attempted to develop and document techniques for mapping locations and alignment. The 1989 publication by the American Society for Photogrammetry and Remote Sensing’s “X-Ray Photogrammetry, Systems and Applications” by S.A. Veress represents the highpoint of literature in the field.

However, despite the eclipse of the x-ray photogrammetry research in the medical field, optical photogrammetry has more recently advanced in fields ranging from accident reconstruction to archaeology. Advances in digital photography and personal computing hardware and software have made photogrammetry more physically portable, cost accessible and simpler to use. The combination of these advantages has led to combined software and hardware bundles costing less than \$1500. Responding to this opportunity, the researchers explored the possibility of coupling the rapidly evolving off-the-shelf photographic software with radiographic image analysis.

Multiple perspectives and calculated dimensions

While photogrammetry is similar to stereo-photography, the possibility of accurately inferring position and measurement of the actual objects from their images distinguishes this technique. Mathematical calculations based on the geometric laws are well established as they relate to optical lenses. This is the basis of modern “optical” photogrammetry (Karara, 1989). Theoretically, x-ray projection is subject to the same laws, albeit several practical problems have impeded the use of x-ray photogrammetry.

A review of the sources of error in x-ray photogrammetry and techniques for correcting or overcoming these demonstrated that controlling the imaging environment, and improving the imaging technology might adequately offset inherent difficulties in post-processing (Veress, 1989). However, at least two key sources of error remain problematic for those attempting to apply photogrammetric principles to x-rays: the penumbra effect, and the ambiguity of the focal point. “The penumbra effect tends to spread out the edge gradients and

results in a soft edge on the film” (Veress, 1989). Even more significant is the problem of calibration. In the absence of the *focal point* and *focal length* properties of a *lens* the *principal point* and *principal distance* provide the necessary metric inputs for post-processing. The principal point is that point on the imaging plate perpendicular to the focal spot, with the principal distance being that from the focal spot to the principal point (Figure 85). Veress’s review of the literature covers apparatus and techniques for overcoming the calibration problem. He distinguished between *physical approaches* and *semi-analytical approaches*.

Veress’s analysis is relevant to the present discussion because it highlights both the nature of the problem and the potential direction for mitigating these problems. Both physical techniques and semi-analytical techniques were tried in our empirical investigations.

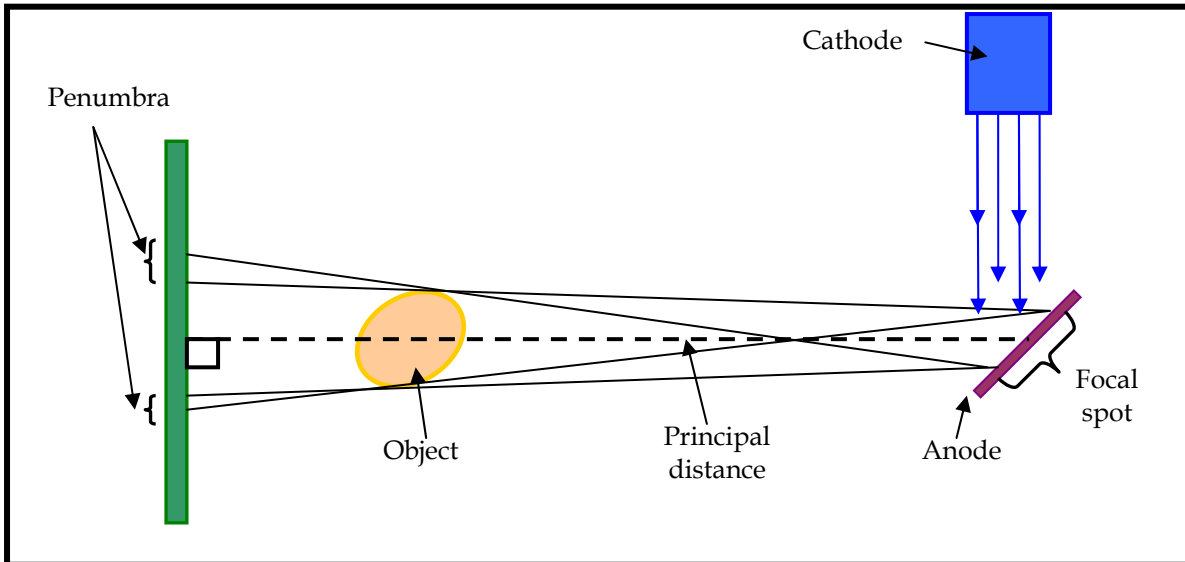


Figure 85. Diagram displaying terms used in image transfer.

Software advances: digital imaging and computational algorithms

Karara (1989) divides the technological development of “non-topographic” (i.e., close range) photogrammetry into eras: 1900-1960 as ‘Analog’; 1960 onward as ‘Analytical’; and 1980 onward as ‘Digital’. The implication of this typology has been a rapid expansion in both recording instrumentation (i.e., ‘cameras’) and in post-processing software. Within the field of architectural photogrammetry this has resulted in several research initiatives, and a smaller number of commercialized software products. Two commercial products marketed for the photogrammetric post-processing of close range photographs are Vexcel Corporation’s FotoG software (<http://www.vexcel.com>) and EOS Systems’s Photomodeler (<http://www.photomodeler.com>).

As Photomodeler has developed a more explicit marketing approach to the architectural market and it was known to one of the author's of this report (Koziol) it was chosen as the product for preliminary assessment in our review. This choice is not meant as an endorsement of this product, and as is concluded below, other products may prove to be more adaptable to the tasks outlined here.

Photomodeler: An off the shelf software possibility

EOS Systems's Photomodeler is an evolving (currently in Release 5) set of tools for processing inputted geometry into spatial coordinates. Some combination of 'camera' properties and graphically picked common 'points' on overlapping images, and/or additional geometric constraints (i.e., known points or relationships) are required for computation to proceed and be successful. In theory, the *principal distance* could be measured between the imaging plate and the x-ray source, and entered as one parameter, and through calibration (e.g., using marker(s) with a known location between the source and imaging plate) several images from differing camera stations should yield a vector model in coordinate space (i.e., x, y, z coordinates).

These several assumptions were used in designing and running a series of analyses. In general, the 'gross' spatial relationships of denser objects within an assembly were discernible, but the amount of effort to attain these results seem inordinate to the information gained. As this preliminary conclusion may be the result of inexperience and inefficiency, we document the procedure here as the basis for possible improvements on the process or logic employed.

In each of the experiments, multiple images were produced by varying the spatial relationships of the imaging plate, object, and source. A variety of assemblies, angles, and distances were tried. For example, Figure 86 shows the assembly with three screws in the 4-inch by 4-inch wood block which were x-rayed with the source shifted three inches each direction from center. Of particular interest is the spatial relationship between the small "marker" on the imaging plate as related to the corner of the wood block (circled). The positioning of the elements is shown in Figure 87.

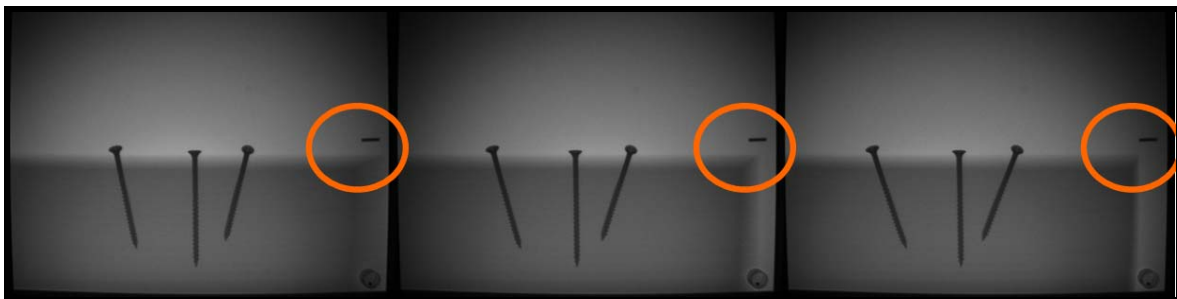


Figure 86. Left, Center, and Right Images of Screws in 4 X 4.

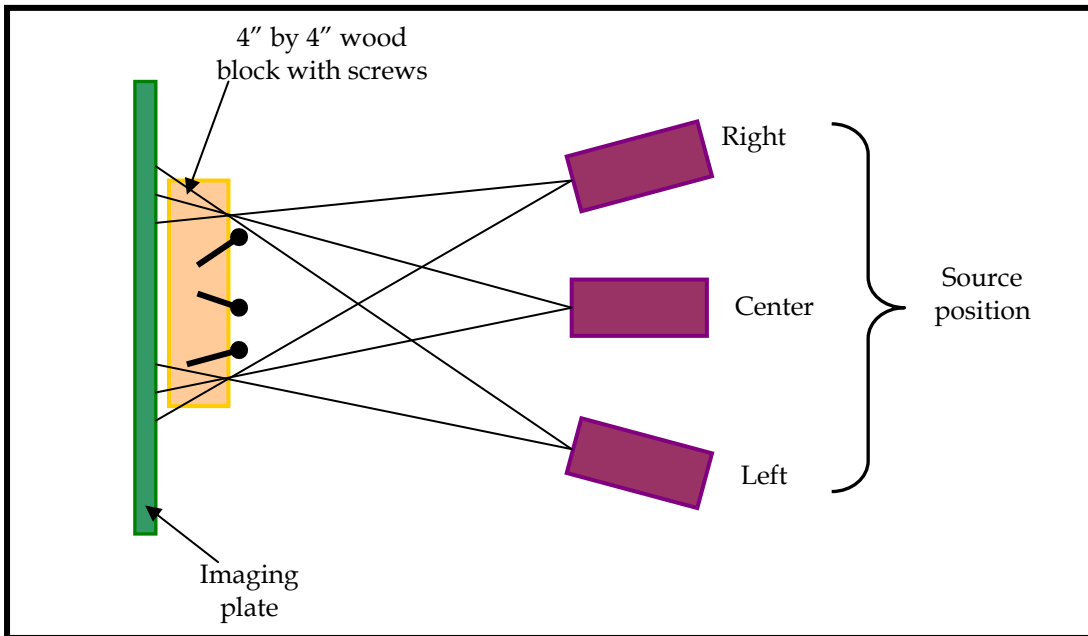


Figure 87. Configuration of imaging elements.

Although it would seem that a more extreme angling of the x-ray source would have yielded a greater difference in perspective, this option, often used by “optical” photographers, was practically limited by the need to minimize both the penumbra effect and the dissipation of x-ray strength at the edges of the imaging plate.

The identification of *common points* between multiple images is a key aspect of inputting adequate data for the Photomodeler computational algorithms to run with minimal error. This software requires the operator to visually identify and mark these points. The screen layout allows this to be done with side-by-side images (Figure 88).

This process is facilitated by several tools provided in the user interface, but it remains a task that is both time-consuming and subject to operator-caused inaccuracies. After a sufficient number of points are identified, it is possible to process the images into a coordinate model. Figure 89 shows marked points and lines, and Figure 90 shows the processed “model”.

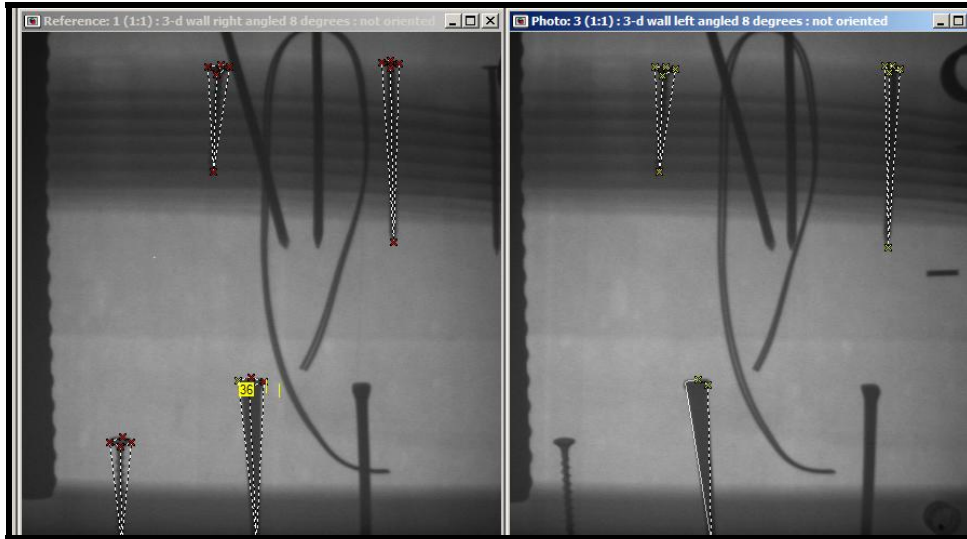


Figure 88. Marking points in Photomodeler.



Figure 89. Marked images ready to be processed

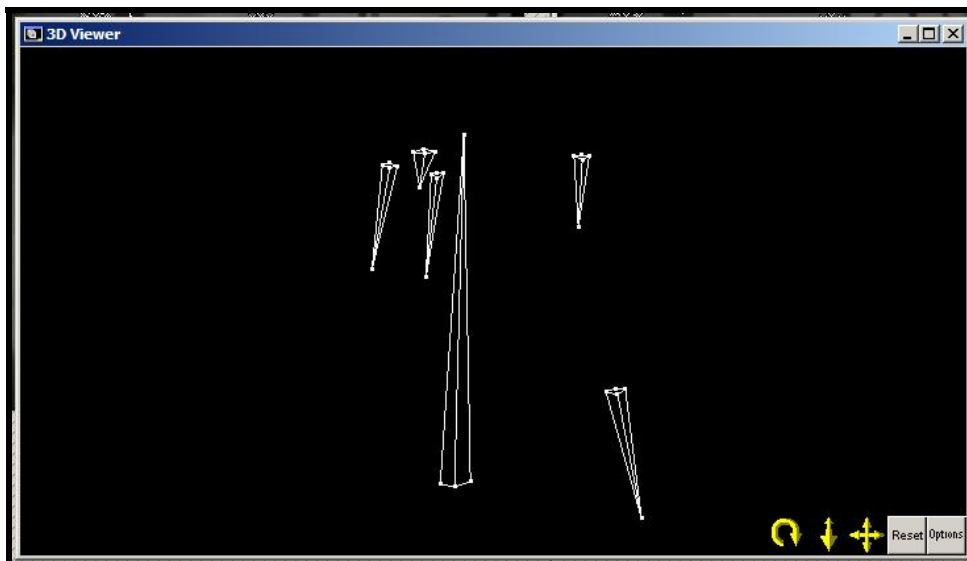


Figure 90. Processed model in viewer window.

Each point and line in this processed model can be located in coordinate space. The built-in viewer in Photomodeler allows the operator to rotate and query the model.

Real-time rotation of the model reveals that the piece of rebar (large triangle in model) sits “forward” of the other inclusions. (The second image of Figure 91 shows this.) While this model provides photogrammetrically derived “information,” the process to attain it was tedious and pending future findings to the contrary, the result seemed to offer few analytical benefits.



Figure 91. Rotations of the model.

Photomodeler creates its files in a proprietary format, but allows for easy export as a ‘dxf’ [Drawing eXport Format] file. Hence, the model can be incorporated into Autodesk AutoCad, or most other three-dimensional software packages.

Although Photomodeler did not prove to be immediately useful for this analysis, experimenting with the software helped identify several of the operational constraints in setting up future studies. The present experiments with Photomodeler would have benefited from better “front end” documentation of physical measurements in a format that could be used in Photomodeler. Additionally, a better means of identifying and recording known spatial positions (e.g., on the imaging plate) may have allowed for more extensive input of point data, and hence, improved the accuracy of the output model. The small pin on the imaging plate was useful, we believe that an even more precise multi-point reference system would have benefited the experiment.

This system might be a modification of some of the calibration systems reviewed by Veress (1989). One possibility would be a grid of known dimension (previous researchers have used one made of lead wire set into an incised grid of Plexiglas) set directly on the imaging plate. This could then be calibrated with known (i.e., marked) locations on the ‘surface plane’ of the object assembly. However, while such a calibration system could in-principle improve the accuracy of the output, it would also require greater attention to setup and data entry.

Recommendations for future research and applications in 3-D analysis

Despite not identifying a “breakthrough application” for the photogrammetric analysis of radiographs of building assemblies, the present study is far from conclusive. Communications between one of the researchers (Koziol) and several industry and academic experts suggests that “the mathematics are known” for developing a set of computer algorithms capable of efficiently converting radiographic images into coordinate models. However, it would take additional effort to (1) “tweak” Photomodeler, (2) develop a sufficiently sophisticated physical calibration apparatus, or (3) identify a different software package without the same limitations (for this application) as Photomodeler. In determining whether to undertake further investigation, it would also be prudent to conduct a potential benefits analysis of such a project before committing additional resources.

Case Studies - Examples of Field Projects Using Digital Radioscopy

St. Anne’s Church, Prague – Examination of Medieval Roof Framing

St. Anne’s Church in Prague, Czech Republic was built in the 1300s. Currently on the World Monuments Fund’s Watch List as an endangered site, the church has functioned as a warehouse for the past two centuries. The original roof timbers are largely intact and appear to be in excellent condition. Questions about whether the trusses had once been covered to produce a wooden vault led to an opportunity to use digital radioscopy to examine some of the truss members.

A catwalk at the base of the trusses allowed for placing the x-ray source on a tripod close to the truss. The image plate was taped to the back of the timber, as shown in Figure 92. Using a distance from the truss of approximately 60 cm and 10 pulses resulted in the radiograph shown in Figure 93. Of interest was the presence of any Gothic nails that may serve as evidence of boards attached to the timber at one time. Such a nail can be seen in the lower left side of the radiograph.

While at St. Anne’s Church, visual inspection of some of the timbers revealed minor pockets of deterioration due to decay fungi. The radioscopy equipment was configured again as shown in Figure 92. The radiograph (Figure 94) was colorized to accentuate the differences in absorption of x-ray energy by the timber. Converting the image to grey scale still allows for noticeable differences in absorption of x-ray energy. The light-colored area in most of the radiograph

represents sound wood. The approximately round, dark area is where a void could be seen in the timber. Although the loss of wood could not be determined visually, it was possible to estimate the extent of the void by measuring the dark area on the radiograph. Using the technique described in the section on Quantification of Decay, the maximum void was estimated at 50 percent loss of section.



Figure 92. Test configuration for digital radiography of a roof truss member in Saint Anne's Church.



Figure 93. Radiograph showing a nail with the head removed.

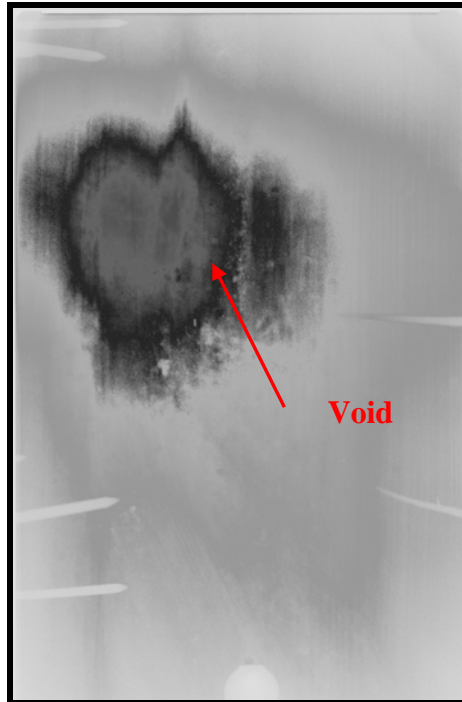


Figure 94. Radiograph showing the location and size of an internal void in a timber.

St. Bernard's Episcopal Church – Hidden Fasteners

The goal of the radioscopy in this study was to identify any evidence of the types of connections within the wood in the connections of the roof trusses, such as iron straps, iron bars, split ring connections, or mortise and tenon joints. Scaffolding allowed for access to the connection locations shown in Figure 95. Location A, at the peak of the truss where the post is connected was evaluated. Location B1, where the tie connects to the diagonal truss chord (which acts somewhat like a principal rafter) was evaluated. Location B2 is the connection between the toe and post at the peak of the arch. Location C could not be evaluated because of the lack of space to set up the imager at the base of the truss chord. Location C is where the majority of the resistance drilling was conducted.

Figure 96 shows the placement of the x-ray source to generate an image through the cross section at Location B1. Figure 97 shows the placement of the imager for this location. There are two metal straps (front and back) secured by a bolt at one end of the straps through the tie and the other end secured by a bolt through the diagonal truss chord (Figure 97). The source position was offset to see both the front and back straps for purposes of identifying any hidden fastener located between the straps.

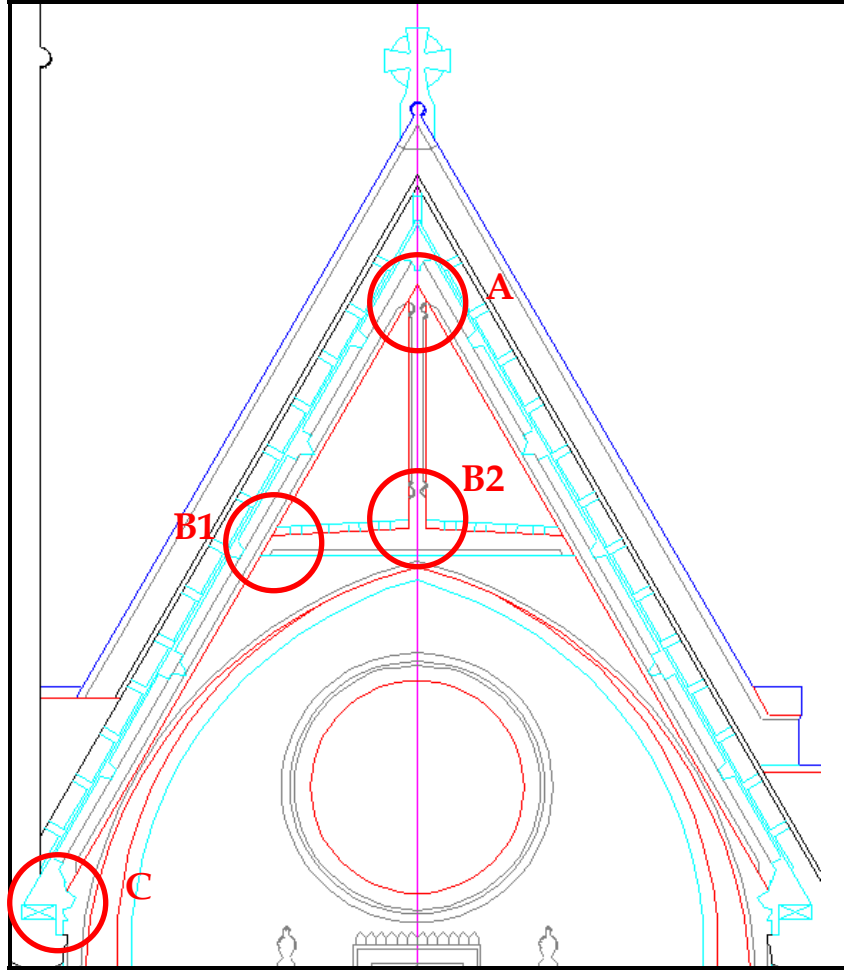


Figure 95. Locations where digital radiography was conducted.



Figure 96. Source placement for conducting digital radiography for one setup at Location B1.



Figure 97. Imager placement for conducting digital radiosity for one setup at Location B1 on Truss 7 (north side).

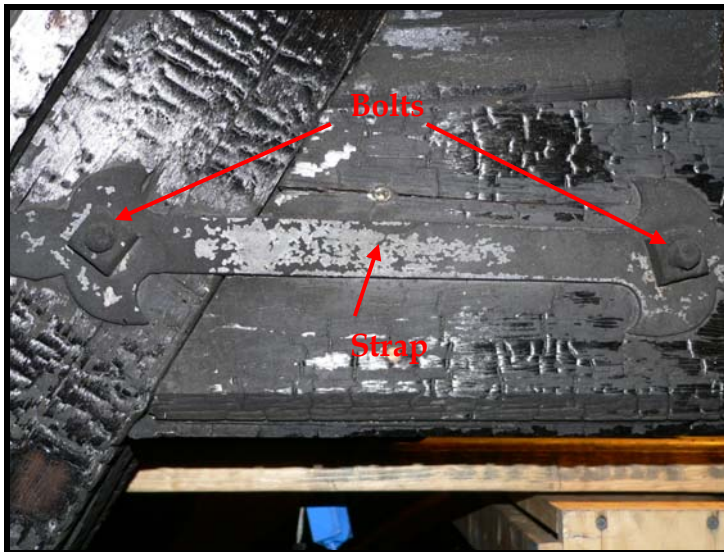


Figure 98. Area of interest showing two bolts and a metal strap at Location B1 on Truss 7 (north side).

The radiograph corresponding to this setup is shown in Figure 99. The image is as seen from the position of the x-ray source and is essentially the left side of the view seen in Figure 98. In the radiograph, the two metal straps are visible, as is metal conduit at the top of the image. The conduit is on the back of the truss tie and is, therefore, not visible in Figure 98 but can be seen in Figure 97. The diagonal line is the edge of the diagonal truss chord. To the right of the truss chord is the truss tie. Nails that secure wood trim to the tie are visible at the bottom of the radiograph. The uneven surface at the bottom of the wood trim is due to charring of the trim.

Note the lack of steel rods or other connectors between the metal straps. This image does not show either of the bolts on the straps because of the position of the source and imager. It is possible to see the grain of the wood in both the diagonal and the tie. There is no mortise and tenon connection between the diagonal and the tie. However, the wood member making up the truss tie does overlap the diagonal truss, as seen (barely) by the cross-hatched pattern of wood grain in the rectangular box in Figure 99.

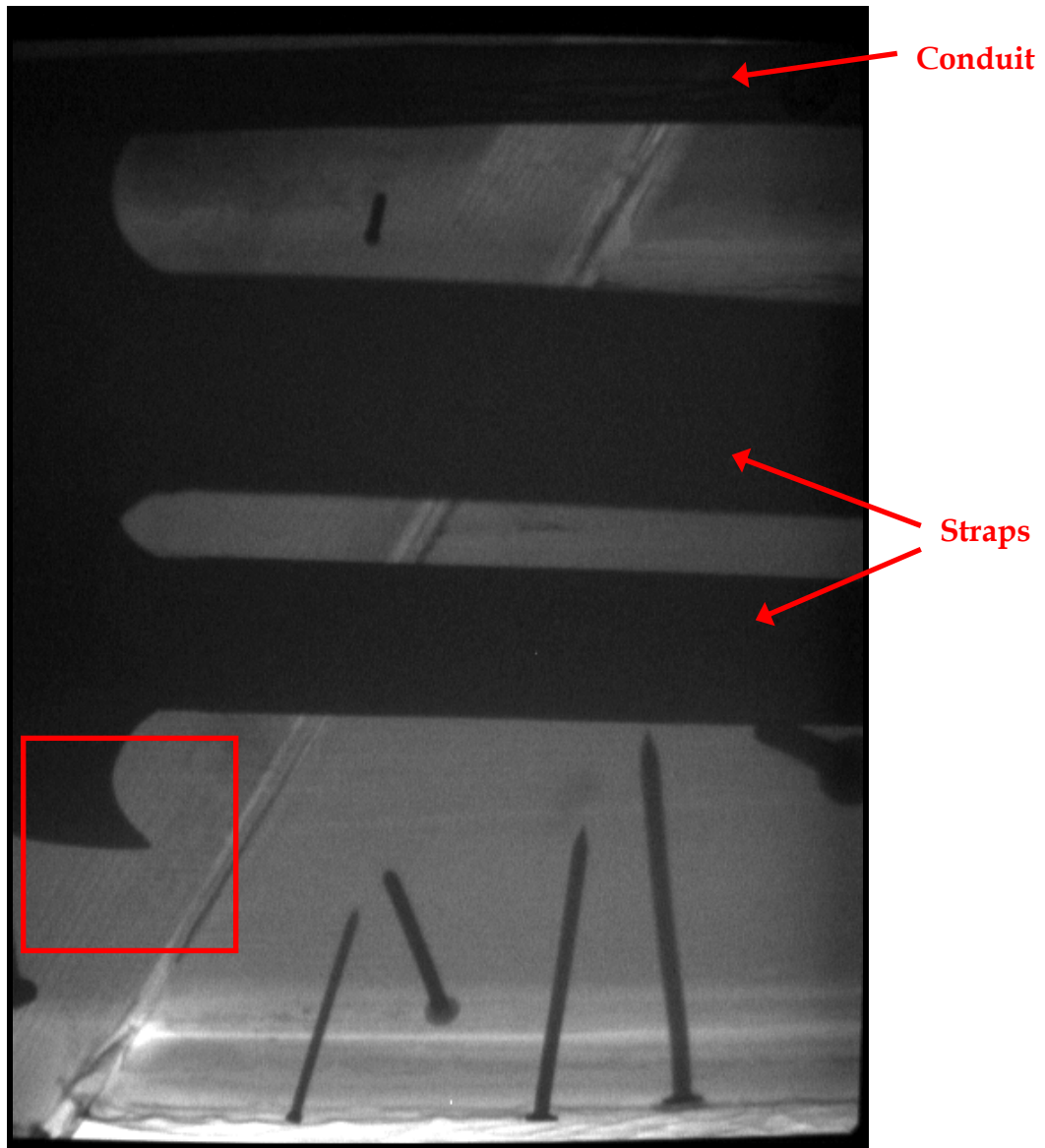


Figure 99. Radiograph of Location B1 on Truss 7 showing no internal rods or other fasteners (view from the x-ray source seen in Figure 24). The source position was offset to see both the front and back straps for purposes of identifying any hidden fasteners located between the straps; there are none.

To attempt to capture any internal fasteners from another perspective, as well as determine the condition of the bolt visible on the surface, the setup was reconfigured as is shown in Figure 100. The imager was placed on top of the tie and the source was positioned to allow x-rays to pass through the tie from the bottom. With this configuration, the bolt should be visible. Figure 101 shows that it is. The bolt is in good condition.

Of interest was what else might be found to support the connection between the tie and the diagonal. No metal fasteners were found in any of the radiographs. The wood member in the truss tie and the diagonal chord simply overlap (like a sandwich). Other than a few nails, the two bolts and metal straps that are visible are the only connection found at this location.



Figure 100. Source and imager placement to view the bolt through the tie at Location B1 on Truss 7 (north side).

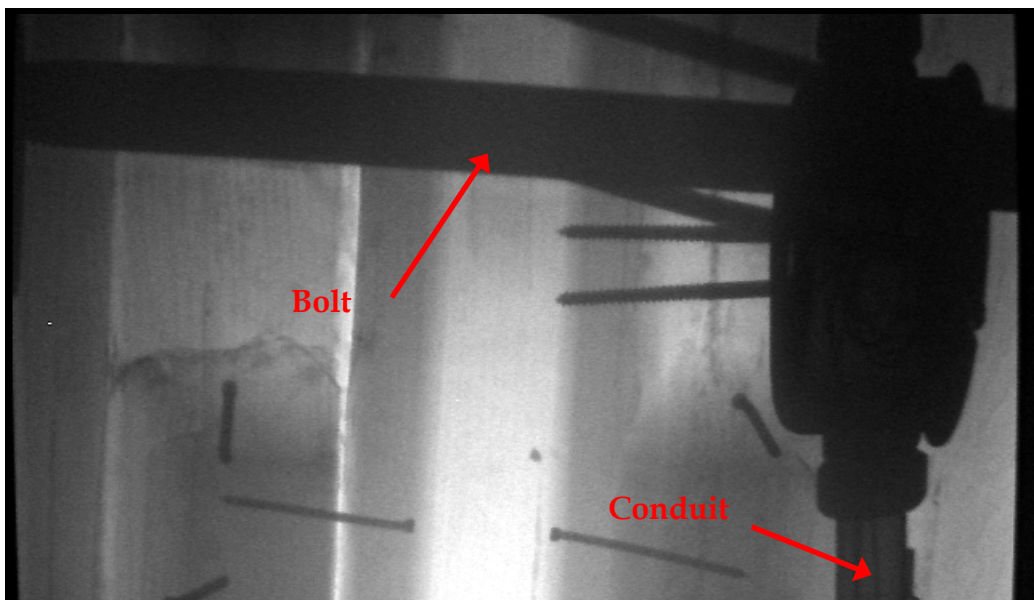


Figure 101. Radiograph of Location B1 on Truss 7 showing one of the bolts and the electrical conduit. No other internal rods or fasteners are visible.

Location B2, where the truss tie and post meet at the apex of the arch below, was the next area of interest (Figure 102). The source was initially placed as shown in Figure 103 to determine whether a mortise and tenon joint connected the tie and the post. The imager was subsequently lowered to determine whether any large metal fasteners secured the arch components to the truss tie.



Figure 102. Area of interest showing two bolts and a metal strap at Location B2 on Truss 6.



Figure 103. Source placement for digital radiography at Location B2 on Truss 6.

Figure 104 shows the placement of the imager for one of the tests. The corresponding radiograph for that setup is shown in Figure 105. As was found with Location B1, the metal straps and the two bolts through the straps provide the primary connection between the truss tie and the post. The wood members overlap but only nails secure the apex of the arch to the truss tie.



Figure 104. Imager placement for digital radiography at Location B2 on Truss 6.

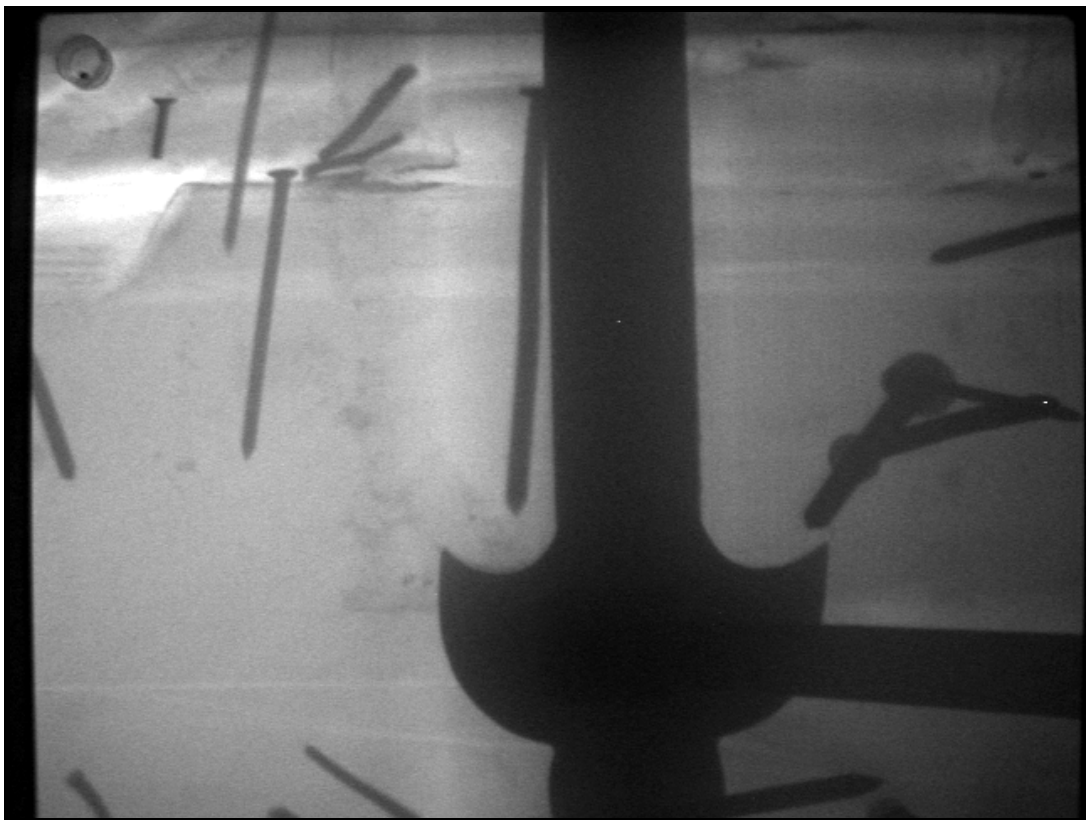


Figure 105. Radiograph of Location B2 on Truss 6 showing one of the bolts securing the metal strap. No other internal rods or fasteners are visible, except for nails.

Location A, at the peak of the truss, was the other location investigated with radiography. The visible connection was the same as at Locations B1 and B2 – metal straps secured by two bolts (Figure 106).



Figure 106. Area of interest showing two bolts and a metal strap at location A on Truss 7.

The x-ray source was initially placed as shown in Figure 107 in an attempt to view fasteners embedded in either the diagonals or the vertical post of the truss. As can be seen in the accompanying radiograph, the internal detail is the same as was found at Locations B1 and B2 (Figure 108). The area where the straps are located was enhanced to verify that no other metal fasteners (other than nails) were used here. None were found. Reconfiguring the setup allowed for confirmation that bolts pass through the diagonals to secure the straps.



Figure 107. Source placement for digital radiography at Location A on Truss 7.

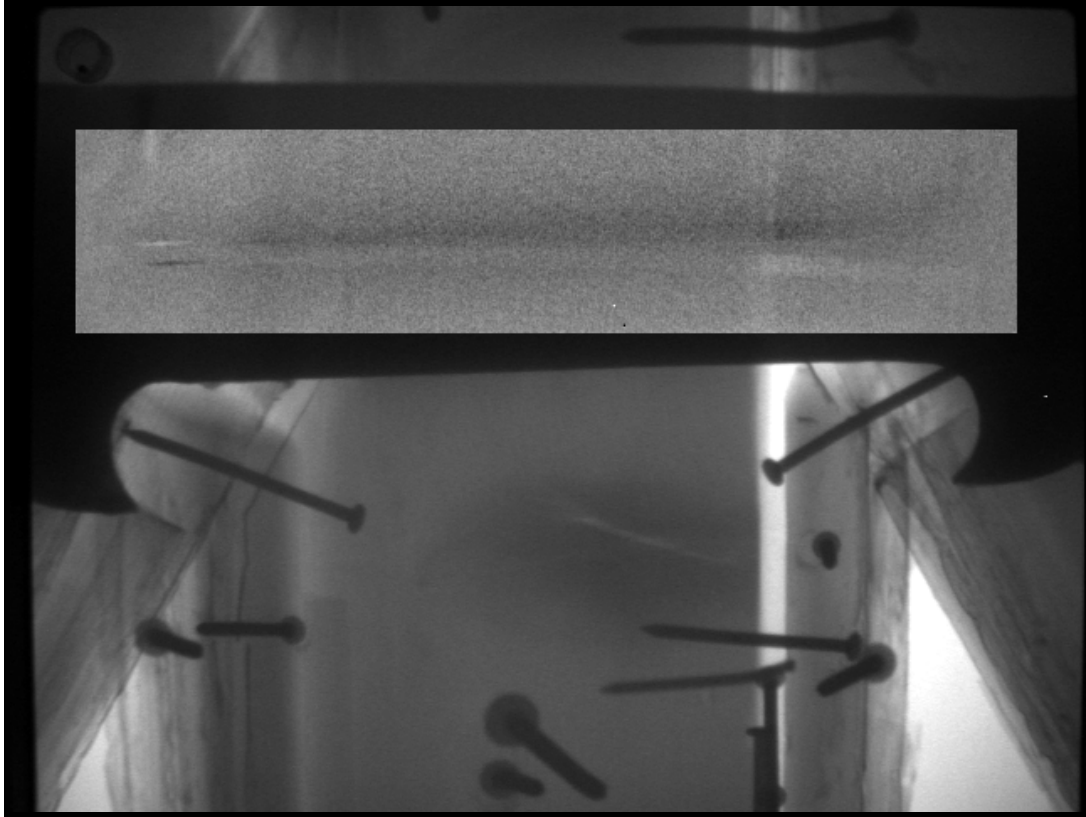


Figure 108. Radiograph of Location A on Truss 7 showing no internal rods or other fasteners. The area between the straps has been enhanced to verify that no metal fasteners are located between the straps.

New York State Capitol - Internal Construction and Failure Investigation

A key concern for the Senate Chamber of the New York State Capital in 2005 was the condition of one of the ceiling trusses that exhibited visible deflection. The construction of the truss connection details and positioning of blocking or other components was unknown. Destructive testing was not desirable because of the placement of the historic decorative wood trim over the lower truss chord. Digital radiography was proposed as a means to examine the truss at key locations identified by the structural engineer to determine the presence or absence of connections and any possible failure of the wooden truss chords.

The purpose of the investigation was to use digital radiography to identify evidence of the types of connections within the lower truss chord of one ceiling truss, such as steel plates, iron straps, iron bars, or bolts. Additionally, a possible failure in one of the truss chords was to be investigated. Scaffolding allowed for direct access to the lower truss chord.

Scaffolding was erected below the truss to allow full access along the length of the lower truss chord. The scaffolding provided a platform for placing the x-ray

source in various positions to capture images at key locations along the lower truss chord (Figure 109). Note that the decorative trim has separated due to deflection of the truss. The truss measures approximately 18 inches from front to back face. The source was typically placed 12 to 20 inches from the front face of the decorative wood trim over the truss chord.



Figure 109. Scaffolding platform used for radioscopy setup.

Prior to conducting the fieldwork, a mock-up was constructed in the lab to determine the likely number of pulses needed to penetrate the steel side plates, if necessary, and the effect of shooting at an angle on the ability to detect internal features. The mock-up was configured from field information provided by the structural engineer. Based on the lab research, it was known that placement of the imaging plate was critical for attempting to accurately locate structural rods, fasteners, plates and, if present, any potential fractures in the truss chords. Shooting perpendicular to the surface of the truss chord was the preferred setup and was used at most of the locations along the truss. Figure 110 shows the position of the source near purlin 8 to shoot perpendicular to the surface of the truss. The imaging plate for this shot is oriented as shown in Figure 111.



Figure 110. X-ray source positioned to take shot #15.



Figure 111. Placement of imaging plate for shot # 15.

Images were captured systematically along the length of the truss chord between three purlins (the area of interest to the structural engineer) so that the radiographs could be “connected” to continuously show the internal construction of the lower truss chord. The schematic shown in Figure 112 shows both the location and orientation of the imaging plate for each shot. The radiographs were oriented to show the internal view of the truss chord as it appears below the imaging plate (as opposed to being viewed from the source side of the truss).

As shown in the radiographs in Figures 113 through 114, the radiographs successfully identified metal connections of the truss system, such as screws, nails, threaded rods, bolts and steel plates. In addition the sensitivity of the radiographs was sufficient to identify more subtle features such as wood grain in

the trusses and decorative carved wooden trim. Key elements were labeled on each radiograph. The important features can be summarized as follows:

- Steel plates were present below where purlins 6 and 8 intersected the truss.
- Vertical threaded rods were visible at purlins 6 and 8.
- No steel plate was present below purlin 7 at truss 3.
- A wood diagonal truss chord was visible at purlin 6.
- A probable fracture (as opposed to a seasoning check in the lumber due to drying) was visible in images 15, 1, 14, 13 and 12 (proceeding from west to east). The fracture extended at least from west of purlin 8 to west of purlin 6, based on the number of images taken. Subsequent destructive testing verified the extent of the fracture.

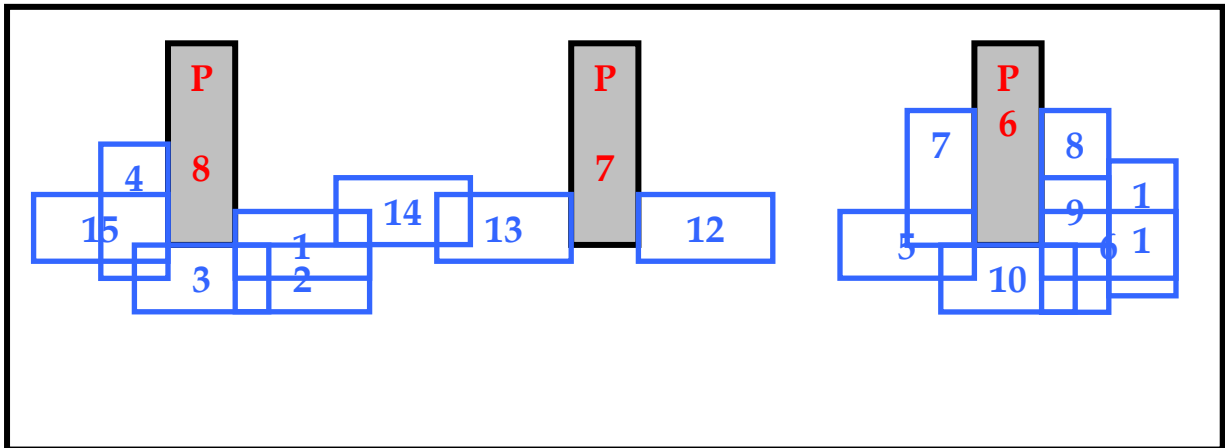


Figure 112. Schematic of radioscopic images. Purlins are colored gray and labeled in red (6 through 8). The imaging plate locations and orientation corresponding to each shot are in blue.

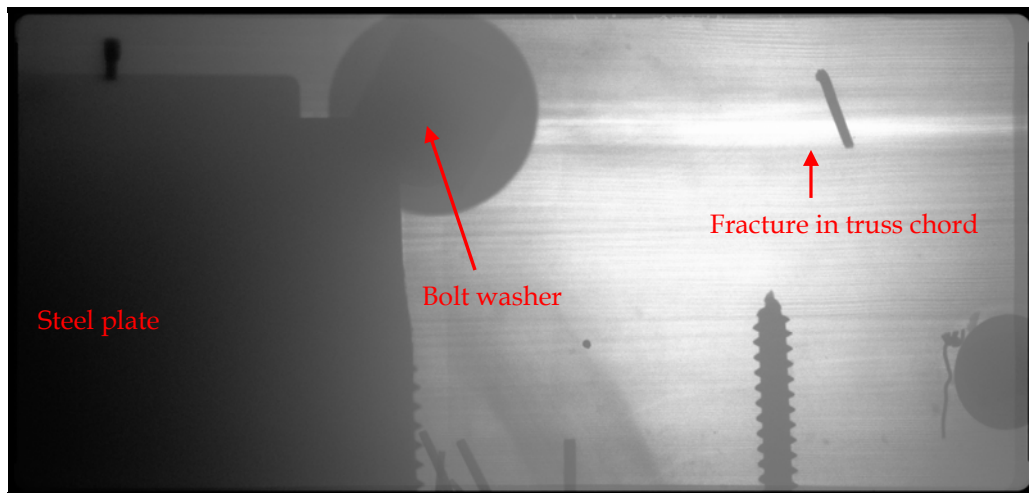


Figure 113. Radiograph of shot #1.

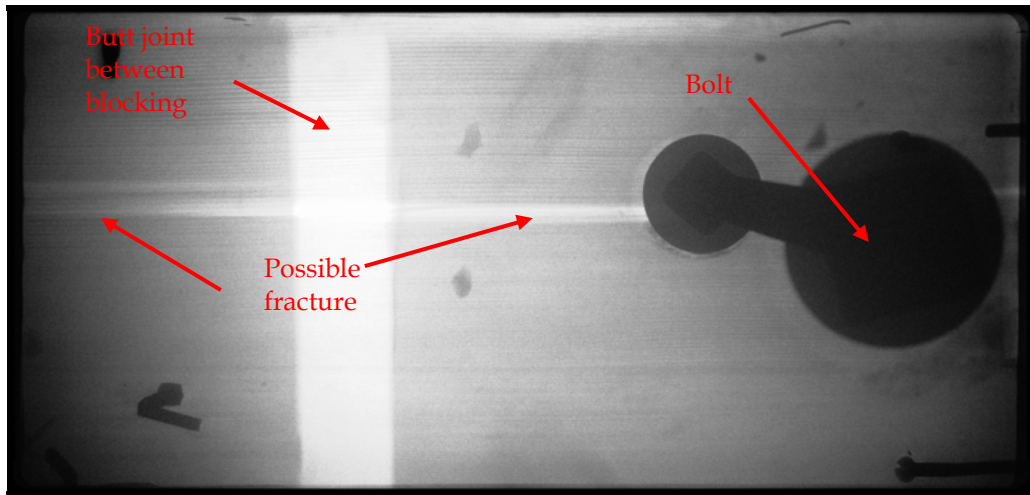


Figure 114. Radiograph of shot #13.

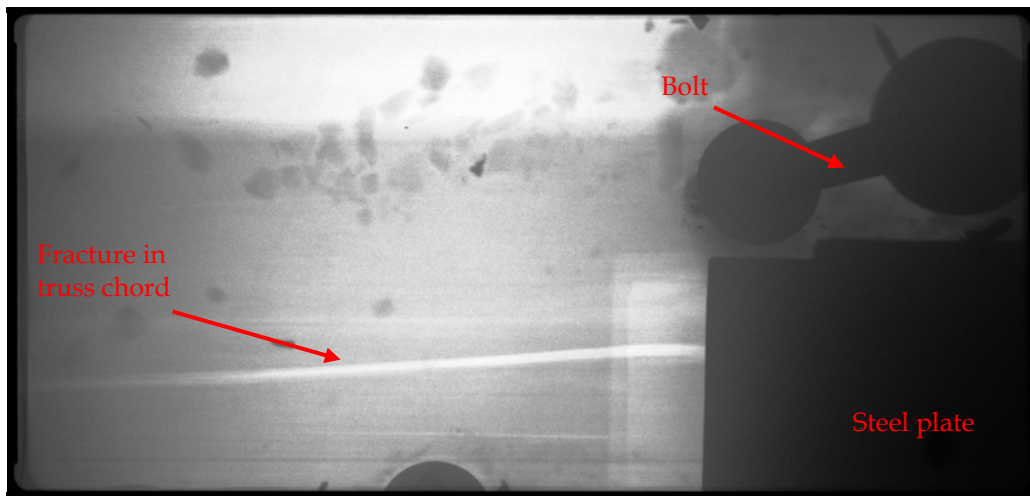


Figure 115. Radiograph of shot #15.

Summary

In the interest of saving as much historic fabric as possible and not altering or scarring historic materials as a result of investigative probes, architectural conservators look to nondestructive testing methods for the evaluation and identification of materials, conditions and alterations made to structures over time. As the answers to these and many other questions are typically concealed in a historic structure, nondestructive techniques of investigation are a necessity, but few are available. Digital radiography is one technique that is available and that can serve historic preservation purposes without destroying significant or historic features.

The goal of this work was to advance the use of digital radiography for assessing wood in historic structures. The work focused on:

- Investigating historic fabric and construction details using stereo-radiography
- Evaluating the extent of wood deterioration using digital imaging techniques
- Investigating licensing and regulatory requirements for use of portable x-ray equipment
- Investigating safety measures needed to operate the equipment in historic structures

In distilling the findings related to post-processing of digital radiographs, three main points are relevant. First, digital imaging affords the field operator the opportunity to modify image capture techniques based on real-time or near real-time (i.e., field processing) image production. This is particularly important in building investigation where conditions are variable, and future access may be difficult.

Second, the availability of relatively inexpensive mass-market (e.g., Adobe® Photoshop®) and multi-market specialty software (e.g., Photoflair®, Photomodeler) raise the possibility that software applications can be found and tweaked so as to extend the power of digital radiography for building investigation without a prohibitively large outlay of research and development (R&D) resources.

Finally, while the intuitively legible graphic (i.e., pictorial) output of radiographic investigation can provide convincing information, the efficient investigator must weigh whether increasing data inputs is worth the investment, and under what circumstances interpretive experience, multi-method data corroboration, and tacit knowledge suffice.

As demonstrated in this project, the potential that real-time digital radiography investigation presents is exciting and could have great positive impact in the field of historic preservation. Practical use can be found in some of the following areas:

- Historic structures reports
- Documentation of original construction details
 - Documentation of the chronology of construction of a historic structure
 - Documentation of material dimensions
 - Documentation of tool markings
 - Documentation of fastener shapes and sizes
- Identification of the alteration of such details due to modifications
- Structural evaluation of conditions and construction details

References:

American Society for Testing and Materials, 1995, 'ASTM D 5652-95, Standard Test Methods for Bolted Connections in Wood and Wood-Based Products', Philadelphia, PA.

Bleich, A. R., 1960, *The Story of X-rays from Rontgen to Isotopes*, Dover Publications, New York, 186 p.

Brown, G. I., 2002, *Invisible Rays, A History of Radioactivity*, Sutton Publishing, Limited, Phoenix Mill, England, 248 p.

Bossi, R., C. Oilen, P. Mengers, 1985, *Fundamental of Real-Time Radiography*, Nondestructive Testing Handbook, Second Edition, Volume 3, Radiography and Radiation Testing, L.E. Bryant, Technical Editor, P. McIntire, Editor, ASCE.

Cheney, M. 1981, *Tesla, Man out of Time*, Simon & Schuster, New York. 396 p.

EPA Website, 2004, www.epa.gov/radiation

Gilberg, M., C. Reigel, B. Melia, and J. Leonard, 2003, "Detecting Subterranean Termite Activity with Infrared Thermography: A Case Study", ART Vol. XXXIV, No.2/3, pp. 47-53

Hallert, B., 1970, *X-Ray Photogrammetry, Basic Geometry and Quality*, Elsevier Publishing Company, New York, 154 p.

Halliday, D. and R. Resnick, 1970, *Fundamental of Physics*, John Wiley & Sons, Inc., New York, 837 p.

Halmshaw, R. 1995, *Industrial Radiography*, Chapman and Hall. London.

Hart, D. 1974, "X-ray Analysis of the Narbonne House", APT Bulletin Vol. VI, No. 1, pp.78-98.

Hart, D. 1975, *X-ray Examination of Historic Structures*, U.S. Department of the Interior, Heritage Conservation and Recreation Service, Washington, D.C.

Harnsberger, D. 1981, "In Delorme's Manner", APT Bulletin Vol. XIII, No. 4, pp. 2-8.

Heipke, C., 1995, State-of-the-art Digital Photogrammetric Workstations for Photogrammetric Applications, *Photogrammetric Engineering and Remote Sensing*, Vol. 61, No. 1, pp. 49-56.

Josephson, M., 1959, *Edison, A Biography*, History Book Club, New York, 511 p.

Karara, H.M., ed., 1989. Non-topographic photogrammetry, 2nd ed; Falls Church, Va. : American Society for Photogrammetry and Remote Sensing

Lang, J. and A. Middleton, 1997, *Radiography of Cultural Material*, Butterworth-Heinemann, Oxford.

Life Magazine, 1896, "The New Roentgen Photography: Look Pleasant Please", February 1896.

Lillesand, T. M. and Kiefer, R. W., 1987, *Remote Sensing and Image Interpretation*, John Wiley and Sons, Inc., New York, N.Y., 721 pages.

Logos Imaging System, no date, Logos Imaging User Manual and Installation Guide.

Nitske, W. R., 1971. *The Life of Wilhelm Conrad Rontgen, Discoverer of the X Ray*, University of Arizona Press, Tucson, Arizona, 355 p.

Okoshi, T., 1976, *Three-dimensional Imaging Techniques*, Academic Press Inc., New York, N.Y., 403 pages.

Z. Rahman, G. A. Woodell, and D. J. Jobson, 2001. Retinex Image Enhancement: Application to Medical Images, presented at the NASA workshop on *New Partnerships in Medical Diagnostic Imaging*, Greenbelt, Maryland, July 2001

Roentgen, W. C., 1895. Über Eine Neue Art von Strahlen, *Sitzungsberichte der Physikalisch-Medizinischen Gesellschaft, Würzburg*, p. 132-141.

Roentgen, W. C., 1896. One a New Kind of Rays, *Nature*, v. 53, p. 274-276.

Science Applications International Corporation (SAIC), no date, Field Radiography Employing Radiation Machines, Environmental Compliance & Health and Safety.

Univ. of Pennsylvania, 1993, The New Light: Discovery and Introduction, http://www.xray.hmc.psu.edu/rci/contents_1.html.

Veress, S.A.. 1989 "X-Ray Photogrammetry, systems, and applications" in Karara, H.M.,ed., Non-topographic photogrammetry, pp. 167-186

Wisehart, M. K., 1928. *Marvels of Science: Modern Discoveries and Inventions and the Part They Play in Our Everyday Life*, The Century Co., New York, NY.

Wrenn, G. 1976. "Questions of Preservation and a New X-ray Investigative Technique", in *Preservation and Conservation: Principles and Practices*, Proceedings of the North American Regional Conference, Williamsburg, VA, September 10-12.

Appendices

- Presentations and publications discussing radioscopy by project staff
- Radiation warning sign
- X-ray set up form
- Survey of state regulations regarding use of x-ray machines
- State radiation control programs

Presentations and publications discussing radioscopy by project staff

1. Anthony, R.W. 2003. "Examination of Connections and Deterioration in Timber Structures Using Digital Radioscopy", Third Forensic Engineering Congress, San Diego, California.
2. Kasal, B. and R. W. Anthony. 2004. "In-situ Evaluation of Timber Structures", *Journal of Progress in Structural Engineering & Materials*. 6(2) pp. 94-103.
3. Anthony, R. W. 2004. "Use of Portable X-ray Equipment to Investigate Historic Timber Structures", *Proceedings of the Workshop on Historic Roof Timber Frames, Trest Castle, Czech Republic, May 2004*.
4. Anthony, R.W. 2004. "Condition Assessment of Timber Using Resistance Drilling and Digital Radioscopy", *Association for Preservation Technology International Bulletin Vol. XXXV No. 4*, p. 21-26.
5. Blaha, J., T. Kyncl, and R. W. Anthony. 2004. "Komplexni nedestruktivni pruzkum pozdne gotickeho dreveneho portalu v Hodinove vezi na hrade Pernstějne", in *Dejiny Staveb 2004*, Plzensky Kra, Plzen, Czech Republic. pp. 165-170.
6. Anthony, R. W. 2005. "Digital Radioscopy of Wood", in *Inspection and Monitoring Techniques for Bridges and Highways*, Woodhead Publishing Ltd., Cambridge, U.K.
7. R. W. Anthony. 2005. "Investigation of Historic Timber Structures Using Portable X-Ray Technology". *Proceedings of the International Conference on Conservation of Historic Wooden Structures, Centro UNESCO di Firenze, Florence, Italy, February, 2005*.
8. Workshop in Preservation Engineering: Diagnostics, Nondestructive Testing for the Evaluation of Historic Structures, Association of Preservation Technology Meeting, Galveston, Texas.
9. Shenandoah-Dives Mill HAER and HSA Workshop, Silverton, Colorado, 2004.
10. Shenandoah-Dives Mill HAER and HALS Workshop, Silverton, Colorado, 2005.

Radiation warning sign



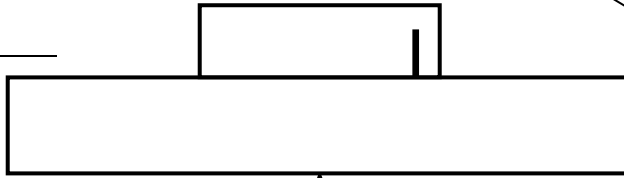
X-ray setup form

Site: _____

Reference pin - length: _____ "

Source #: _____

width: _____ "



Test location: _____

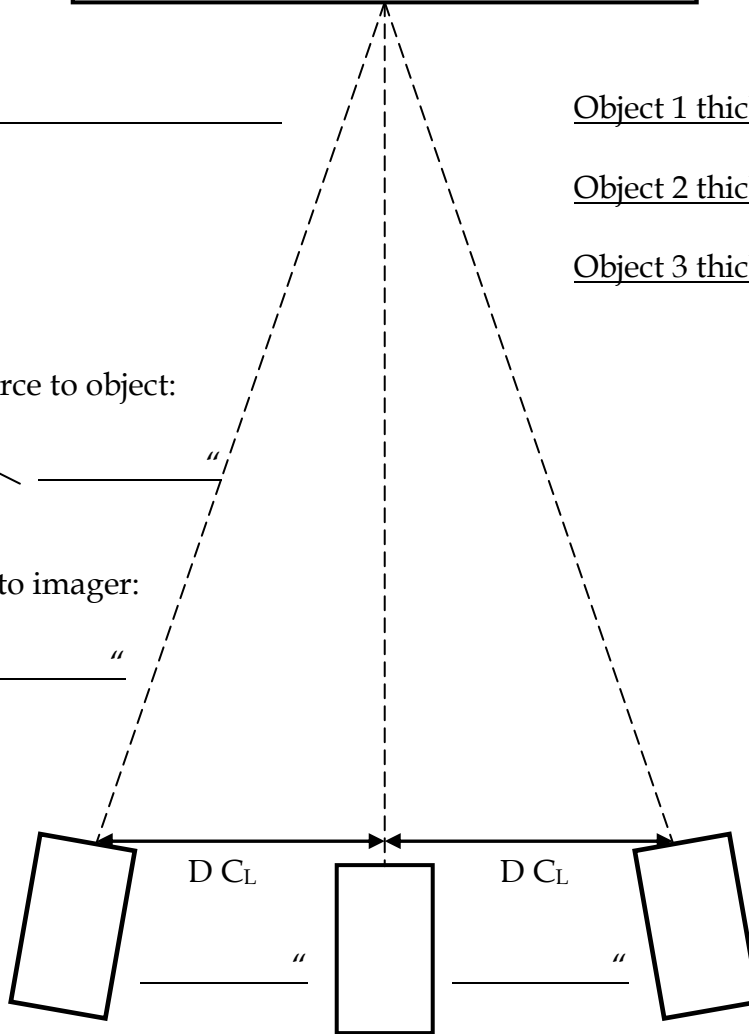
Object 1 thickness: _____ "

Object 2 thickness: _____ "

Object 3 thickness: _____ "

Distance- source to object: _____ "

Distance- source to imager: _____ "



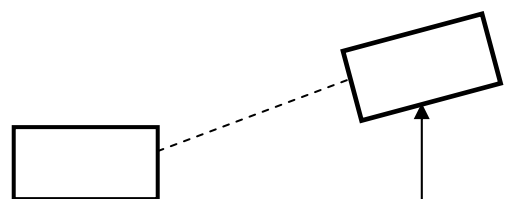
Pulses _____

Imager orientation _____

File name _____

Photo # _____

Vertical rise: _____ "



Survey of state regulations regarding use of x-ray machines

Phone surveys were done with Alabama, Colorado, New Jersey, New York, Oregon, and Virginia. The tables below describe the regulatory requirements for use of this equipment for historic preservation research. Each table identifies the agency to contact, the contact person (in 2004), what is required to bring radiology equipment into that state and if there is reciprocity or the ability to use licensing from your home state.

AGENCY	CONTACT PERSON(S)	BRINGING IN EQUIPMENT	RECIPROCITY
<p>NEW YORK State of NY -Dept. of Labor Division of Safety and Health Radiological Health Unit Registration: Building 12, Rm. 169 State Office Campus Albany, NY 12240 Phone:518-457-1202 Contact: Bill Varcasio USAWTV@labor.state.ny.us</p> <p>Reciprocity: Mail Stop #7F PO Box 683 New York, NY 10014-0683 Office: 212-352-6120 Fax: 212-627-9081</p>	<p>The Dept. of Labor regulates use of industrial x-ray equipment. Reciprocity is dealt with through the NYC office listed. Licensing is handled through the Albany office listed.</p>	<p>The manufacturing company notifies the state of the sale. The end user registers equipment at no cost. A licensing application is filed in Albany. It is good for three years. The form is the "Registration of X-Ray Machines and Particle Accelerators for Nonhuman Use."</p>	<p>For reciprocity one must file a request for reciprocity with the NYC office. Seven days notice is required. The form is called the "Notice of proposed use of radioactive material under reciprocity." This can be obtained by calling the number listed. When the form is submitted, a copy of one's current license must be included. (If authorized users are not named on the license, all sources users in NY state must carry some evidence of training and/or authorization to use your sources in NY (source: Notice to Reciprocity Applicants dated 3/1/04)</p> <p>As of March 2004, reciprocity is only allowed for a total of 30 days in a calendar year. Those companies exceeding this limit and failing to apply for a license lose future eligibility for reciprocity.</p>

AGENCY	CONTACT PERSON(S)	BRINGING IN EQUIPMENT	RECIPROCITY
<p>ALABAMA Alabama Office of Radiation Control</p> <p>Alabama Dept. of Public Health RSA Tower 201 Monroe St. Montgomery AL 36104</p> <p>334-206-5300 Fax: 334-206-5387</p> <p>Mailing address: PO Box 303017 Montgomery AL 36130-3017 The website is: www.adph.org/ADMINISTRATION/guidetoservices.pdf</p>	<p>David Walter at 334-206-5391 is the Director of Radioactive Materials Licensing</p> <p>Dave Turberville is in charge of inspection.</p> <p>Note: Jefferson County regulates X-ray equipment usage within that county only.</p>	<p>If work is longer than 30 days in a calendar year, the operator is required to apply for an Alabama radioactive material license. The application is available on the forms page of the website: www.adph.org/radiation/ or by calling the numbers listed.</p> <p>The state also requires that certain shielding plans are approved and that the agency has been notified that you are entering the state with the machine.</p> <p>Their safety requirements for Industrial Radiographic Operations require an annual refresher in safety training and hands on experience of 2000 hours. Industrial radiography Rule 420-3-26-04 is available on the website. The definition appears there: “(t) “Industrial radiography” means an examination of the structure of materials by the nondestructive method of utilizing ionizing radiation to make radiographic images.</p> <p>Alabama does not currently require a license to operate an x-ray machine. There are however, two paragraphs in the rules that apply to all persons who operate x-ray machines. The first one is in Rule 420-3-26-.10, Notices, Instructions, And Reports To Workers; Inspections. This paragraph basically requires that persons who work around radioactive materials or radiation machines receive radiation safety training to whatever level is required for them to work safely while performing their duties. The second paragraph is found in Rule 420-3-26-.06, Radiation Safety Requirements For Users Of X-Ray In Healing Arts Or Servicers Of X-Ray Equipment. This paragraph requires that each x-ray machine operator be instructed in safe operating procedures and must be competent in the safe use of the equipment.</p> <p>www.adph.org/RADIATION/ Q&A)</p>	<p>There is reciprocal recognition. Two days written notice is required which can be faxed to the number listed above marked, attention: David Turberville. The information needed is: the type of machine, where it is licensed, the nature, duration and scope of use, and the location of planned use. A copy of your current radioactive material license is also needed. One needs to comply with local rules. There is no time limit using reciprocity.</p>

AGENCY	CONTACT PERSON(S)	BRINGING IN EQUIPMENT	RECIPROCITY
<p>COLORADO Colorado Dept. of Public Health and Environment</p> <p>HMWMD – Radiation Management –XRP</p> <p>4300 Cherry Creek Drive South Denver, CO 80246-1530</p> <p>303-692-3448 Fax: 303-759-5355 Attn: Radiation-XRP</p> <p>Regulations governing the use of x-ray machines are available at: www.cdphe.state.co.us/hm/rad/xray/op/regs</p>	<p>Pamela Harley is the current Policy and Regulation / Radiation Management Manager of Radiation Services.</p> <p>Chris Irving, 303-692-3448, Chris.Irving@state.co.us, is with the X-Ray Certification Program (Registers all x-ray machines in Colorado)</p>	<p>The manufacturer needs to contact the state when it sells equipment to someone in the state. The new owner then needs to contact the state or go on-line to get the list of privatized and qualified inspectors. The owner meets with an inspector who inspects the machine and is paid a fee. The inspector then applies a “blue” certification label with a specific number and an expiration date, (provided by the state at a fee of \$50 to the inspector). This shows that the machine has been inspected. This inspection is good for a two-year period.</p> <p>“The inspection must be scheduled directly with the Qualified Inspector. Once the inspection has been completed, the Qualified Inspector will send the Department the necessary paperwork to complete the process. The inspectors are private individuals, approved by the Department to inspect x-ray machines. They may charge what they want for their services. Please contact the Radiation Management Unit at 303-692-3300 to receive a copy of the list of approved Qualified Inspectors in Colorado, or to get the telephone number of the Qualified Inspector who performed the last inspection in your office.” Source: www.cdphe.state.co.us/hm/rad/radiationservices.asp.</p> <p>To register the machine, the owner fills out a two page form, the RCD-4 and provides information on the ownership of the machine with an emergency contact and the number of the label provided by the inspector. Operators need to have proof of training. For this, you can show an industrial radiographers card or some other proof of training.</p> <p>It takes two weeks lead time to get the machine inspected if there is no reciprocity. The inspector gets the registration number and gives the application form and inspection number to the state. Applicants can get forms using an internet source: www.cdphe.state.co.us/hm/rad/xray. Regulations governing the use of x-ray machines are available at: www.cdphe.state.co.us/hm/rad/xray/op/regs.</p>	<p>Currently there is reciprocity with several states including: TX, OH, and NY. Usually, these are the states who are in agreement with the rules of the Nuclear Regulatory Commission. If machine is coming from a state with a comparable program and has been inspected in the last year, there is also reciprocity. If not, the machine needs to be registered and inspected in Colorado.</p> <p>Reciprocity rules: notify state three days before entering state. Describing type of equipment, who will be using it and where you will be. Use the X-Ray</p> <p>Reciprocity request form “LRS 200” is available on the Internet address listed above.</p> <p>There is a 180 day time limit on reciprocity within a one year period.</p>

AGENCY	CONTACT PERSON(S)	BRINGING IN EQUIPMENT	RECIPROCITY
NEW JERSEY New Jersey Dept. of Environmental Protection Bureau of Radiological Health P.O. Box 415 Trenton NJ 08625-0415 Website: http://www.state.nj.us/dep/rpp	Catherine Clausen, Supervisor, Machine Source Section, 609-984-5370 Catherine.Clausen@dep.state.nj.us	Within 30 days of entering the state with the equipment the responsible party needs to fill out a registration form and file it with the office. This will include a copy of the radiation safety survey, which provides radiation readings at three, six and nine feet from the equipment. One also needs to prove that the operator was trained and tested. The Agency will then send an invoice for the annual fee. Forms are available on the website.	Contact the office providing the registration form with a letter describing the dates and location of the anticipated work. Also include a copy of the radiation safety survey and proof of operator training and testing. This needs to be done a week prior to your visit. Include a letter that you expect to be in the state temporarily. Notification once a year should be sufficient.

AGENCY	CONTACT PERSON(S)	BRINGING IN EQUIPMENT	RECIPROCITY
OREGON Dept. of Human Services – Oregon Health Services, Radiation Protection Services 800 NE Oregon, Suite 260, Portland OR 97232 www.ohd.hr.state.or.us/rps/index.cfm	J. Robert Ropcinski, X-ray Program Manager, 503-731-4014, Ext. 676	The owner would have to register the x-ray control with Oregon and contact them by mail to inform them of the dates and locations where they will be using the equipment. Divisions 101 and 103 of their Administrative Rules describe this. Operators need to show 40 hours of training and 160 hours of “active participation in the performance of industrial radiography utilizing radiation machines and meet the requirements in sections(2) (a), (b), (c) and (d). In addition there is a bi-annual fee of \$115 to register the machine with us. Contact the registrar at (503) 731-4014, Ext. 666.	With temporary use from out of state, written notice shall be provided two working days prior to arrival. This notice shall include: a) The type of radiation machine; b) The nature, duration and scope of use; c) The exact locations where the radiation machine is to be used; d) The States in which this machine is registered. http://arcweb.sos.state.or.us/rules/OAR_333/333_101.html) Temporary use is limited to 30 days and not more than 180 days per year.

AGENCY	CONTACT PERSON(S)	BRINGING IN EQUIPMENT	RECIPROCITY
<p>VIRGINIA Virginia Public Health Radiation Health Program James Madison Bldg, 7th Fl. 109 Governor St. Room 730 Richmond VA 23219 804-864-8150 Fax: 804-864-8175 The website is: www.vdh.state.va.us/rad/rad_about.htm</p>	<p>Contact: Stan Orchel, Jr. X-ray program Coordinator. sorchel@vdh.state.va.us. Telephone: 804-864-8150.</p>	<p>If use will exceed 180 days, equipment needs to be registered with the state. An inspection report may be required. (Industrial registrations are completed the third week of each month.)</p>	<p>For reciprocal use not exceeding 180 days, seventy-two hours notice is needed. Provide the office with: purpose of the visit, operator contact name and number, location of work, a copy of the inspection report or certificate showing licensing in state the unit resides, and a statement that the state has no requirements for analytical equipment (if this is true).</p>

State Rad. Control Programs: Ind. Radiographer Certification Contacts & Status (3/2004)

****NOTE:** Effective 10/02/2001 FL requires IR certification for both x-ray and RAM and will accept certification from any approved CE**

State	RCP Status	Phone No.	IR Cert. Contact(s)	E-mail	RAM CE	X-Ray CE	Notes
Alabama	AS	(334) 206-5391	David Turberville	dturberville@adph.state.al.us	Yes	Yes	IR cert. rule became effective 5/25/00, AL has given exams since 2002
Alaska	non-AS	(907) 269-7942	Clyde Pearce	cepearce@alaska.net	No	No	NRC certifies AK's RAM IRs; no current plans to require IR certification for x-ray
Arizona	AS	(602) 255-4845	Aubrey Godwin	agodwin@arra.state.az.us	Yes	Yes	
Arkansas	AS	(501) 661-2173	Jared Thompson	jthompson@mail.doh.state.ar.us	No	No	AR will require RAM IRs to be certified, and will accept certs from any approved certifying entity; no current plans to require IR certification for x-ray
California	AS	(916) 322-3482	Ed Bailey	e.bailey@dhs.ca.gov	No	No	CA plans to become a CE for both RAM and x-ray IR in 2002
Colorado	AS	(303) 692-3036	Steve Tarlton	steve.tarlton@state.co.us	No	No	CO will require RAM IRs to be certified, and will accept certs from any approved CE; no current plans to require IR certification for x-ray
Connecticut	non-AS	(860) 424-3029	Edward Wilds	edward.wilds@po.state.ct.us	No	No	NRC certifies CT's RAM IRs; no current plans to require IR certification for x-ray
Delaware	non-AS	(302) 739-3787	Gary Lynn	---	No	No	NRC certifies DE's RAM IRs; no current plans to require IR certification for x-ray
Dist. of Columbia	non-AS	(202) 535-2180	Harold Monroe	hmonroe@dcchealth.com	No	No	NRC certifies DE's RAM IRs; no current plans to require IR certification for x-ray

KEY: AS = Agreement State CE = Certifying Entity	IR = industrial radiography, ind. radiographer non-AS = non-Agreement State	RAM = radioactive material RCP = radiation control program
---	--	---

State Rad. Control Programs: Ind. Radiographer Certification Contacts & Status (3/2004)

State	RCP Status	Phone No.	IR Cert. Contact(s)	E-mail	RAM CE	X-Ray CE	Notes
Florida	AS	(850) 245-4545 (904) 359-6363	RAM: Walter Cofer X-ray: Phil Thoma	walter_cofer@doh.state.fl.us philip_thoma@doh.state.fl.us	No	No	FL will require both RAM and x-ray IRs to be certified, and will accept certs from any approved CE
Georgia	AS	(404) 362-2675	Eric Jameson	eameson@mail.dnr.state.ga.us	Yes	No	GA has no current plans to require certification for x-ray IRs
Hawaii	non-AS	(808) 586-4700	Russell Takata	nriaq@keystroke.net	No	No	NRC certifies HI's RAM IRs; HI plans to become a CE for x-ray IR in 2002
Idaho	non-AS	(208) 334-2235 Ext 245	David Eisentrager	eisentra@idhw.state.id.us	No	No	NRC certifies ID's RAM IRs; no current plans to require IR certification for x-ray
Illinois	AS	(217) 785-6982	Steven Collins	collins@iemn.state.il.us	Yes	Yes	IL began IR certification in 1994
Indiana	non-AS	(317) 233-7153	Rex Bowser	rbowser@isdh.state.in.us	No	No	NRC certifies IN's RAM IRs; no current plans to require IR certification for x-ray
Iowa	AS	(515) 725-0301	Ramona Ubaldo-Mealey	rubaldo@idph.state.ia.us	Yes	Yes	
Kansas	AS	(785) 296-1563	Justin Spence	jspence@kdhe.state.ks.us	No	No	KS will require RAM IRs to be certified, and will accept certs from any approved CE; no current plans to require IR certification for x-ray
Kentucky	AS	(502) 564-7818, Ext 3697	Robert L. Johnson	robertl.johnson@ky.gov	No	No	KY will require both RAM and x-ray IRs to be certified, and will accept certs from any approved CE
Louisiana	AS	(225) 219-3027 (225) 219-3041	Tabitha Rice Ann Troxler Brad Schexnayder	tabitha.rice@la.gov ann.troxler@la.gov brad.schexnayer@la.gov	Yes	Yes	
Maine	AS	(207) 287-5696	Shawn Seeley	shawn.seeley@maine.gov	Yes	Yes	

KEY:	AS = Agreement State	IR = industrial radiography, ind. radiographer	RAM = radioactive material
	CE = Certifying Entity	non-AS = non-Agreement State	RCP = radiation control program

State Rad. Control Programs: Ind. Radiographer Certification Contacts & Status (3/2004)

State	RCP Status	Phone No.	IR Cert. Contact(s)	E-mail	RAM CE	X-Ray CE	Notes
Maryland	AS	(410) 631-3300	Ray Manley	rmanley@mdc.state.md.us	No	No	MD will require RAM IRs to be certified, and will accept certs from any approved CE; no current plans to require IR certification for x-ray
Massachusetts	AS	(617) 727-6214	Agostino Savastano Ken Traegde	agostino.savastano@state.ma.us kenath.traegde@state.ma.us	No	No	MA will not give exams, but will become a CE by accepting certs from other CEs, and will issue state ID cards for both RAM and x-ray
Michigan	non-AS	(517) 335-8204 (517) 241-1989	RAM: Bob Skowronek X-ray: Jim Camburn	skowronb@state.mi.us jim.camburn@cis.state.mi.us	No	No	NRC certifies MI's RAM IRs; no current plans to require IR certification for x-ray
Minnesota	non-AS	(651) 215-0935	Tim Donakowski	timothy.donakowski@health.state.mn.us	No	No	MN has notified NRC of intent to become an AS, and plans to become a CE for both RAM and x-ray IR, but will not proctor exams; state ID cards will be issued based on IR certs from other CEs
Mississippi	AS	(601) 987-6893	Robert Goff	rgoff@msdh.state.ms.us	No	No	MS will require RAM IRs to be certified, and will accept certs from any approved certifying entity; no current plans to require IR certification for x-ray
Missouri	non-AS	(573) 751-6111	Keith Henke	henkek@dhss.mo.gov	No	No	NRC certifies MO's RAM IRs; no current plans to require IR certification for x-ray
Montana	non-AS	(406) 444-5266	Denzel Davis	ddavis@state.mt.us	No	No	NRC certifies MT's RAM IRs; no current plans to require IR certification for x-ray
Nebraska	AS	(402) 471-0528	Julia Schmitt	julia.schmitt@hss.state.ne.us	No	No	NE will require RAM IRs to be certified, and will accept certs from any approved CE; no current plans to require IR certification for x-ray

KEY: AS = Agreement State IR = industrial radiography, ind. radiographer RAM = radioactive material
 CE = Certifying Entity non-AS = non-Agreement State RCP = radiation control program

State Rad. Control Programs: Ind. Radiographer Certification Contacts & Status (3/2004)

State	RCP Status	Phone No.	IR Cert. Contact(s)	E-mail	RAM CE	X-Ray CE	Notes
Nevada	AS	(775) 687-5394 Ext. 276	Stan Marshall	smarshall@bhps.state.nv.us	No	No	NV requires RAM IRs to be certified; accepts certs from any approved CE; no current plans to require IR certification for x-ray
New Hampshire	AS	(603) 271-4585	Diane Tefft	dtefft@dhhs.state.nh.us	No	No	NH requires RAM IRs to be certified; accepts certs from any approved CE; no current plans to require IR certification for x-ray
New Jersey	non-AS	(609) 984-5636	Jill Lipoti	jlipoti@dep.state.nj.us	No	No	NRC certifies NJ's RAM IRs; no current plans to require IR certification for x-ray
New Mexico	AS	(505) 476-3236	Bill Floyd	william_floyd@mneuv.state.nm.us	No	No	NM will require RAM IRs to be certified, and will accept certs from any approved CE; no current plans to require IR certification for x-ray
New York	AS	(518) 457-1202	Clayton Bradt	dolhu@nysnet.net	No	No	NY will require RAM IRs to be certified, and will accept certs from any approved CE; no current plans to require IR certification for x-ray
North Carolina	AS	(919) 571-4141	Robin Haden	robin.haden@ncmail.net	No	No	NC will require RAM IRs to be certified, and will accept certs from any approved CE; no current plans to require IR certification for x-ray
North Dakota	AS	(701) 328-5188	Ken Wangler	kwangler@state.nd.us	Yes	Yes	ND offers their exam once or twice a year, depending on the number of requests received
Ohio	AS	(614) 644-2727	Mike Snee	msnee@gw.odh.state.oh.us	No	No	OH requires RAM IRs to be certified; accepts certs from any approved CE; no current plans to require IR certification for x-ray

KEY:	AS = Agreement State	IR = industrial radiography, ind. radiographer	RAM = radioactive material
	CE = Certifying Entity	non-AS = non-Agreement State	RCP = radiation control program

State Rad. Control Programs: Ind. Radiographer Certification Contacts & Status (3/2004)

State	RCP Status	Phone No.	IR Cert.Contract(s)	E-mail	RAM CE	X-Ray CE	Notes
Oklahoma	AS	(405) 702-5141	Pamela Bishop	pamela.bishop@deq.state.ok.us	Yes	No	OR will require RAM IRs to be certified, and will accept certs from any approved CE; no current plans to require IR certification for x-ray
Oregon	AS	(503) 731-4014 Ext 669	Terry Lindsey	terry.d.lindsey@state.or.us	No	No	PA has notified NRC of intent to become an A.S., but does not plan on becoming a CE; will require RAM IRs to be certified, and will accept certs from any approved CE; no current plans to require IR certification for x-ray
Pennsylvania	non-AS	(717) 787-3720	William Kirk	kirk.william@dep.state.pa.us	No	No	NRC certifies PR's RAM IRs; no current plans to require IR certification for x-ray
Puerto Rico	non-AS	(787) 274-7816	Osiris Siurano	osurano@salud.gov.pr	No	No	RI will require RAM IRs to be certified, and will accept certs from any approved CE; no current plans to require IR certification for x-ray
Rhode Island	AS	(401) 222-3434	Bill Dundulis	billd@doh.state.ri.us	No	No	SC will require RAM IRs to be certified, but has not finalized its process; no current plans to require IR certification for x-ray
South Carolina	AS	(803) 737-7407	James Peterson	petersjk@columb54.dhec.state.sc.us	No	No	NRC certifies SD's RAM IRs; no current plans to require IR certification for x-ray
South Dakota	non-AS	(605) 773-6719	Bob McDonald		No	No	TN will require RAM IRs to be certified, and will accept certs from any approved CE; no current plans to require IR certification for x-ray
Tennessee	AS	(615) 532-0383	Johnny Graves	Johnny.Graves@state.tn.us	No	No	

KEY: AS = Agreement State IR = industrial radiography, ind. radiographer RAM = radioactive material
 CE = Certifying Entity non-AS = non-Agreement State RCP = radiation control program

State Rad. Control Programs: Ind. Radiographer Certification Contacts & Status (3/2004)

State	RCP Status	Phone No.	IR Cert. Contact(s)	E-mail	RAM CE	X-Ray CE	Notes
Texas	AS	(512) 834-6688, Ext. 2229	Jan Endahl	Jan.Endahl@tdh.state.tx.us	Yes	Yes	TX developed the first IR cert exam; other state RCPs can contract to use it
Utah	AS	(801) 536-4250	Craig Jones	cwjones@utah.gov	No	No	UT requires RAM IRs to be certified; accepts certs from any approved certifying entity; no current plans to require IR certification for x-ray
Vermont	non-AS	(802) 865-7743	Carla White	cwhite@vdh.state.vt.us	No	No	NRC certifies VT's RAM IRs; no current plans to require IR certification for x-ray
Virginia	non-AS	(804) 786-5932	Les Foldesi	lfoldesi@vdh.state.va.us	No	No	NRC certifies VA's RAM IRs; no current plans to require IR certification for x-ray
Washington	AS	(360) 236-3224	Arden Scroggs	arden.scroggs@doh.wa.gov	No	No	WA will require RAM IRs to be certified in 2001, and will accept certs from any approved CE; no current plans to require IR certification for x-ray
West Virginia	non-AS	(304) 558-3526	Beattie DeBord	bdebord@wvdbh.org	No	No	NRC certifies WV's RAM IRs; no current plans to require IR certification for x-ray
Wisconsin	AS	(608) 267-4784	Mark Bunge	bungemc@dhsf.state.wi.us	No	No	WI has no plans to become a CE, but will require both RAM and x-ray IRs to be certified; will be accepting certs from any approved CE
Wyoming	non-AS	(307) 777-7753	David Finley	dfinle@state.wy.us	No	No	NRC certifies WY's RAM IRs; no current plans to require IR certification for x-ray

KEY: AS = Agreement State IR = industrial radiography, ind. radiographer RAM = radioactive material
 CE = Certifying Entity non-AS = non-Agreement State RCP = radiation control program